TABLE OF CONTENTS

VI. THERMAL ANALYSIS

		Page
6.1	INTRODUCTION	6-1
6.2	PROCEDURES AND CALCULATIONS	6-1
6.2.1	Introduction	6-1
6.2.2	THTD Computer Program	6-3
6.2.3	IF-300 Cask Computer Model	6-5
6.3	THTD RESULTS - DESIGN BASIS CONDITIONS	6-24
6.3.1	Normal Cooling	6-24
6.3.2	Loss-of-Mechanical Cooling (LOMC)	6-25
6.3.3	50% Shielding Water Loss	6-26
6.3.4	30 Minute Fire	6-27
6.3.5	Post-Fire Equilibrium (PFE)	6-29
6.4	FUEL CLADDING TEMPERATURES	6-34
6.4.1	Wooten-Epstein Correlation	6-34
6.4.2	Analysis	6-37
6.5	MISCELLANEOUS THERMAL CONSIDERATIONS	6-43
6.5.1	Cask Operation at -40°F	6-43
6.5.2	Effects of Antifreeze on Cask Heat Transfer	6-43
6.5.3	Thermal Expansion of Neutron Shielding Liquid	6-44
6.5.4	Effects of Residual Water on Inner Cavity Pressure	6-47
6.5.5	Sensitivity of the Results to Changes in Outer Shell Emissivity	6-52
6.6	PRESSURE RELIEF DEVICES AND FILL, DRAIN, AND VENT VALVES	6-52
6.6.1	Rupture Disk Device	6-52
6.6.2	200 psig Pressure Relief Valve	6-55
6.6.3	1-Inch Globe Valve	6-56
6.7	CONFIRMATION OF CASK THERMAL PERFORMANCE	6-63
6.7.1	Thermal Test Description	6-63
6.7.2	Equipment and Test Facilities	6-63

CONTENTS (Continued)

		Page
6.7.3	Test Preparation	6-66
6.7.4	Testing	6-66
6.7.5	Thermal Test Report	6-67
6.7.6	Cask Surface Temperature	6-77
6.7.7	Thermal Test Acceptance Criterion	6-77
6.8	SECTION CONCLUSIONS	6-80
6.9	REFERENCES	6-81

LIST OF ILLUSTRATIONS

Figure	Title	Page
VI-1	THTD Nodal Network	6-6
VI-2	Corrugated Area	6-20
VI-3	Fire Transient and Cooldown	6-28
VI-4	Zircaloy Cladding Perforation Temperatures	6-31
VI-5	THTD Results - Dry Cavity Temperature Profile for PFE Conditions	6-32
VI-6	Fuel Basket Configurations	6-35
VI-7	IF300 Cask - Hottest Fuel Rod vs. Ambient Temperature for BWR Configuration with Dry Cavity and Group I Fuel	6-38
VI-8	IF300 Cask - Hottest Fuel Rod vs. Ambient Temperature for PWR Configuration with Dry Cavity and Group I Fuel	6-39
VI-9	IF300 Cask - Hottest Rod vs. Decay Heat for BWR Configuration with Dry Cavity and Group I Fuel	6-40
VI-10	IF300 Cask - Hottest Rod vs. Decay Heat for PWR Fuel Configuration with Dry Cavity and Group I Fuel	6-41
VI-11	Shield Barrel Surge Tank	6-44
VI-12	Burst Disk Device Installation	6-53
VI-13	Circle Seal Relief Valve (5100 Series)	6-56
VI-14	Globe Valve (1-inch)	6-58
VI-15	Valve Test	6-59
VI-16	Valve Test	6-60
VI-17	Globe Valve Assembly	6-61
VI-18	Thermocouple Locations	6-64
VI-19	Ambient Correction Factors	6-70
VI-20	Bulk Cavity Water Temperature Comparisons - LOMC	6-74
VI-21	Cask Surface Temperature Profile Measurement	6-77

N

LIST OF TABLES

Table	Title	Page
VI-1	Characteristics of Cask and Design Basis Fuels	6-2
VI-2	Effective Areas of End Nodes	6-8
VI-3	Film Coefficients and Equivalent Conductivity (A_e x H_c) of End Nodes	6-9
VI-4	Film Coefficients and Equivalent Conductivity (A_e x H_c) of Side Nodes - Natural Convection	6-11
VI-5	Emissivity Parameters	6-13
VI-6	Radiation Parameters	6-15
VI-7	Stainless Steel and Depleted Uranium Thermal Conductivity	6-16
VI-8	Fuel Properties	6-16
VI-9	Water Equivalent Conductivity	6-17
VI-10	Air Equivalent Conductivity	6-18
VI-11	Water Properties	6-23
VI-12	150°F Water Conductivity	6-24
VI-13	Cask Temperatures and Pressures - Normal Cooling	6-25
VI-14	Cask Temperatures and Pressures - LOMC	6-26
VI-15	Cask Temperatures and Pressures - 50% SWL	6-27
VI-16	Cask Temperatures and Pressures - End of 30 Minute Fire	6-29
VI-17	Cask Temperatures and Pressures - PFE	6-30
VI-18	Wooten-Epstein Correlation Input Parameters - PFE	6-36
VI-19	Cask Shielding Tank Liquid	6-42
VI-20	Expansion Volumes	6-46
VI-21	Cavity Volumes	6-48
VI-22	Emissivity Comparison - PFE, 17 x 17 PWR Fuel	6-52
VI-23	Cask 301 LOMC	6-71
VI-24	Cask 302 LOMC	6-72
VI-25	Cask 303 LOMC	6-72
VI-26	Cask 304 LOMC	6-73
VI-27	Cask Heat Load to Produce 422°F Water Temperature	6-75

N

VI. THERMAL ANALYSIS

6.1 INTRODUCTION

This section describes thermal analyses of the IF-300 shipping cask with the 7-cell PWR and 18-cell BWR baskets licensed prior to 1991. The characteristics of the types of fuels licensed prior to 1991 which may be transported in the cask are described in Section 3.0.

The analyses described in this section assume that the IF-300 cask is used in the "dry" shipping mode with a design basis heat load of 40,000 Btu/hr. The per bundle maximum decay heat rates are as follows:

- PWR fuel - 5725 Btu/hr
- BWR fuel - 2225 Btu/hr

Thermal analyses were originally done in 1973 for wet shipments of high heat load Group I BWR and PWR fuels. Additional analyses were completed for the Group I fuels in 1974 for low heat load dry shipments and in early 1980 for high pressure fuel pins. The newer Group II BWR and PWR fuels were analyzed in late 1980 with their results being similar to those of the Group I fuels. Fuel designs licensed since 1991 are presented in Volume 3, Appendices A and B.

Table VI-1 tabulates the characteristecs used in the thermal analyses of the Group I 7 x 7 BWR and 15 x 15 PWR fuels (14 x 14 PWR is bounded by the 15 x 15 fuel) and the Group II 8 x 8 BWR and 17 x 17 PWR fuels (16 x 16 PWR is bounded by the 17 x 17 fuel) licensed prior to 1991.

This section contains five "Design Basis Heat Load Conditions"; normal cooling, loss-of-mechanical cooling (LOMC), 50% shielding water loss, 30 minute fire, and post-fire equilibrium (PFE).

The mechanical cooling system is not required by the NRC. This system has been partially or completely removed from all four IF-300 casks. The thermal results are shown in this section. The LOMC results replace all normal cooling results.

Volume 3, Appendix A, Section A-3.0 has four design basis heat load conditions; normal cooling (NOC), 30 minute fire, 3-hour post fire, and post-fire equilbrium (PF3). NOC is natural convection in 130° ambient air, which is eqivalent to the LOMC in this section.

6.2 PROCEDURES AND CALCULATIONS

6.2.1 Introduction

The thermal analyses described in this section have been, with minor exceptions, calculated by computer. These calculations are based on parameters specified in Table VI-1. This section of the report describes the methodology incorporated in the various computer codes, discusses the bases for the procedures used, and details the calculations performed.

Table VI-1

CHARACTERISTICS OF CASK AND DESIGN BASIS FUELS

CASK

Type	BWR	PWR
Cavity Length, in.	180.25	169.50
Cavity Diameter, in.	37.5	37.5
Inner Shell Thickness, in.	0.5	0.5
Shielding Thickness, in.	4.0	4.0
Outer Shell Thickness, in.	1.5	1.5
Cask Linear Surface Area, ft^2/ft	39.2	32.2
Cask Length (Excluding Fins), in.	192.3	182.1
Shielding Water, lb	4,540	4,540
Cavity Relief Pressure, psig at 443°F	350 - 400	350 - 400
Neutron Shielding Relief Pressure, psig	200	200
Maximum Heat Load, Btu/hr - Air Filled	40,000	40,000

FUELS

Type	BWR	PWR
Number of Fuel-Bearing Rods/Bundle - Group I	49 (7 x 7)	208 (15 x 15)
Number of Fuel-Bearing Rods/Bundle - Group II	62 (8 x 8)	264 (17 x 17)
Exposure, GWd/MTU (average)	35.0	35.0*
Operating Power, kW/kgU	30.0	40.0
Assembly Decay Heat Rate, (max) BTU/hr, Air Filled	2,225	5,725
Assemblies per Cask Load	18	7
Uranium, kgU/Bundle	198	465

* See Volume 3, Appendix B for high burnup PWR fuel.

(BLANK PAGE)

It should be reemphasized that the thermal analysis is not based on specific fuels but rather on a "design basis" configuration that sets an analyzed upper limit on the cask thermal capacity. The cask is intended as a general purpose container and, as long as the design basis conditions are not exceeded, will function adequately and safely for any light water moderated reactor fuel that may be placed in the cavity fuel baskets. See Section 3 for a detailed fuels description.

6.2.2 THTD* Computer Program

The THTD computer program computes transient and steady-state temperature solutions for three-dimensional heat transfer problems. Over 1200 temperature nodes have been handled in a single problem, but the actual number possible depends on the available computer memory and the amount of nongeometrical data. Problems can include:

Node-to-node heat transfer by conduction, convection, and radiation.

Node-to-boundary heat transfer by convection and radiation.

Latent heat for an isothermal phase change for any material.

User-supplied input includes:

1. Geometrical dimensions, connections, and material reference for temperature nodes which can have up to six faces. (Dimensional data can be detailed or, if applicable, approximated by three mutually orthogonal dimensions for rectangular parallelepipeds.)
2. Flow geometry and convection data references for nodes through which fluid flows.
3. Radiation linkages between nodes or between nodes and external boundaries without limit to the number of linkages for a node face.
4. Initial rates for fluid flow, surface flux, and internal heating.

---

*Transient Heat Transfer Version D, General Electric Company, computer code.

5. Convective heat transfer coefficient data. These take the form of tables of Nusselt number as a function of Reynolds number for which linear interpolation is done between the natural logarithms.
6. Thermal resistance coefficients which can be assigned between faces of neighboring nodes.
7. Temperature-dependent tables for material properties, including emissivities for boundary radiation. Material property tables can also indicate the isothermal energy absorption (assuming heating) which is to take place during phase change and can indicate another material property table to be used by a node which completes phase change.
8. Time-dependent tables which can include fluid inlet temperature, convective heat transfer coefficients, fluid flow, surface flux, internal heating, and temperature.
9. Temperature-dependent multipliers for use with internal generation rates.

Considerable data checking is done to assure consistent, complete problem input and thus avoid wasted computer time. Edited output in the form of tables of physically connected nodes and tables of temperatures as functions of time can be obtained to enhance readability of output and to facilitate data plotting.

Temperature solutions are obtained by iterative solution of simultaneous algebraic equations for node temperatures derived from finite difference analysis.

The use of simultaneous equations (the implicit method of formulating nodal heat balances) precludes any stability limitations on time increments and permits a direct steady-state solution at any stage of a computer run, including solutions to serve as initial conditions for a transient. Convergence of a temperature solution is recognized and controlled by tolerances on the residual heat balances which provide a measure of the imperfection" of a solution, as well as by the conventional maximum change in any node temperature during an iteration sweep.

6.2.3 IF-300 Cask Computer Model

6.2.3.1 Introduction

The following describes the boundary conditions and properties used in the THTD thermal analysis of the IF-300 shipping cask. Figure VI-1 shows the nodal model used to represent the IF-300 cask.

The model represents the cask base and 84 inches of height as measured from the cavity bottom. The 32-series nodes represent the cask mid-length where axial symmetry is assumed. The fuel region is representative only in heat generation, axial distribution and thermal property terms. The actual temperature distribution within the fuel matrix is computed by techniques discussed in Section 6.5.

6.2.3.2 External Boundary Conditions

The exterior surface (finned, unfinned, or corrugated) of the cask is represented by a series of "dummy" materials whose temperature-dependent conductivities yield the same ΔT's as do the actual temperature-dependent convection film coefficients of these surfaces. These nodes are 1010 through 1910 (at the cask end), and 2004 through 3204 (along the corrugated barrel), as shown in Figure VI-1.

Equivalency of k and h_c is obtained in the following manner (A_e = effective area):

For convection:

$$q = A_e h_c \Delta T$$

For conduction:

$$q = \frac{kA\Delta T}{\Delta X}$$

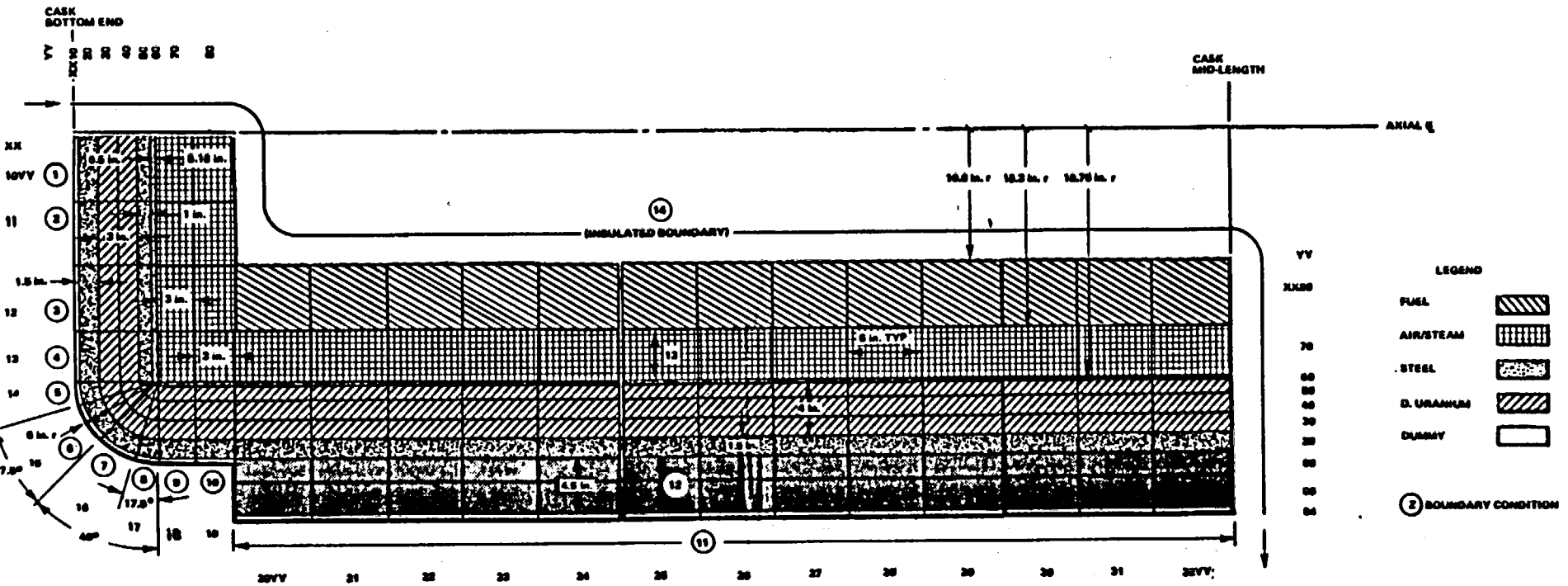

Figure VI-1: THTD Nodal Network

Equating these we obtain:

$$\frac{kA}{\Delta X} = A_e h_c$$

By choosing ΔX = 1 foot and A = 1 ft^2 (THTD input) then:

$$k = A_e h_c \tag{6.1}$$

Thus, a film coefficient whose value is a function of $(T_s - T_{amb})$ can be converted into an equivalent conductivity that is a function of T_s, since T_{amb} is constant. Values of k for each surface node as a function of temperature are calculated below.

a. Equivalent Conductivity of End Nodes - Natural Convection

The "dummy" nodes bound by the circled numbers 1 through 10 on Figure VI-1 are subject to natural convection. Nodes corresponding to boundaries 1 and 10 are unfinned; those corresponding to boundaries 2 through 9 are finned. The extended areas vary from node to node depending on the number and shape of the fins.

i. Effective Areas (A_E)

The effective area of a finned surface is given by:

$$A_E = A_B + \eta A_F \tag{6.2}$$

where:

A_B = Base Area
A_F = Fin Area
η = Fin Effectiveness

Fin effectiveness is defined on page 60 of Reference 6.3. Using a representative range of values for h_c, the average value for fin effectiveness was determined to be 0.85. Table VI-2 lists the resulting effective areas for the end nodes:

Table VI-2

EFFECTIVE AREAS OF END NODES

Boundary	Effective Area, A_e (ft^2)
1	0.61
2	10.2
3	9.2
4	12.6
5	11.5
6	21.6
7	16.4
8	9.6
9	9.7
10	6.3

ii. Film Coefficients (h_c)

The following coefficient correlation for natural convection from the end nodes is from Reference 6.6:

$$h_c = 0.29\ (\Delta T/L)^{0.25} \qquad (6.3)$$

where:

h_c = natural convection film coefficient Btu/hr-ft^2-°F

ΔT = surface-to-ambient temperature differential, °F

L = average surface height, ft

Film coefficients generated from equation 6.3 are listed in Table VI-3.

Table VI-3

FILM COEFFICIENTS AND EQUIVALENT CONDUCTIVITY ($A_e \times h_c$) OF END NODES

Nodal Temperature	Film Coefficient	Equivalent Conductivity at Boundary									
		1	2	3	4	5	6	7	8	9	10
130°F	0	0	0	0	0	0	0	0	0	0	0
150°F	0.624	0.38	6.4	5.7	7.9	7.2	13.5	10.2	6.0	6.1	3.9
200°F	0.853	0.52	8.7	7.8	10.7	9.8	18.4	14.0	8.2	8.3	5.4
250°F	0.977	0.60	10.0	9.0	12.3	11.2	21.1	16.0	9.4	9.5	6.2
300°F	1.065	0.65	10.9	9.8	13.4	12.2	23.0	17.5	10.2	10.3	6.7
500°F	1.294	0.79	13.2	11.9	16.3	14.9	28.0	21.2	12.4	12.6	8.2
1000°F	1.603	0.98	16.4	14.7	20.2	18.4	34.6	26.3	15.4	15.5	10.1

iii. Equivalent Conductivity

Equivalent conductivities ($A_e \times h_c$) for the end nodes are also listed in Table VI-3.

b. Equivalent Conductivity of Side Nodes - Forced Convection

The dummy nodes in Figure VI-1 bound by the circled number 11 represent the heat transfer surface of the corrugated neutron shielding barrel.

i. Area

Calculations for the linear surface area of the corrugated barrel structure are documented in subsection 6.2.3.5. The area is 32.82 ft^2 per foot of cask length, or approximately 16 ft^2 per 6 inch wide node. Since there is no radial thermal gradient along a convolution, no effectiveness correction is required.

ii. Film Coefficients (h_c)

Heat transfer from the side nodes occurs by forced convection when the mechanical cooling system described in section 4.1 is operating.

The original forced convection heat transfer coefficient was based on a correlation developed in Reference 6.20. However, the results of thermal tests on cask 301 suggested that the calculated coefficient (7.63 Btu/hr-ft^2-°F) was too high.

iii. Equivalent Conductivity

To account for the test results described above, the THTD input for equivalent conductivity of the side nodes, under forced convection conditions, was reduced from 112 Btu/hr-ft^2-°F to 60 Btu/hr-ft^2-°F.

c. Equivalent Conductivity of Side Nodes - Natural Convection

i. Area

The area for natural convection is the same as for forced convection, i.e., 16 ft^2 per node.

ii. Film Coefficients

Heat transfer from the side nodes occurs by natural convection when the mechanical cooling system is not operating.

The following film coefficient correlation for natural convection from the side nodes is from Reference 6.4:

$$h_c = 0.18\ \Delta T^{1/3} \qquad (6.4)$$

where h_c = film coefficient, Btu/hr-ft^2-°F
ΔT = surface to ambient temperature differential

Film coefficients generated from equation 6.4 are listed in Table VI-4.

Table VI-4

FILM COEFFICIENTS AND EQUIVALENT CONDUCTIVITY ($A_e \times h_c$) OF SIDE NODES — NATURAL CONVECTION

E

Nodal Temperature	Film Coefficient	Equivalent Conductivity at Boundary II
130	0	0
150	0.488	7.8
200	0.742	11.9
250	0.888	14.2
300	0.997	16.0
500	1.292	20.7
1000	1.718	27.5

iii. Equivalent Conductivity

Equivalent conductivities for the side nodes under natural convection conditions are also listed in Table VI-4.

d. Radiation Boundary Properties

Under normal, 50% shielding water loss, and loss-of-mechanical cooling conditions the cask end is radiatively linked to its cradle and the sides "see" the skid and ducting as well as the ambient. Under fire and post-fire conditions the cask "sees" only the ambient. The ability to do multiple radiation linkages is an integral feature of THTD and only requires the proper entry in the appropriate tables.

Emissivities of extended surfaces were computed using the cavity radiator equation (see 6.2.3.6). Material emissivities were taken from References 6.6 and 6.25. The LOMC view-factors were computed using the crossed-strings method as described in Reference 6.17.

THTD can compute the overall radiative exchange factor by two methods, one using computed areas and the other using input geometric view-factors. Since the skid and ducting are not part of the model, the latter method was chosen. The code computes the exchange factor (F) as follows:

$$F = (\text{Geometric view-factor}) \cdot (\varepsilon_E) \cdot (\varepsilon_R \text{ or } \varepsilon_B)$$

where:

ε_E = Emitter emissivity
ε_R = Receptor emissivity
ε_B = Boundary emissivity

Table VI-5 summarizes the parameters which describe end and side radiation boundary conditions.

In order to handle certain situations such as the corrugated barrel, where the effective emissivity differs from the material emissivity and the radiative area differs from the modeled area, the dummy node material emissivities were set to unity and the values entered as geometric view factors were modified to include other terms of "F".

Table VI-5

EMISSIVITY PARAMETERS

Condition	Linkage	Emitter: Emissivity*	Emitter: Geometric View Factor	Receptor: Absorptivity	Receptor: Temperature (°F)
Normal, 50% SWL and LOMC	End-to-Ambient	0.84	1.0	1.0	130
	End-to-Cradle	0.84	1.0	0.3	130
	Side-to-Skid/Ducts	0.83	0.55	0.25	130
	Side-to-Ambient	0.83	0.45	1.0	130
Fire	Ambient-to-All	0.90 (1475°F)	1.0	0.8	-
Post-Fire	End-to-Ambient	0.84	1.0	1.0	130
	Side-to-Ambient	0.83	1.0	1.0	130

*Real or effective emissivity

e. Solar Heat Flux

When transported on its skid, the IF-300 cask is shielded from direct solar heat gain by its retractable enclosure. During hypothesized accident conditions, however, the cask is assumed to be separated from the skid and railcar so that a solar heat flux must be applied to the cask exterior surfaces. For the PFE analysis, a value of 61.5 Btu/hr-ft^2 is applied to boundaries 1-5 and 123 Btu/hr-ft^2 to boundaries 6-11 (Figure VI-1). Due to its insignificance in the 30-minute fire, no solar heat flux is applied in that analysis.

6.2.3.3 Internal Boundary Conditions

a. Internal Radiation

From Figure VI-1 it can be seen that there are two internal radiation boundary conditions. The first condition, labeled 12, is the radiation linkage from each outer shell node to the corrugated barrel node directly opposite it. This linkage is established under conditions where the neutron shielding annulus is void of water. The second condition labeled 13 is the radiation linkage from each fuel node to the inner shell node directly opposite it. This linkage is made under all dry cavity conditions.

It should be mentioned that the linkages described above represent a certain amount of conservatism because they couple only with the opposite node. Clearly there is radiative heat exchange between one emitter and several receptors. Due to program complexity, multiple internal linkages were not performed.

b. Exchange Factors

For BC 12 the following was used to compute the exchange factor:

$$F_{12} = \frac{VF}{\frac{1}{E_1} + \frac{A_1}{A_2}\left(\frac{1}{E_2} - 1\right)} \qquad (6.6)$$

For BC 13 the exchange factor was calculated using the following:

$$A_1F_{12} = \frac{1}{\frac{P_1}{A_1E_1} + \frac{1}{A_1} + \frac{P_2}{A_2E_2}}$$

Since $A_1 \approx A_2$ this becomes,

$$F_{12} = \frac{1}{\frac{P_1}{E_1} + 1 + \frac{P_2}{E_2}} \qquad (6.7)$$

Table VI-6 lists the radiation parameters for boundary conditions 12 and 13.

Table VI-6

RADIATION PARAMETERS

BC Number	Condition	Exchange Factor	View-factor	Emissivity E_1	Emissivity E_2
12	Post-Fire	0.545	1.0	0.6	0.83
13	Post-Fire	0.54	-	0.7	0.7

c. Insulated Boundary

The boundary labeled 14 is located at the "inside" of the model. This condition simply establishes the direction of heat transmission as radially outward and axial.

6.2.3.4 Internal Material Properties

a. Introduction

The cask model consists of the following materials: 317/216 stainless steel, depleted uranium, fuel, steam and water. Material properties of stainless steel and depleted uranium are shown in Table VI-7.

Fuel and water properties require modification to be used in the THTD model.

Table VI-7

STAINLESS STEEL AND DEPLETED URANIUM THERMAL CONDUCTIVITY

Material	100°F	300°F	500°F	800°F	1200°F
317/216 SST	7.6	8.5	9.5	10.8	12.6
Depleted Uranium	14.3	15.9	17.4	19.6	22.5

Note: Units are Btu/hr-ft-°F

b. Fuel Properties

As mentioned previously, the fuel region does not geometrically simulate the actual matrix. However, for the purposes of THTD the region was given a "lumped" set of thermal properties which is a reasonable representation of the fuel. The individual properties and the composite values are shown in Table VI-8.

Table VI-8

FUEL PROPERTIES

Component	Specific Heat (Btu/lb-°F)	Density (lb/ft^3)	Weight (lb)	Volume (in.^{3})
Stainless Steel	0.12	493	Not Individually Computed	
Zircaloy	0.075	409		
UO_2	0.070	650		
Weighted Average	0.085	430	7162	2.878×10^4

The conductivity of the fuel region was taken at 5.0 Btu/hr-ft-°F. This value is that of uranium dioxide at lower temperatures. Although meaningless for a homogenized fuel term in the radial direction, it does represent a good approximation of the fuel's axial conductivity.

c. Water Properties

There are two annuli in the model; one surrounding the fuel and the other on the cask exterior (see Figure VI-1). These annuli are 3.45 and 5.00 inches wide respectively. The water in the neutron shielding annulus transfers heat by natural circulation. It is, therefore, necessary to compute an equivalent conductivity which takes this circulation into consideration. Using a 4.5 inch wide annulus and equation 6.10 of subsection 6.2.3.9, a series of calculations were performed based on a range of expected water temperatures (150°F to 400°F). The results of these computations are shown in Table VI-9 as equivalent conductivity vs. water temperature. The detailed equivalent conductivity calculations are in subsection 6.2.3.9.

Table VI-9

WATER EQUIVALENT CONDUCTIVITY
(Neutron Shielding)

$\bar{T}$, Average Temperature (°F)	k_{Eq}, Equivalent Conductivity, (Btu/hr-ft-°F)
150	14.75
200	17.33
250	19.15
300	20.83
400	23.35

The small difference in annuli width has little effect on the value of equivalent conductivity.

d. Air Properties

For the empty neutron shielding annulus under fire and post-fire conditions, a value of 0.1 Btu/hr-ft°F is used as the conductivity. This represents the small amount of natural circulation that will occur.

For the air filled cask cavity, a temperature dependent set of conductivity entries was chosen to model the natural circulation occurring around the fuel bundles. These values are shown in Table VI-10.

Table VI-10

AIR EQUIVALENT CONDUCTIVITY
(Cask Cavity)

Temperature (°F)	Keg, Equivalent Conductivity (Btu/hr-ft-°F)
75	0.1504
500	0.2457
1000	0.3369
1500	0.4139
3500	0.7299

e. Internal Heat Generation - Fuel

The total heat generated by the model is 21,645 Btu/hr. This is the appropriate fraction of the total 40,000 Btu/hr which is contained in the lower 7 feet of the cavity. The volume of the fuel region (nodes 2080 through 3280) is 16.66 cu ft, yielding a volumetric heat generation rate of 1299 Btu/hr-ft^3. This value was used as THTD input. The linear heat generation rate is:

$$q_{lin.} = \frac{40,000}{12} \quad 3333 \text{ Btu/hr-ft}$$

6.2.3.5 Corrugated Area Computation

The corrugated structure was chosen as an extended surface due to its light weight, ruggedness and large area. Figure VI-2 shows a typical convolution.

Unlike fins, a corrugated surface needs no correction for efficiency. Since cooling medium backs each increment of extended surface, there is no temperature gradient along a corrugation in the radial direction.

Referring to Figure VI-2:

$$A_T = A_{\text{Convex Section}} + A_{\text{Concave Section}} + A_{\text{Straight Section}}$$

$$= \left\{2\pi r_1 R_1 \left[\theta_1\right]_0^{90^\circ} + 2\pi r_1^2 \left[-\cos\theta_1\right]_0^{90^\circ}\right\}$$

$$+ \left\{2\pi r_2 R_2 \left[\theta_2\right]_0^{90^\circ} - 2\pi r_2^2 \left[-\cos\theta_2\right]_0^{90^\circ}\right\}$$

$$+ \left\{\frac{\pi}{4}\left[D_1^2 - D_2^2\right]\right\} \qquad (6.8)$$

where:

r_1 = 0.6875 in.
R_1 = 31.25 in.
θ_1 = 1.57 rad
$-\cos\theta_1$ = 1
r_2 = 0.562 in.
R_2 = 30.6875 in.
θ_2 = 1.57 rad
$-\cos\theta_2$ = 1
D_1 = $2R_1$
D_2 = $D_1 + 2H$
H = 0.5625 in.

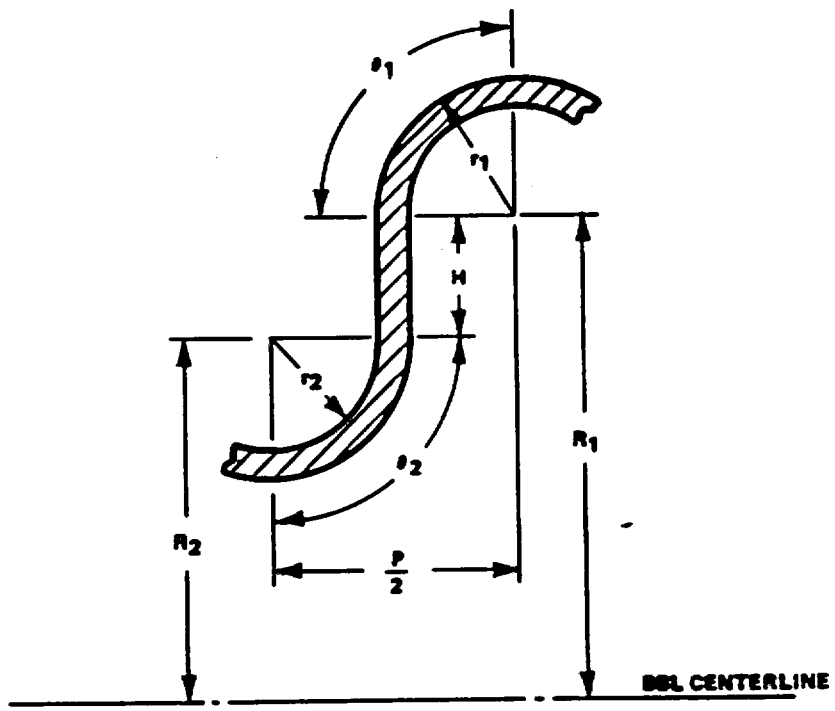

Figure VI-2. Corrugated Area

Solving:

$$A_T = (214.85 + 168.04 + 109.43)\ \text{in.}^2$$
$$= 492.32\ \text{in.}^2$$

and, Linear Area, A_2

$$A_L = \frac{A_T}{P/2}$$

$$= \frac{(492.32)}{(2.5/2)(12)} = 32.82\ \text{ft}^2/\text{ft of length}$$

6.2.3.6 Cavity Radiator Effect

Protrusions from or depressions in a surface have the effect of increasing the emissivity of the surface over that for just the material itself. This effective emissivity is computed using the following relationship from Reference 6.1:

$$\varepsilon_e = \left[1 + \frac{S}{S+2h}\left(\frac{1}{\varepsilon_r} - 1\right)\right]^{-1} \qquad (6.9)$$

where:

S = average face-to-face distance of corrugations (in.)

h = corrugation height (in.)

ε_r = material emissivity

6.2.3.7 Effective Emissivity - Ends

For the radial end fins, average values were used.

S = 3 in.

h = 6 in.

ε_r = 0.55 in.

Using equation 6.9:

$$\varepsilon_e = 0.84$$

6.2.3.8 Effective Emissivity - Side

For the corrugated containment, from Figure VI-2;

$$S = 2r_2 = 1.25 \text{ in.}$$
$$h = r_1 + H + r_2 = 1.1825 \text{ in.}$$
$$\varepsilon_r = 0.55$$

Using equation 6.9:

$$\varepsilon_e = 0.83$$

6.2.3.9 Water Equivalent Conductivity

The relation used for the thermal conductivity, k, of an intervening liquid medium is that developed by Liu, Mueller, and Landis (Reference 6.21). The relation assumes a naturally convecting media contained between walls in a concentric, annular space and is presented in the form of an effective conductivity. The relation is:

$$k = 0.135k_m \left(\frac{Pr^2Gr}{1.36+Pr}\right)^{0.278} \qquad (6.10)$$

where:

k = Effective thermal conductivity of medium (Btu/hr-ft-°F)

K_m = Actual thermal conductivity of medium (Btu/hr-ft-°F)

Pr = Prandtl number of medium

Gr = Grashof number of medium, based on annulus width

$$= \left(gB\frac{\rho^2}{\mu^2}\right)L^3\Delta T$$

g = Gravitational constant, ft/sec^2

B = Volume expansion coefficient, 1/°F

ρ = Density, lb/ft^3

μ = Viscosity, lb/sec-ft

L = Annulus width, ft

ΔT = Temperature differential across annulus, °F

A width of 4-1/2 inches was chosen as a reasonable representation of the annuli found in the IF-300 cask. Natural circulation systems such as this are quite insensitive to small changes in "L".

Figure 6 of reference 6.21 plots J vs. k_{eq}/k where:

$$J = \frac{(Pr^2 Gr_L)}{(1.36\ S + Pr)} \qquad (6.11)$$

k_{eq}/k = conductivity ratio

From reference 6.24, the water properties shown in Table VI-11 were extracted:

Table VI-11
WATER PROPERTIES

Average Temperature (°F)	Pr	$gB\frac{\rho^2}{\mu^2}$	K	$Gr_L \cdot \Delta T$	$J \cdot \Delta T$
150	2.74	0.44×10^9	0.364	$2.32 \times 10^7 \Delta T$	$4.24 \times 10^7 \Delta T$
200	1.88	1.11×10^9	0.384	$5.86 \times 10^7 \Delta T$	$6.39 \times 10^7 \Delta T$
250	1.45	2.14×10^9	0.394	$11.30 \times 10^7 \Delta T$	$8.44 \times 10^7 \Delta T$
300	1.18	4.00×10^9	0.396	$21.10 \times 10^7 \Delta T$	$11.6 \times 10^7 \Delta T$
350	1.02	6.24×10^9	0.395	$32.90 \times 10^7 \Delta T$	$14.4 \times 10^7 \Delta T$
400	0.93	8.95×10^9	0.391	$47.20 \times 10^7 \Delta T$	$17.8 \times 10^7 \Delta T$

From the initial calculations it is known that the temperature differential across an annulus under these thermal conditions is between 10°F and 40°F (10°F < ΔT < 40°F). Thus, for each average temperature in Table VI-11 four ΔT values were chosen and the equivalent conductivities calculated. The average of the four values was then taken as the water conductivity for the particular temperature. As an example, Table VI-12 is the conductivity calculation for an average temperature of 150°F.

Table VI-12

150°F WATER CONDUCTIVITY

$\bar{T}$	ΔT	J	log J	log (k_{eq}/k)	(k_{eq}/k)	k_{eq}
150	10	4.24×10^8	8.627	1 1.51	32.4	11.8
150	20	8.48×10^8	8.928	1.59	38.9	14.2
150	30	12.7×10^8	9.104	1.64	43.7	15.9
150	40	17.0×10^8	9.230	1.67	46.8	17.1
						4 | 59.0

$\bar{k}_{eq}$ = 14.75

The equivalent conductivities for all of the average water temperatures are shown in Table VI-9 of subsection 6.2.3.4. These values were used in the THTD property tables for water-filled annuli.

6.3 THTD RESULTS - DESIGN BASIS CONDITIONS

6.3.1 Normal Cooling

The configuration referred to as "normal cooling" consists of the cask mounted on the skid in its normal (horizontal) position with one of the two blowers of the mechanical cooling system directing 10,000 CFM air flow at the cask surface. It should be noted that use of this cooling system is optional.

The inner cavity of the cask is air-filled and the neutron shielding cavity is water-filled. Heat dissipation is by convection and radiation from the fuel to the cavity walls, conduction through the cask body, convection across the neutron shielding containment, and a combination of convection and radiation from the cask exterior to the environment and the skid.

The THTD computed cask temperatures and corresponding pressures for normal cooling at a heat load of 40,000 BTU/hr are shown in Table VI-13. The maximum fuel rod temperature for normal cooling

conditions is 508°F, based on a maximum inner cavity surface temperature of 173°F.

Table VI-13

CASK TEMPERATURES AND PRESSURES - Normal Cooling

Parameter		
Ambient Air Temperature, °F		130
Internal Heat Load, Btu/hr		40,000
Maximum Barrel Surface Temperature, °F		155
Maximum Outer Shell Temperature, °F		163
Maximum Inner Cavity Surface Temperature, °F		173
Maximum Fuel Cladding Temperature, °F		
Gp. I	7x7 BWR	492
	15x15 PWR	503
Gp. II	8x8 BWR	498
	17x17 PWR	508
Inner Cavity Pressure, psig		14

N

6.3.2 Loss-of-Mechanical Cooling (LOMC)

LOMC is essentially the same as normal cooling, discussed in 6.3.1, with the exception that the mechanical cooling system is no longer in operation. Since use of the mechanical cooling system is optional, the tital of this condition is something of a carryover from earlier work.

Elimination of the effects of the mechanical cooling system requires that natural convection coefficients replace the forced convection coefficients along the corrugated barrel.

The results of this change are reflected in the increased temperatures and pressures shown in Table VI-14. The maximum fuel rod temperature for LOMC conditions is 554°F, based on a maximum inner cavity surface temperature of 229°F.

Table VI-14

CASK TEMPERATURES AND PRESSURES - LOMC

Parameter		
Ambient Air Temperature, °F		130
Internal Heat Load, Btu/hr		40,000
Maximum Barrel Surface Temperature, °F		213
Maximum Outer Shell Temperature, °F		219
Maximum Inner Cavity Surface Temperature, °F		229
Maximum Fuel Cladding Temperature, °F		
GP. I	7x7 BWR	537
	15x15 PWR	549
Gp. II	8x8 BWR	544
	17x17 PWR	555
Inner Cavity Pressure, psig		29

N

6.3.3 50% Shielding Water Loss (50% SWL)

The neutron shielding cavity encircling the cask body is partitioned at mid-length, forming two separate structures. Each cavity has its own vent, fill, and relief capability and has been pressure tested at 200 psig. In addition, they are each protected by a pressure relief valve set at 200 psig.

In Section V the possibility of neutron shielding containment puncture is discussed. The conclusion reached is that the loss of water from one of the two containments is possible but of a low probability. None-the-less, the effect on the cask temperature distribution of a 50% loss of shielding water has been analyzed.

The 50% SWL analysis uses the normal cooling model discussed in 6.3.1, with the exception that nodes 2608 through 3208 and nodes 2606 through 3206 are assumed to have the thermal properties of air rather than water. This assumption simulates a loss of 54% of the shielding water from the center (hottest part) of the cask, thus conservatively modeling a 50% loss of shielding water from one end.

Temperatures and pressures resulting from the above described simulation are shown in Table VI-15. The maximum fuel rod temperature for 50% SWL conditions is 607°F, based on a maximum inner cavity surface temperature of 292°F.

Table VI-15
CASK TEMPERATURES AND PRESSURES - 50% SWL

Parameter		
Ambient Air Temperature, °F		130
Internal Heat Load, Btu/hr		40,000
Maximum Barrel Surface Temperature, °F		173
Maximum Outer Shell Temperature, °F		284
Maximum Inner Cavity Surface Temperature, °F		292
Maximum Fuel Cladding Temperature, °F		
Gp. I	7x7 BWR	587
	15x15 PWR	601
Gp. II	8x8 BWR	595
	17x17 PWR	607
Inner Cavity Pressure, psig		70

6.3.4 30 Minute Fire

This analysis was performed to comply with regulatory requirements that the cask be designed to withstand a 30 minute exposure to a 1475°F radiation environment having an emissivity of 0.9, assuming that the cask has an absorption coefficient of 0.8.

The cask is separated from the skid and cooling system for this evaluation. The corrugated barrel surrounding the neutron shielding cavity is assumed to be in place but ruptured due to the 30-ft drop. The cask cavity remains sealed due to the integrity of the closure, valves, and ruptive disk (See Section V). It is assumed that the initial temperature distribution within the cask at the start of the fire is that shown in Table VI-14 for LOMC.

Table VI-16 and Figure VI-3 summarize the input conditions and transient results of this analysis. An examination of the transient

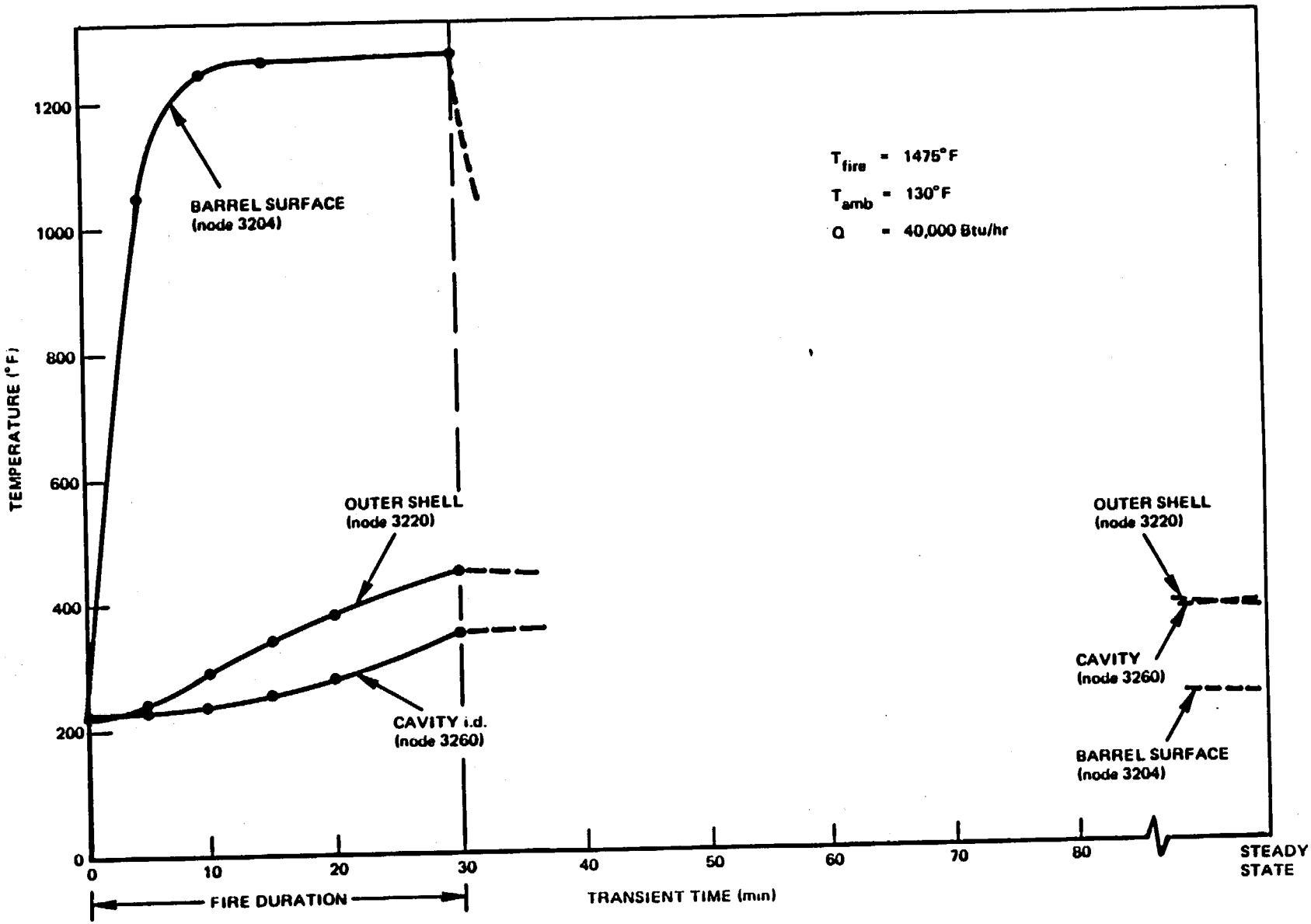

Figure VI-3. Fire Transient and Cooldown

Table VI-16

CASK TEMPERATURES AND PRESSURES - End of 30 Minute Fire

Parameter		
Ambient Air Temperature, °F		1475
Internal Heat Load, Btu/hr		40,000
Maximum Barrel Surface Temperature, °F		1274
Maximum Outer Shell Temperature, °F		452
Maximum Inner Cavity Surface Temperature, °F		353
Maximum Fuel Cladding Temperature, °F		
Gp. I	7x7 BWR	635
	15x15 BWR	651
Gp. II	8x8BWR	643
	17x17BWR	658
Inner Cavity Pressure, psig		152

curves for the various shells (Figure VI-3) shows that the air-filled neutron shielding containment structure acts as a radiation barrier, thus limiting the heat input to the cask body from the fire. At the end of the fire the maximum fuel rod temperature is 658°F, based on a maximum inner cavity surface temperature of 353°F.

6.3.5 Post-Fire Equilibrium (PFE)

The most limiting thermal conditions experienced by the cask internals are in the period following the 30-minute fire. The limiting nature of this analysis is due to the corrugated barrel of the empty neutron shielding containment. This structure, which acted as a barrier to external radiation during the fire, now acts as an insulator to internal heat dissipation.

Heat transfer from the cask to the 130°F ambient environment is by natural convection and radiation. Heat is transferred across the empty neutron shielding containment by radiation and a small amount of natural convection. Conduction is the mechanism for heat

transmission through the solid body components. Due to the insulating effect of the external containment there is more axial heat flow through the uranium and steel than in the other cases examined.

Temperatures of the various shells at equilibrium conditions are shown in Figure VI-3 and Table VI-17.

A maximum fuel rod temperature of 677°F results from the maximum cavity wall temperature of 377°F at equilibrium conditions. This fuel rod temperature is well below the 1000°F plus temperatures at which cladding failure by creep rupture would be predicted from Figure VI-4.

Cavity wall temperatures along the cavity length, and at PFE conditions, are shown in Figure VI-5.

Table VI-17

CASK TEMPERATURES AND PRESSURES - PFE

Parameter		
Ambient Air Temperature, °F		130
Internal Heat Load, Btu/hr		40,000
Maximum Barrel Surface Temperature, °F		228
Maximum Outer Shell Temperature, °F		369
Maximum Inner Cavity Surface Temperature, °F		377
Maximum Fuel Cladding Temperature, °F		
Gp. I	7x7 BWR	654
	15x15 PWR	670
Gp. II	8x8 BWR	662
	17x17 PWR	677
Inner Cavity Pressure, psig		267*

* Assumes 100% fission gas release

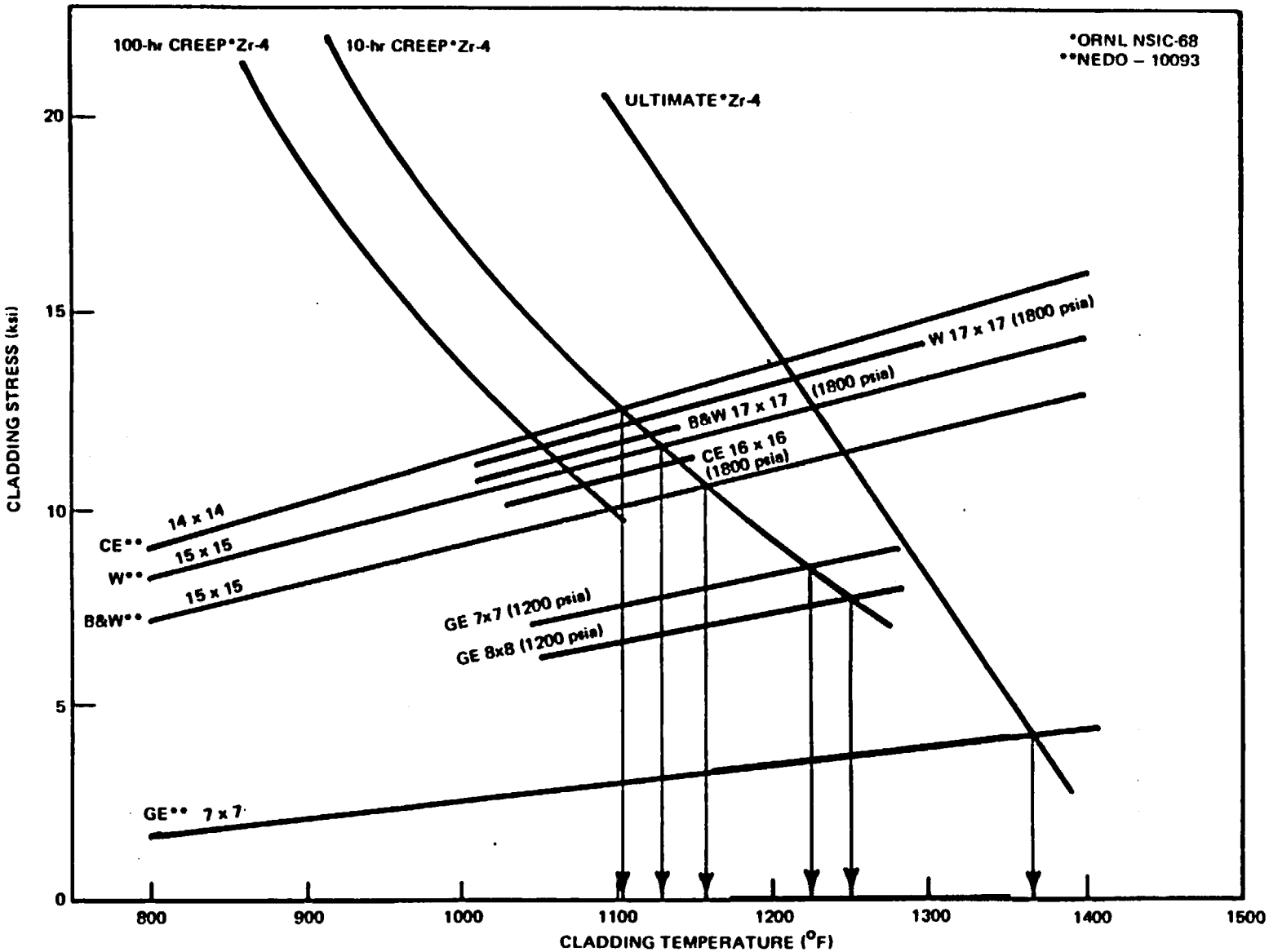

Figure VI-4. Zircaloy Cladding Perforation Temperatures

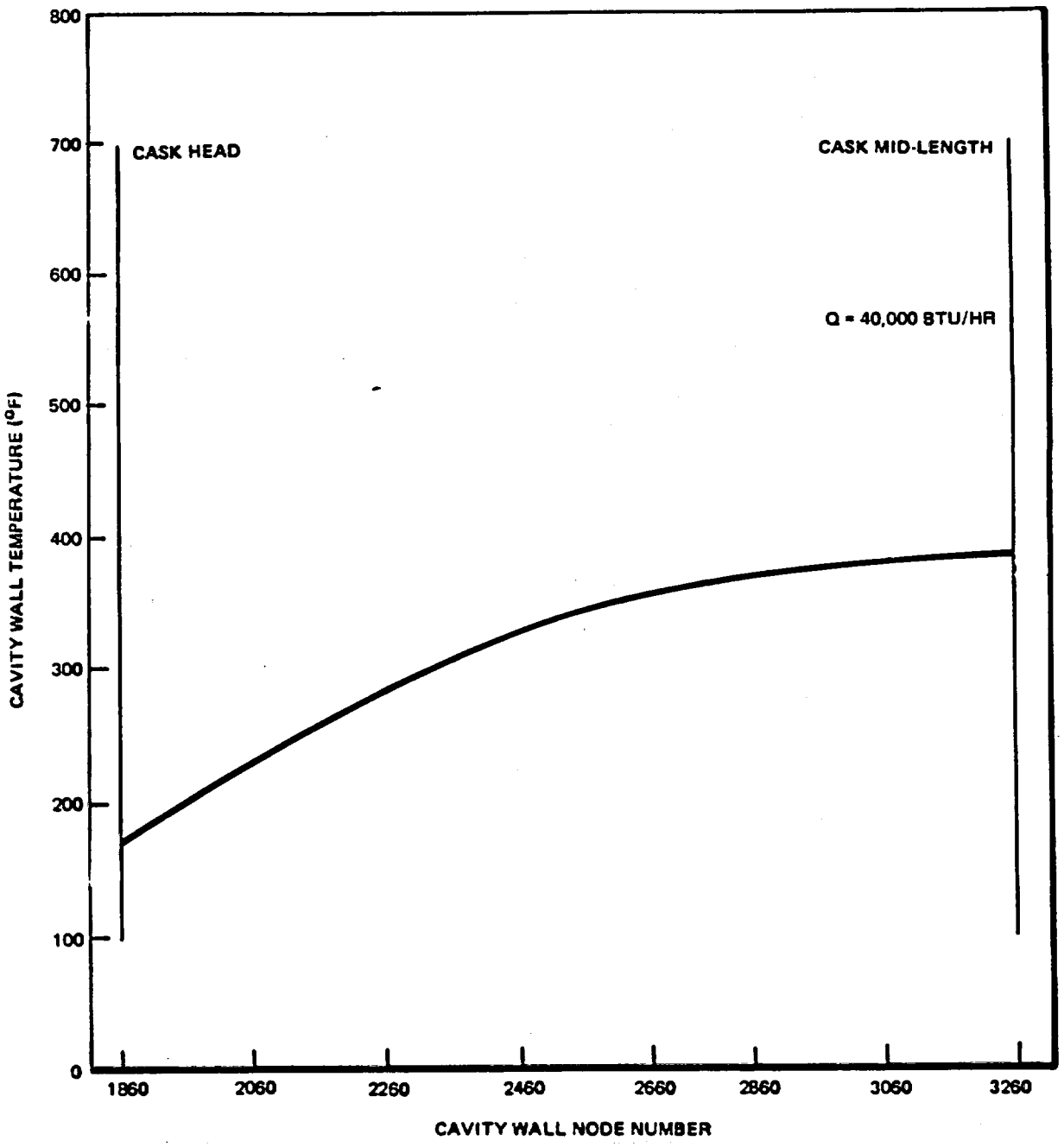

Figure VI-5. THTD Results - Dry Cavity Temperature Profile for PFE Conditions

6.4 FUEL CLADDING TEMPERATURES

This section presents analyses for fuels licensed prior to 1991. See Volume 3, Appendices A and B for fuels licensed since 1991.

6.4.1 Wooton-Epstein Correlation

Since there has been no work done in testing a configuration similar to the IF-300 cask, the work of Wooton and Epstein (Ref. 6.23) has been selected as the best available basis for predicting fuel rod temperatures in a "dry" If-300 cask. As a benchmark, this method was applied to the experimental work of Watson (Ref. 6.10) and succeeded in predicting hottest rod cladding temperature within 1% of the measured value.

The analytical approach of Wooton and Epstein is based primarily on radiation, with a convective term added to reflect heat removal from the fuel bundle exterior. The radiation term is derived by assuming that the bundle consists of a series of concentric surfaces where the area ratio between any two such surfaces is approximately one. This ratio makes the radiative exchange factor (F) between any two surfaces only emissivity dependent.

This correlation relates the cask cavity wall temperature to the hottest rod cladding temperature for any given heat load and fuel bundle configuration.

$$Q = \sigma C_1 F_1 A_1 (T_E^4 - T_C^4) + C_2 A_1 (T_E - T_C)^{4/3} \qquad (6.12)$$

where:

$$C_1 = \frac{4N}{(N + 1)^2} (N \text{ odd})$$

or:

$$C_1 = \frac{4}{N + 2} \quad (N \text{ even})$$

and:

N = number of rod rows in bundle

F_1 = exchange factor

$$= \left(\frac{1}{\varepsilon E} + \frac{1}{\varepsilon C} - 1\right)^{-1}$$

A_1 = bundle surface area

= 4HL

H = height of one side of bundle (ft)

L = length of bundle (ft)

T_E = hottest rod cladding temperature (°R)

T_C = cavity wall temperature (°R)

C_2 = convection constant

= 0.118 (air)

Q = decay heat rate (Btu/hr)

ε = material emissivity

δ = Stefan - Boltzmann Constant

It is assumed that the above equation can be applied to both BWR and PWR fuel rod arrays within the IF-300 cask by modeling each with a square, NxN, uniformly spaced array having approximately the same number of fuel rods, the same heat load, and the same perimeter. The BWR & PWR fuel bundle arrays are shown in Figure VI-6.

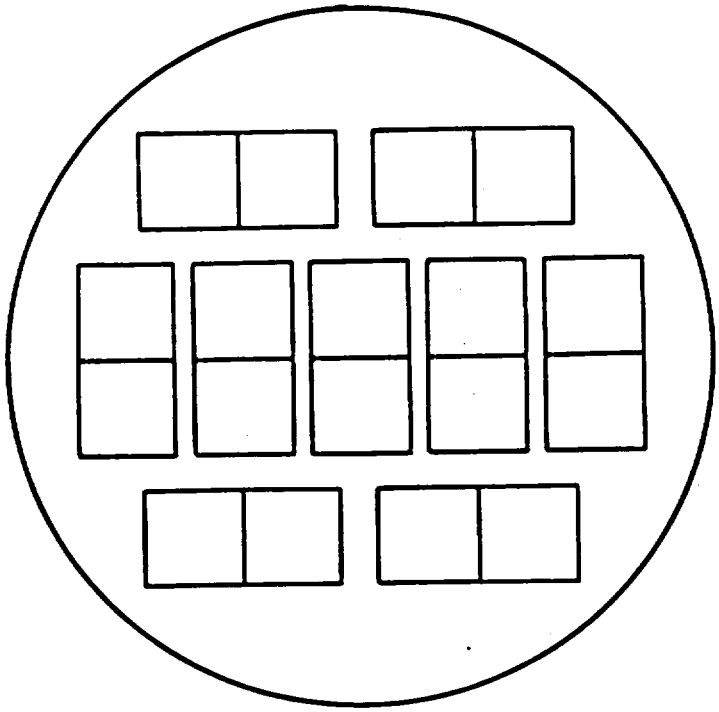

(a)

18-CELL BWR CONFIGURATION*

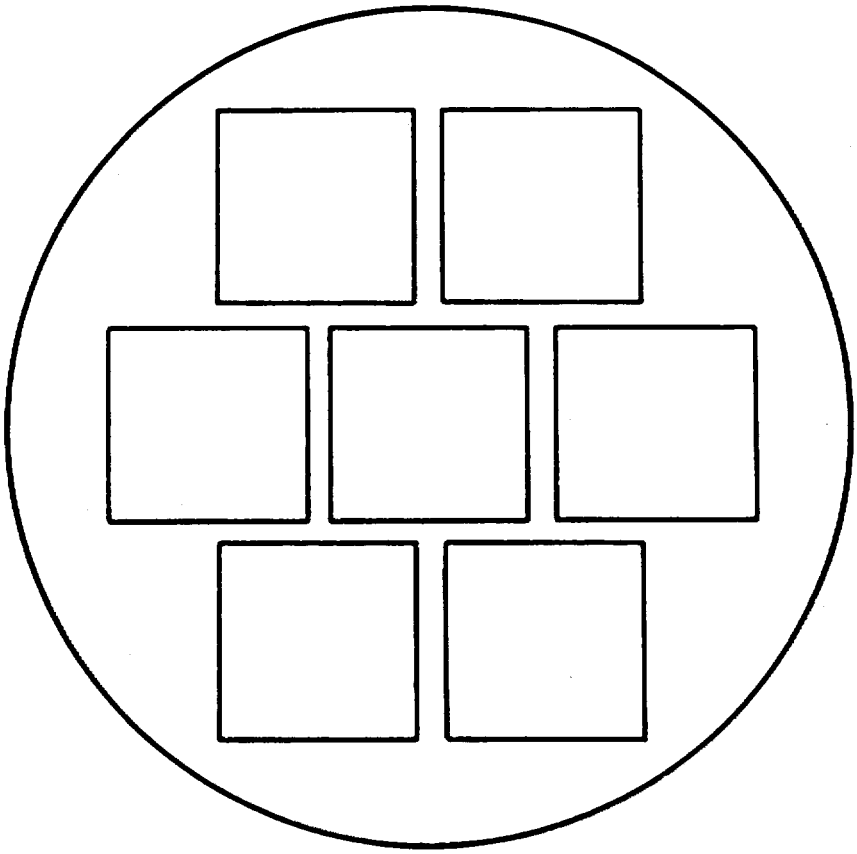

(b)

7-CELL PWR CONFIGURATION*

Figure VI-6. Fuel Basket Configurations

* See Volume 3, Appendix A for 17-Cell Channelled BWR Fuel Basket

There are several features of this analytical method which make it conservative:

a. The Wooton-Epstein correlation is inherently conservative in that it is based on the assumption of concentric surfaces. In a fuel rod bundle radiation occurs through the spaces between rods thus reducing the effective number of rows. The actual test results conducted at BMI demonstrated that the correlation consistently overpredicted the hottest rod cladding temperature.

b. The cavity wall temperatures used in the analysis are maximums. Use of average cavity wall temperatures would result in lower fuel rod temperature predictions.

6.4.2 Analysis

6.4.2.1 Example Problem - PFE

As previously noted, both BWR and PWR configuration are analyzed using a direct application of the W-E equation. Table VI-18 shows the input parameters for PFE conditions for BWR 8x8 fuel and PWR 17x17 fuel.

Table VI-18

WOOTEN-EPSTEIN CORRELATION INPUT PARAMETERS - PFE

Parameter	BWR-8x8	PWR-17x17
C_1	0.111	0.085
N	34	45
H, ft	2.50	2.53
Q, Btu/hr	40,000	40,000
L, ft	12	12
C_2	0.118	0.118
T_c, °F	377	377
F_1	.539	.539
ε	0.7	0.7

The number of rod rows (N) is taken as the square root of the total number of fuel rods in the cask. The height (H) of the assumed array is taken as the perimeter around the fuel bundle array divided by four.

The resultant temperatures for the hottest fuel rod of each array are as follows:

	BWR	PWR
T_e =	662°F	677°F

This example demonstrates that everything else being equal, arrays with fewer fuel rods have lower rod temperatures due to the relationship between C_1 and T_E in equation 6.12.

6.4.2.2 Fuel Rod Temperatures vs. Ambient Temperatures

Combining the WEC computer code input/output with the thermal test results of cask #301, yields a plot of ambient air temperature vs. maximum fuel cladding temperature for a series of heat loads with and without the cooling system in operation. These relationships are shown as Figures VI-7 and VI-8 for the BWR and PWR Group I fuel rods, respectively.

6.4.2.3 Fuel Rod Temperatures vs. Heat Load

By cross-plotting the data from Figures VI-7 and VI-8, the relationship between heat load and maximum fuel cladding temperature can be obtained for any given ambient temperature. Figures VI-9 and VI-10 show heat load vs. maximum fuel cladding temperature for ambient temperatures of +130°F and -40°F, with and without the cooling system in operation, for Group I fuel rods.

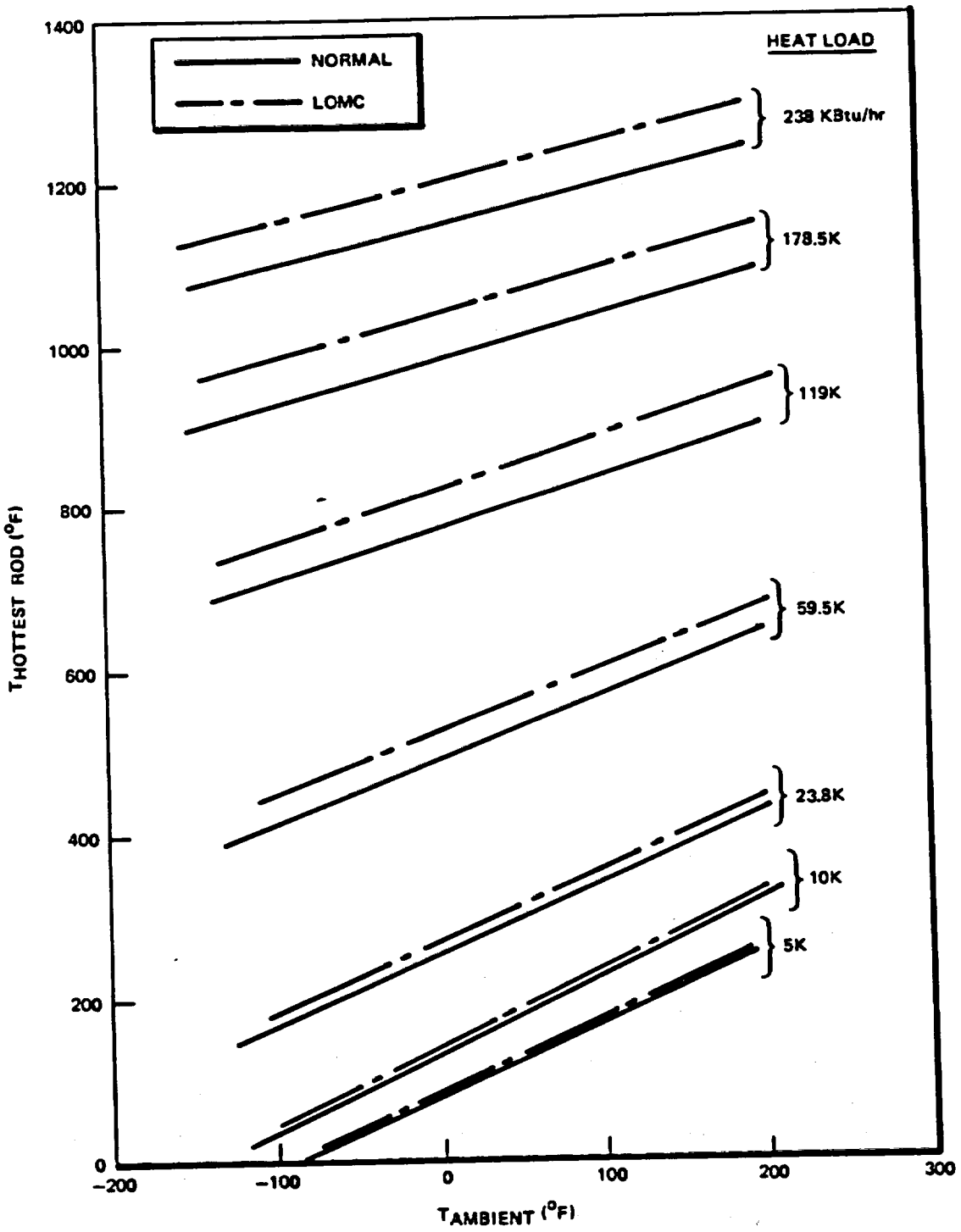

Figure VI-7. IF300 Cask - Hottest Fuel Rod Vs. Ambient Temperature for BWR Configuration with Dry Cavity and Group I Fuel

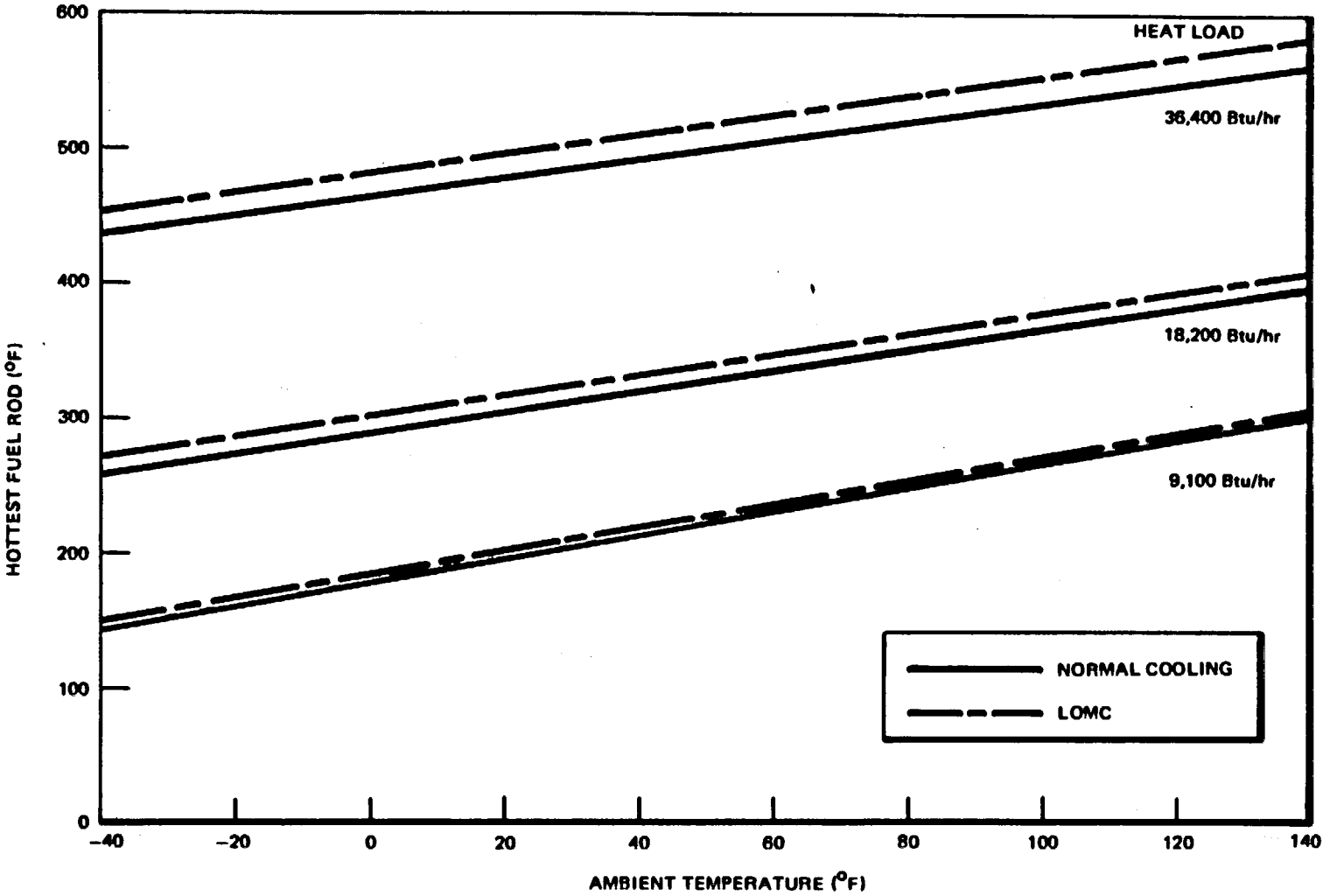

Figure VI-8. IF300 Cask - Hottest Fuel Rod Vs. Ambient Temperature for PWR Configuration With Dry Cavity and Group I Fuel

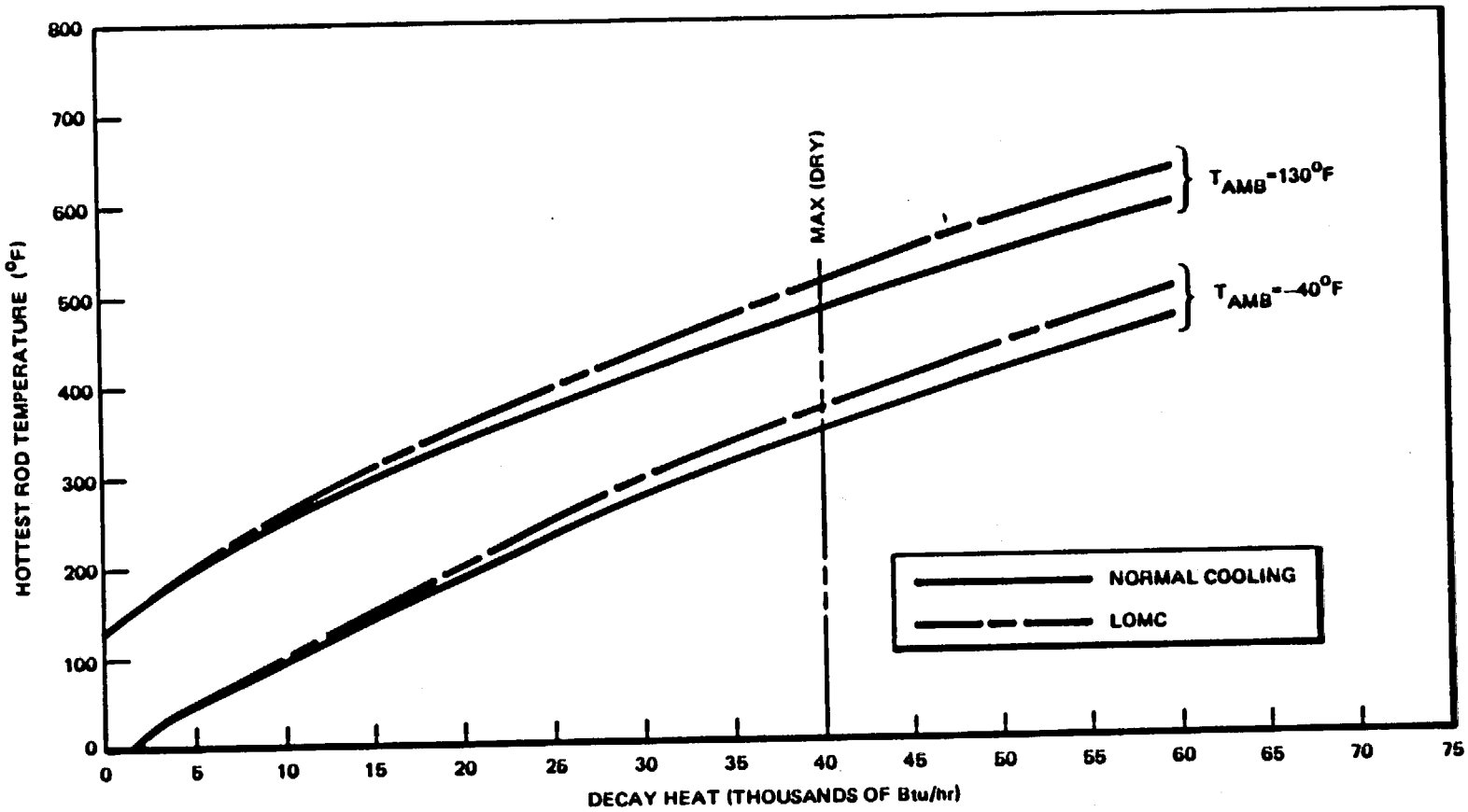

Figure VI-9. IF300 Cask - Hottest Rod Vs. Decay Heat for BWR Configuration With Dry Cavity and Group I Fuel

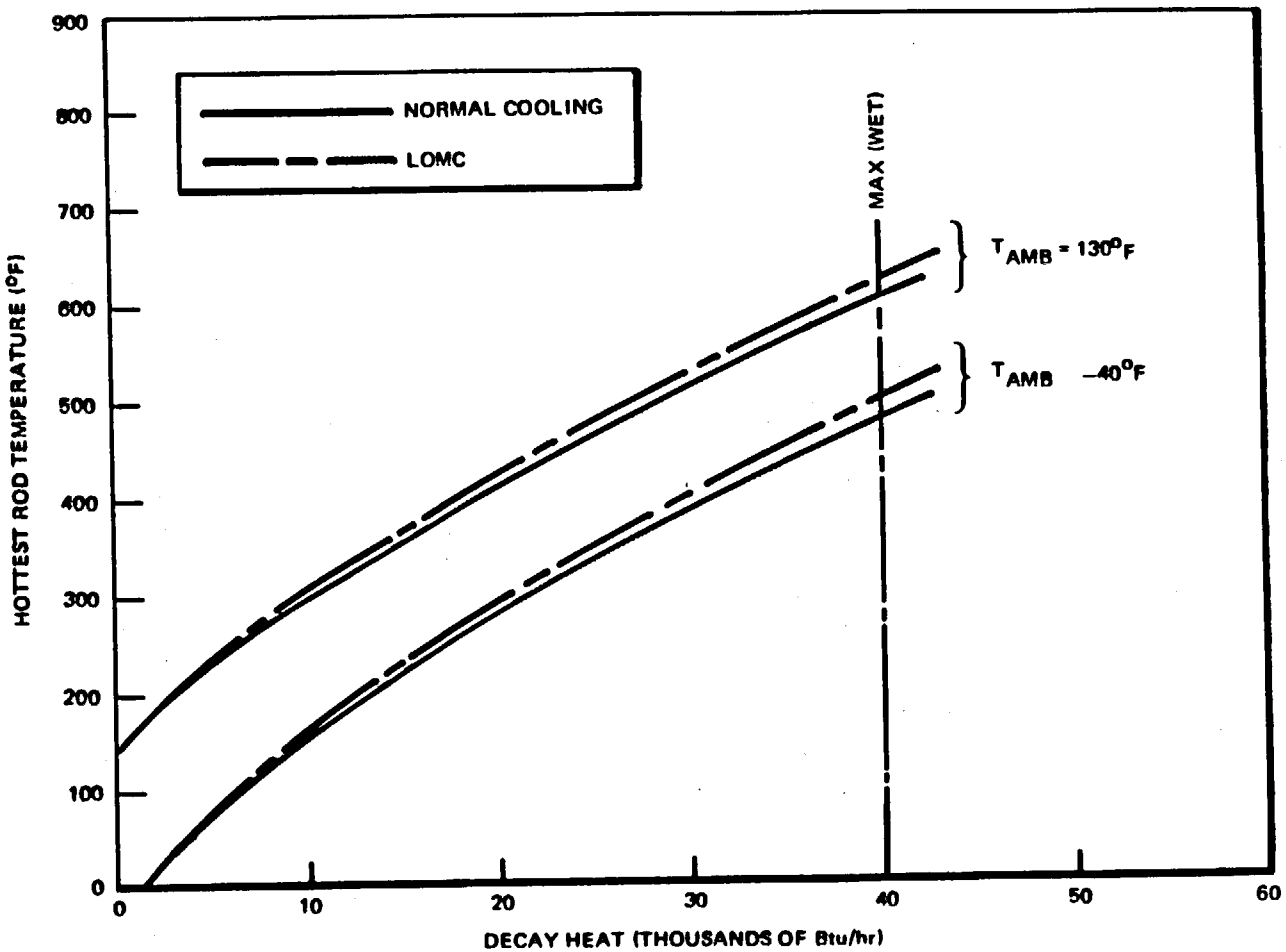

Figure VI-10. IF300 Cask - Hottest Rod Vs. Decay Heat for PWR Configuration with Dry Cavity and Group I Fuel

6.5 MISCELLANEOUS THERMAL CONSIDERATIONS

6.5.1 Cask Operation at -40°F

Operation of an air-filled cask at -40°F would result in fuel cladding temperatures which are significantly reduced from those occurring at 130°F. This is shown graphically on Figures VI-7 through VI-10.

To prevent freezing of the neutron shielding water, an antifreeze solution of ethylene glycol, or equivalent, is added to form a 50/50 volume percent mixture.

6.5.2 Effects of Antifreeze on Cask Heat Transfer

The thermal testing of cask #302 included a determination of the cask's heat dissipation capabilities with only water in the neutron shield and then with the 50/50 antifreeze mixture in place. Table VI-19 compares inner cavity bulk water temperatures at 196,500 BTU/hr.

Table VI-19

CASK SHIELDING TANK LIQUID

	302 w/antifreeze	302 w/water
Bulk water Temp, F (T_{amb} = 130°F)	428	412

The use of ethylene glycol and water in place of only water in the shielding tank resulted in a 4% increase in cavity bulk water temperature. This is considered negligible for the lower temperatures associated with dry shipments at 40,000 Btu/hr.

6.5.3 Thermal Expansion of Neutron Shielding Liquid

6.5.3.1 Discussion:

There are two neutron shielding cavities which contain a mixture of ethylene glycol and water when in service. Each cavity is equipped with a surge tank assembly mounted directly above it as shown in Figure VI-11. The purpose of this surge tank is to permit the filling of the barrels to provide maximum neutron shielding while maintaining a void space for water expansion during heat up. Two different surge tank assembly volumes are required due to the volume differences between the upper and lower neutron shielding cavities.

6.5.3.2 Required Tank Volumes

a. Upper Barrel Section.

Barrel free volume = 33.69 ft^3

Assume: (1) the barrel is filled at 70°F
(2) the max. normal water temp. is 250°F
(3) the max. normal BBL pressure is 100 psig

Expansion of water 70°F to 250°F

$$\Delta V = \frac{v_f \text{ @ } 250}{v_f \text{ @ } 70} \left(V_B\right) - V_B$$

$$= \frac{0.01700}{0.01606} (33.69) - 33.69$$

$$= 1.97 \text{ ft}^3$$

$$P_2 = P_1 \frac{V_1}{V_2} \frac{T_2}{T_1}$$

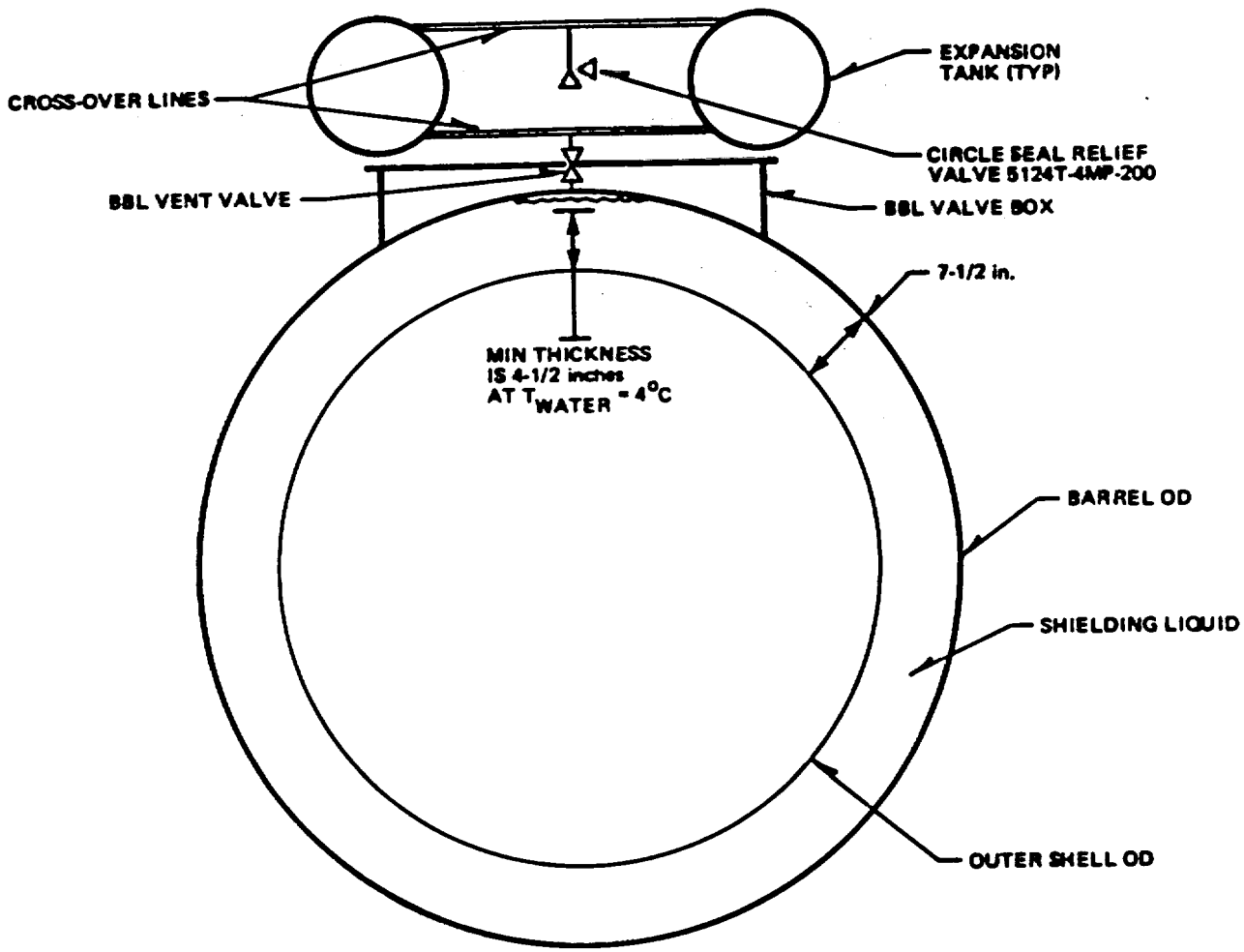

Figure VI-11. Shield Barrel Surge Tank

Solving for surge tank volume, V_T

$$114.7 = 14.7 \frac{V_T}{V_T - 1.97} \left(\frac{710}{530}\right)$$

$V_T = 2.38\ ft^3$ required tank volume

Water Contraction:

The Δ density from 70°F to 40°F (water's max. density) is quite small. At 40°F the water level in the barrel will drop a fraction of an inch. Since the full barrel provides from 5-1/8 to 7-1/8 inches of water shielding whereas only 4-1/2 inches is required, the slight decrease in level under cold conditions has no effect.

b. Lower Barrel Section

Following the method of the upper barrel section:

Barrel free volume - $46.34\ ft^3$

$$\Delta V = \frac{0.01700}{0.01606} (46.34) - 46.34 \qquad 70°F \text{ to } 250°F$$

$$= 2.71\ ft^3$$

then:

$$114.7 = 14.7 \left(\frac{710}{530}\right) \frac{V_T}{V_T - 2.71}$$

$V_T = \underline{3.27\ ft^3}$ required tank volume.

6.5.3.3 c. Actual Expansion Volumes

The neutron shielding barrel expansion volume consists of space within the barrel and in the expansion tank system. The in-barrel space is represented by the uppermost corrugation sections that do not fill with liquid when the cask is horizontal. This space is additive to that provided by the externally mounted expansion tanks. Table VI-20 compares the required expansion space to the actual expansion space.

Table VI-20
EXPANSION VOLUMES

BBL Section	Tank Req'd, ft^3	Tank Actual, ft^3	Tank Actual Plus Corrugations, ft^3
Upper	2.38	2.32	2.82
Lower	3.27	2.73	3.23

Thermal tests on the casks demonstrate that the neutron shielding liquid expansion void is sufficient to prevent barrel venting under 210,000 Btu/hr, LOMC conditions. The relief pressure setting for the shielding tanks is 200 psig.

6.5.4 Effects of Residual Water on Inner Cavity Pressure

The design of the IF300 cask inner cavity does not permit complete draining; a small volume of water remains. The presence of this residual water and the temperature of the cavity wall and contents act to pressurize the cavity under certain circumstances. The following analysis examines the effects of this residual water on cask cavity pressure.

6.5.4.1 Amount of water remaining in cavity

The cavity can be drained down to the 1-in. drain pipe diameter. A depth of 1.182 in. of water remains in the cask when it is vertical. Cask basket components displace some of this water and the net residual water for each of the two basket types is as follows:

Fuel Basket	Water Vol., ft^3	Water Wt., lb
BWR	0.605	37.8
PWR	0.420	26.2

When the cask is horizontal, this water will form a segment with the cylindrical cask cavity. This segment will have a maximum depth of 0.8 inches and a chord length of 11.0 inches. It covers a maximum of 9.3% of the total cavity wall area.

6.5.4.2 Cavity free volume

The empty cavity volumes, PWR and BWR, are based on nominal cavity lengths and diameter. The head spacer volume was calculated based on actual dimensions. The basket volumes were computed based on the actual weights of the fabricated units. Since they are stainless steel of known density, the volume is easily obtained. The fuel bundle volume is also obtained by dividing the weights of the various components by their respective densities. The net free volume is the cavity empty volume less the cavity components. Table VI-21 summarizes the computations.

6.5.4.3 Cask cavity pressure - LOMC conditions

The cask cavity pressure under LOMC conditions is the summation of (a) the cask air pressure, and (b) the residual water vapor pressure.

Table VI-21

CAVITY VOLUMES

Item	BWR	PWR
Cavity length, ft	15.02	14.125
Cavity dia., ft	3.125	3.125
Empty volume, ft^3	115.2	108.3
Total bundle vol, ft^3	21.4 (18)	17.0 (7)
Fuel spacer vol, ft^3	0.65	0.53
Basket vol, ft^3	11.0 (5675#)	9.01 (4520#)
Total contents vol, ft^3	33.05	26.54
Net free vol, ft^3	82.15	81.76

a. Air pressure - The cavity air pressure is assumed to follow the ideal gas-temperature-pressure relationship. For this calculation, it is conservatively assumed that the air temperature is midway between the maximum fuel cladding temperature of 555°F and the maximum cavity wall temperature of 229°F for LOMC conditions and 17 x 17 PWR fuel as tabulated in Table VI-14. Then the air pressure is given by

$$P_{air} = P_1 \frac{T_2}{T_1} = \frac{14.7 \times (392+460)}{(460+70)} = 23.6 \text{ psia}$$

b. Water vapor pressure - The residual water vapor pressure is determined by the cask cavity wall temperature. For this evaluation, it is conservatively assumed that the water temperature is at the maximum LOMC cavity wall temperature of 229°F. Then the water vapor pressure is found in the steam tables to be E

$$P_{vapor} = 20.4 \text{ psia}$$

c. Total pressure - The total pressure in the cask is the sum of the partial pressures or

$$P_{total} = P_{air} + P_{vapor}$$

$$= 23.6 + 20.4 = 44.0 \text{ psia}$$

$$= 29.4 \text{ psig}$$

For LOMC conditions, the cask maximum cavity pressure of 29.4 psig is quite low in comparison to 350 psig, the minimum relief pressure.

6.5.4.4 Cask cavity pressure - PFE conditions

The cask cavity pressure is calculated by the same methods used for LOMC conditions, except that it is conservatively assumed that all of the fuel rods release their fission gas into the cask cavity.

a. Air pressure - It is conservatively assumed that the air temperature is midway between the maximum fuel cladding temperature of 677°F and the maximum cavity wall temperature of 377°F, as tabulated in Table VI-17. Then the air pressure is given by

$$P_{air} = P_1 \frac{T_2}{T_1} = \frac{14.7 \times (527 + 460)}{(460+70)} = 27.4 \text{ psia}$$

b. Water vapor pressure - It is conservatively assumed that all of the water is at the middle of the cask and has the maximum cavity surface temperature of 377°F (PFE conditions). Then the water vapor pressure from the steam tables is

$$P_{vapor} = 189 \text{ psia}$$

c. Fuel rod residual gas pressure - In the dry shipping mode ($\leq$ 40,000 Btu/hr), it is expected that no fuel rods will rupture. If in the extreme case it is assumed that all of the fuel rods rupture, then the residual gases in the fuel rods will increase the cavity pressure.

The number of moles, n, of residual gas that could be released into the cask cavity is estimated by

$$n = \frac{P_r V_g}{RT_r} = \frac{2500 \times 1.5}{10.73 \times (900+460)} = 0.257 \sim 0.26 \text{ moles}$$

where,

P_r = 2500 psia, end-of-life rod pressure

T_r = 900°F rod gas temperature at reactor conditions

V_G = 1.5 ft^3 total gas volume in all rods available for release

To allow for new fuel designs, a value of 0.5 lb moles residual gas is used below. It is assumed that the temperature of the residual gas released is the same as that used for the cavity air (see above). Then the maximum residual gas pressure is

$$P_{gas} = \frac{nRT}{V_c} = \frac{0.50 \times 10.73 \times (527 + 460)}{81.76} = 64.8 \text{ psia}$$

d. Total gas pressure - The total pressure in the cask cavity is the sum of the partial pressures, or

$$P_{total} = P_{air} + P_{vapor} + P_{gas}$$
$$= 27.4 + 189 + 64.8 = 281.2 \text{ psia}$$
$$= 266.5 \text{ psig}$$

Thus for PFE, the most limiting accident condition, the maximum cask cavity pressure still remains significantly below the minimum relief pressure of 350 psig.

6.5.4.5 Conclusions

The preceding calculations show that at a maximum "dry" shipping heat load of 40,000 Btu/hr and LOMC conditions, the cask inner cavity pressure will not exceed 30 psig. Under PFE conditions the cask inner cavity pressure will not exceed 267 psig. The minimum inner cavity relief pressure is 350 psig, which is substantially higher; hence, the cask will not relieve any contents under either of these conditions.

6.5.5 Emissivity Sensitivity

Under accident conditions, the decay heat is transferred by radiation and convection across the void created by the assumed loss of neutron shielding water. In order to determine the sensitivity of cask temperatures to changes in the emissivity of the cask outer shell, an additional THTD case was run using an emissivity of 0.4 for the outer shell. The input conditions and steady state results of this case are tabulated in Table VI-22 as they compare to the basic case results for the 17 x 17 PWR case.

It is concluded that a relatively large change in emissivity produces a much smaller change in the calculated fuel rod temperatures and a comparable change in cask cavity pressure.

6.6 PRESSURE RELIEF DEVICES AND FILL, DRAIN, AND VENT VALVES

6.6.1 Rupture Disk Device

6.6.1.1 Description

For dry shipments of spent fuel the maximum allowable heat load is 40,000 Btu/hr. As conservatively calculated in 6.5.4.4, the maximum inner cavity pressure generated under accident conditions for dry shipments is 267 psig. The design pressure of the IF-300 cask is 400 psig. Since the maximum inner cavity pressure generated

Table VI-22

EMISSIVITY COMPARISON FOR PFE CONDITIONS
17 x 17 PWR FUEL

(Heat Load = 40,000 Btu/hr)

Item	Case I	Case II	Δ%
Emissivity, ε	0.6	0.4	-33.3
Ambient Air Temp, °F	130	130	0
Internal Heat Load, Btu/hr	40,000	40,000	0
Maximum Barrel Surface Temp, °F	228	226	0.9
Maximum Outer Shell Temp, °F	369	402	8.9
Maximum Inner Cavity Surface Temp, °F	377	410	8.8
Maximum Fuel Cladding Temp, °F	677	704	4.0
Cavity pressure, psig	267	357	33.7

under accident conditions is well below the cask design pressure the cask will not vent and a cavity relief valve is not needed for overpressure protection. Instead, a properly rated rupture disk device may be used to seal the cask cavity from the environment for dry shipments.

The rupture disk device is installed per the manufacturer's instructions. A typical rupture disk device installation is shown in Figure VI-12. The rupture disk holder is a Black, Silvas and Bryson (BS&B) unit, part number (F) FA7R or equivalent, rated at 600-lb. The holder is designed and fabricated from Type-304 stainless steel by processes and procedures which comply with the ASME code, Section III. The holder is provided with a 1/8 in. NPT gage tap and stainless steel pipe plug on the downstream side for special testing or monitoring needs.

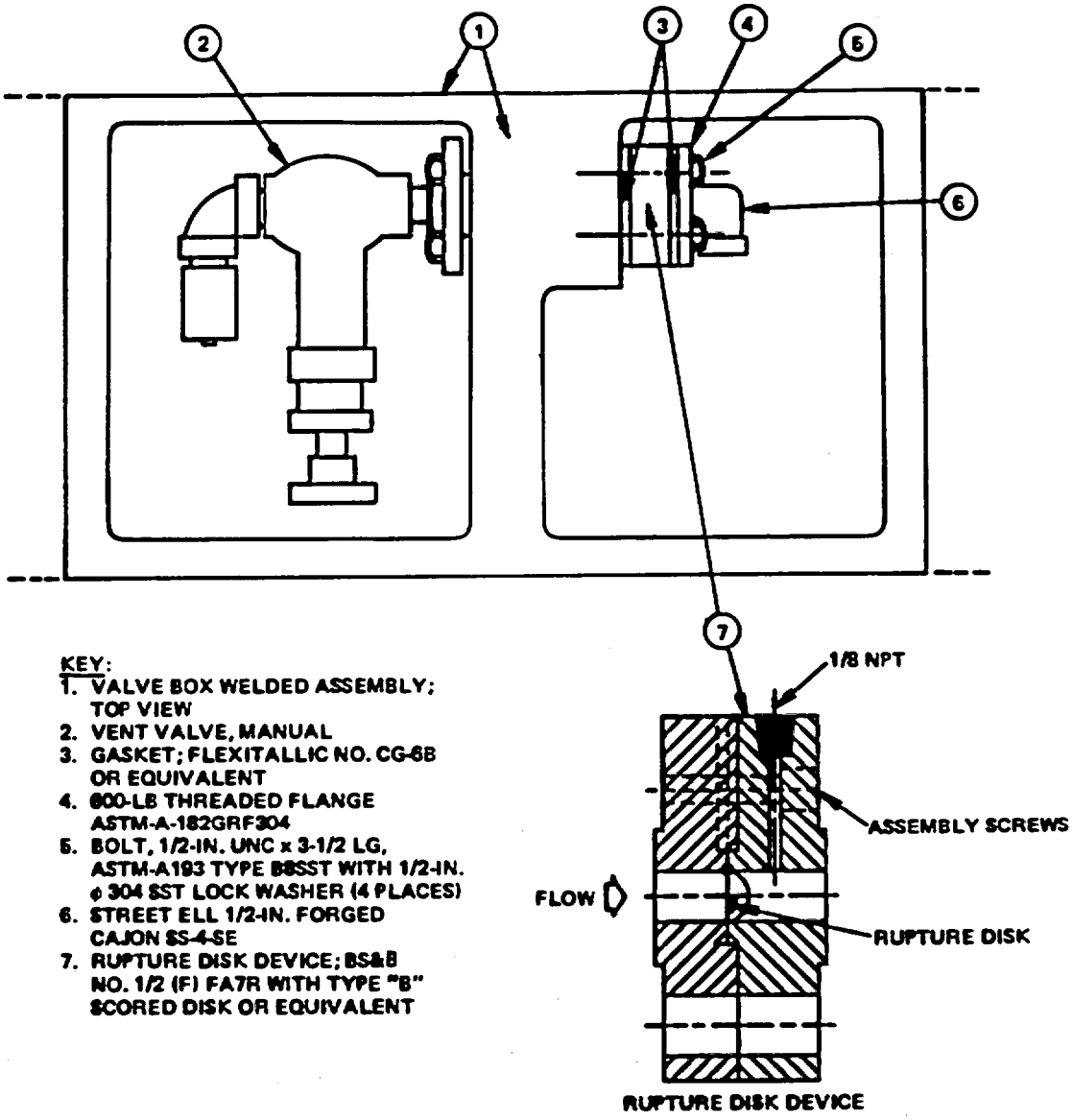

Figure VI-12. Burst Disk Device Installation

The rupture disk is a BS&B type "B" scored disk or equivalent made from nickel material and marked per ASME code Section VIII, Division I requirements. The stamped bursting pressure of each lot of rupture disks is between 350 and 400 psig at 443°F including all manufacturing and burst tolerances and is established by testing per the ASME code Section VIII, Division I. A 304 stainless steel street ell is installed downstream of the rupture disk device to protect the rupture disk from accidental puncture.

6.6.1.2 Periodic Replacement

See Section 10.2 N

6.6.2 200 psig Pressure Relief Valve

6.6.2.1 Description

This valve is used to provide over-pressure protection to the neutron shielding barrel and expansion tanks. One such unit is on each of the two segments of the shielding barrel. The currently qualified valve is a Circle Seal relief valve #5124T-4MP-200. A typical valve was tested to check cracking and reseating pressures, and reliability.

The valve is a simple spring-loaded poppet unit with a soft seat. The silicon seat material is good for temperatures to 500°F (maximum barrel water temperature is 216°F at LOMC conditions). The unit is rated for air, steam, and liquid.

6.6.2.2 Qualification Testing

The qualification test set-up was simply a pressure pump and gauge. The valve inlet pressure was raised and the cracking and reseat points observed. The valve opened at 210 psig (room temperature) and reseated at 190 psig. The unit was cycled 50 times to demonstrate repeatability and reliability. It functioned as specified by the manufacturer. A notarized copy of the test certification is shown in Figure VI-13.

Any substitute unit for the Circle Seal 5124T-4MP-200 will have to undergo the following qualification tests:

a. Cracking and reseating pressure verification

b. Reliability cycling 50 times.

6.6.2.3 Periodic Testing

These neutron shielding pressure relief valves will be tested for functioning and pressure setting on an annual basis. Testing will be done at room temperature, removed from the cask.

6.6.3 1-Inch Globe Valve

6.6.3.1 Description

This valve is used for draining, filling and venting of the cask inner cavity and, optionally, the neutron shielding cavities. The N

S.O. B-53734
Rt. 561

Stearns-Roger
INCORPORATED

700 SOUTH ASH
GLENDALE, COLORADO

DATE August 6, 1973

STEARNS-ROGER ORDER NO. C-10210 SHOP ORDER NO. 51775

CUSTOMER'S NAME General Electric ADDRESS San Jose, California

NAME OF VESSEL Circle Seal Relief Valve (5100 Series)

H.S.B. NO. None SERIAL NO. M37-6, S/N 1

X-RAY None STRESS RELIEVE None

DIAMETER N/A THICKNESS N/A LENGTH N/A

TYPE OF CONSTRUCTION Stainless Steel C.R.N.

WORKING PRESSURE 200 PSIG DESIGN PRESSURE 3700 PSIG

TEMPERATURE None °F. FINAL HYDROSTATIC TEST PRESSURE N/A PSIG

REMARKS: Hydro Test Relief Valve to relieve pressure, after valve relieves pressure lower pressure from pump unit to allow valve to automatically close itself, again raise pressure to make valve relieve pressure. *

THIS IS TO CERTIFY THAT THE ABOVE PRESSURE VESSEL WAS TESTED AND INSPECTED ON July 27, 1973, AND FOUND SATISFACTORY BY E. J. Weil INSPECTOR AT GENERAL IRON WORKS COMPANY.

SIGNED E. J. Weil
INSPECTOR

P. C. Valyunsk
Q. C. Representative
General Electric

Subscribed and sworn to before me on this 6 day of August

Jerome Nockels
NOTARY PUBLIC

My Commission expires May. 11, 1974

*Circle Seal Relief Valve was cycled 50 times.
Relief Valve was set for 210 p.s.i.g., reseated at 190 p.s.i.g.
Circle Seal Valve Serial Number 5124T-4MP-200.

Figure VI-13. Circle Seal Relief Valve (5100 Series)

Inner cavity is serviced by two such valves, one in each cavity valve box. Each half of the neutron shielding annulus may be serviced by such a valve (or a blind flange) housed in its respective valve box. N

Figure VI-14 shows the type of globe valve used on the IF-300 cask cavity (and shielding barrel). This stainless steel unit is manufactured by Precision Products and Controls, Inc. ("PRECON").

6.6.3.2 Qualification Testing

The valve was hydrostatically tested at a pressure of 600 psig by the manufacturer. This test was conducted with water at room temperature.

A typical PRECON valve was tested by Stearns-Roger under accident conditions. The valve was placed in an oven and raised to 500°F. Nitrogen gas at a pressure of 400 psig was introduced to the valve inlet. The valve discharge was routed to a water tank where any leakage bubbles could be visually detected. The inlet pressure was monitored by a calibrated gauge.

The valve was held for 50 hours at 500°F, 400 psig. No signs of leakage were observed. Fluctuations in nitrogen pressure occurred due to changes in ambient temperature. The test data sheet and a notarized test certificate are shown as Figures VI-15 through VI-17.

The 48-hour valve test is quite reasonable for this type of unit. The valve is all stainless steel; there are no organic components which might degrade in a short time span. The stem is sealed with a stainless steel bellows.

FIGURE WITHHELD UNDER 10 CFR 2.390

Figure VI-14. Globe Valve (1-Inch)

[illegible]	S.O. 51775	[illegible] C-10210	VALVE TEST	[illegible]	[illegible]		
[illegible]	ROUTE [illegible] 5/0						
DATE	TIME	INSPECTOR	FURNACE TEMP. °F	GAS PRESSURE (MUST BE 40")	BUBBLE TEST	COMMENTS	
8/10/73	3:00PM	[illegible]	500°	410	[illegible]	[illegible]	7/6/73
8/11/73	3:15	[illegible]	500°	410	[illegible]		
8/11/73	3:30	[illegible]	500°	410	[illegible] – 2 min		
8/11/73	3:45	[illegible]	500°	410	[illegible] – 2 min		
8/11/73	4:00	[illegible]	500°	410	[illegible] – 2 min		
8/11/73	4:15	[illegible]	500°	410	2 every 5 min		
8/11/73	4:30	[illegible]	500°	410	1 every 5 min		
8/11/73	4:45	[illegible]	500°	410	1 every 5 min		
8/11/73	5:00	[illegible]	500°	410	0 – 5 min		
8/11/73	5:30	[illegible]	500°	410	0 – 5 min		
8/11/73	6:00	[illegible]	500°	410	0 – 5 min		
8/11/73	6:30	[illegible]	500°	410	0 – 5 min		
8/11/73	7:00	[illegible]	500°	410	0 – 5 min		
8/11/73	8:00	[illegible]	500°	410	0 – 5 min		
8/11/73	9:00	[illegible]	500°	410	0 – 5 min		
8/11/73	10:00	[illegible]	500°	410	0 – 5 min		
8/11/73	11:00	[illegible]	500°	410	0 – 5 min		
8/11/73	12:00	[illegible]	500°	410	0 – 5 min		
8/12/73	1:00	[illegible]	500°	410	0 – 5 min		
8/12/73	2:00	[illegible]	500°	410	0 – 5 min		
8/12/73	3:00	[illegible]	500°	409	0 – 5 min		
8/12/73	4:00	[illegible]	500°	408	0 – 5 min		
8/12/73	5:00	[illegible]	500°	408	0 – 5 min		
8/12/73	6:00	[illegible]	500°	408	0 – 5 min		
8/12/73	7:00	[illegible]	500°	405	0 – 5 min		
8/12/73	8:00	[illegible]	500°	401	0 – 5 min		
8/12/73	9:00	[illegible]	500°	401	0 – 5 min		
8/12/73	10:00	[illegible]	500°	400	0 – 5 min		
8/12/73	11:00	[illegible]	500°	402	0 – 5 min		
8/12/73	12:00	[illegible]	500°	400	0 – 5 min		
8/12/73	1:00	[illegible]	500°	400	0 – 5 min		
8/12/73	2:00	[illegible]	500°	400	0 – 5 min		
8/12/73	3:00	[illegible]	500°	400	0 – 5 min		
8/12/73	4:00	[illegible]	500°	400	0 – 5 min		
8/12/73	5:00	[illegible]	500°	400	0 – 5 min		

Figure VI-15. Valve Test

[illegible] IRON WORKS	51775	C-10210	VALVE TEST	M43-43

DATE	TIME	INSPECTOR	FURNACE TEMP. °F	GAS PRESSURE (INCHES H2O)	BUBBLE TEST	COMMENTS
8/3/73	1:00	A.Z.	500°	400	0-5 min	
8/3/73	2:00	A.Z.	500°	405	0-5 min	
8/3/73	3:00	A.Z.	500°	405	0-5 min	
8/3/73	4:00	A.Z.	500°	405	0-5 min	
8/3/73	10:00	A.Z.	500°	405	0-5 min	
8/3/73	11:00	A.Z.	500°	405	0-5 min	
8/3/73	12:00	A.Z.	500°	405	0-5 min	
8/3/73	1:00	A.Z.	500°	405	0-5 min	
8/3/73	2:00	A.Z.	500°	405	0-5 min	
8/3/73	3:00	A.Z.	500°	405	0-5 min	
8/3/73	4:00	A.Z.	500°	405	0-5 min	
8-3-73	5:00	A.Z.	500°	410	0-5 min	
8-3-73	6:00	A.Z.	500°	410	0-5 min	
8-3-73	7:00	A.Z.	500°	410	0-5 min	
8-3-73	8:00	A.Z.	500°	410	0-5 min	
8/3/73	8:00	G.J.K.	500°	410	0-5 min	
8/3/73	9:00	G.J.K.	500°	410	0-5 min	
8/3/73	10:00	G.J.K.	500°	410	0-5 min	
8/3/73	11:00	G.J.K.	500°	410	0-5 min	
8/3/73	12:00	G.J.K.	500°	410	0-5 min	
8/3/73	1:00	G.J.K.	500°	410	0-5 min	
8/3/73	2:00	G.J.K.	500°	410	0-5 min	
8/3/73	3:00	G.J.K.	500°	410	0-5 min	
8/3/73	4:00	G.J.K.	500°	410	0-5 min	
8/3/73	5:00	G.J.K.	500°	410	0-5 min	

Figure VI-16. Valve Test

S.O.B53734
Rt. 590

Stearns-Roger
INCORPORATED
700 SOUTH ASH
GLENDALE, COLORADO

DATE August 3, 1973

STEARNS-ROGER ORDER NO. C-10210 SHOP ORDER NO. 51775

CUSTOMER'S NAME General Electric ADDRESS

NAME OF VESSEL Globe Valve Assembly

H.S.B. NO. None SERIAL NO. M43-43 S/N 2

X-RAY None STRESS RELIEVE None

DIAMETER N/A THICKNESS N/A LENGTH N/A

TYPE OF CONSTRUCTION Stainless Steel C.R.N.

WORKING PRESSURE 400 PSIG DESIGN PRESSURE 400 PSIG

TEMPERATURE 500 °F. FINAL ~~HYDROSTATIC~~ Pressure TEST PRESSURE 400 PSIG

REMARKS: * Test started @ 1500 hours on August 1, 1973, & completed @ 1700 hours on August 3, 1973. Furnace charts & pressure log are maintained in G.I.W. files.

THIS IS TO CERTIFY THAT THE ABOVE PRESSURE VESSEL WAS TESTED AND INSPECTED ON August 3, 1973, AND FOUND SATISFACTORY BY E. J. Weil

INSPECTOR AT GENERAL IRON WORKS COMPANY.

Signed [illegible] 8-3-73
Witness

SIGNED George J. Kunrade
INSPECTOR

Subscribed and sworn to before me on this 3 day of August

Jerome Nochis
NOTARY PUBLIC

My Commission expires Mar. 11, 1974

* Test to consist of using Nitrogen Gas at 400 P.S.I. into cask side of valve with valve closed in furnace #474 with temp. @ 500° F. & held for a minimum of 48 hours w/Insp. check on temp., pressure & bubble test for leak thru of valve each 15 min. of first 2 hours, each half hour of second 2 hours, & each hour thereafter.

Figure VI-17. Globe Valve Assembly

Any substitute unit for the PRECON valve will have to undergo the following qualification test without leakage:

a. 600 psi hydrostatic test @ room temperature.

b. Gas leakage test at 400 psi, 400°F for 48 hours.

6.6.3.3 Periodic Testing

See Section 10.2 N

6.7 CONFIRMATION OF CASK THERMAL PERFORMANCE

6.7.1 Thermal Test Description

Following fabrication, each IF 300 shipping package is subjected to a series of tests designed to verify the analytical thermal analysis. The cask is equipped with electrical heaters to simulate fuel elements and instrumented with thermocouples to give an accurate measurement of temperature distribution. The test series includes normal cooling and loss of mechanical cooling. Only the LOMC test is required for thermal performance verification, the other tests are for operational information.

The following is a general description and discussion of the thermal demonstration testing performed on IF301 through 304. Also included is the thermal acceptance criteria and its basis.

6.7.2 Equipment and Test Facilities

The following basic equipment and instrumentation was used for the thermal capability tests.

6.7.2.1 Immersible tubular heater units each capable of continuously generating 37,500 Btu/hr, uniformly over a twelve-foot length. These units must be sized such that they can be inserted in a square channel having an inside dimension of 8.75 inches. Seven of these units were required to yield the original cask maximum heat load of 210,000 Btu/hr. The center rod of each heater unit will have two sheath thermocouples.

6.7.2.2 Compensated multipoint recording equipment capable of continuously monitoring 40 thermocouple channels as listed below:

a. A set of three thermocouples mounted circumferentially on the cask surface, on a plane equidistant from the ends of the heater active zone. As viewed from the end of the cask, one thermocouple would be mounted in the nine o'clock position and the other two at 45 degrees aboge and below that position. (See Figure VI-18.)

b. A set of three thermocouples installed on or near the cask cavity wall adjacent to the thermocouples on the external surface.

c. A set of three thermocouples mounted on the exterior of the fuel basket adjacent to the cavity wall thermocouples.

d. One thermocouple penetrating the outer jacket, designed to record the bulk water temperature. This may be contained in a well.

e. A second series of thermocouples mounted similar to a. through d. above, in a plane five feet below (toward the cask bottom) the midplane thermocouple set.

f. One thermocouple or thermometer which records the test area ambient temperature.

g. Suitable equipment for monitoring and controlling the heaters over their operating range (0-100%).

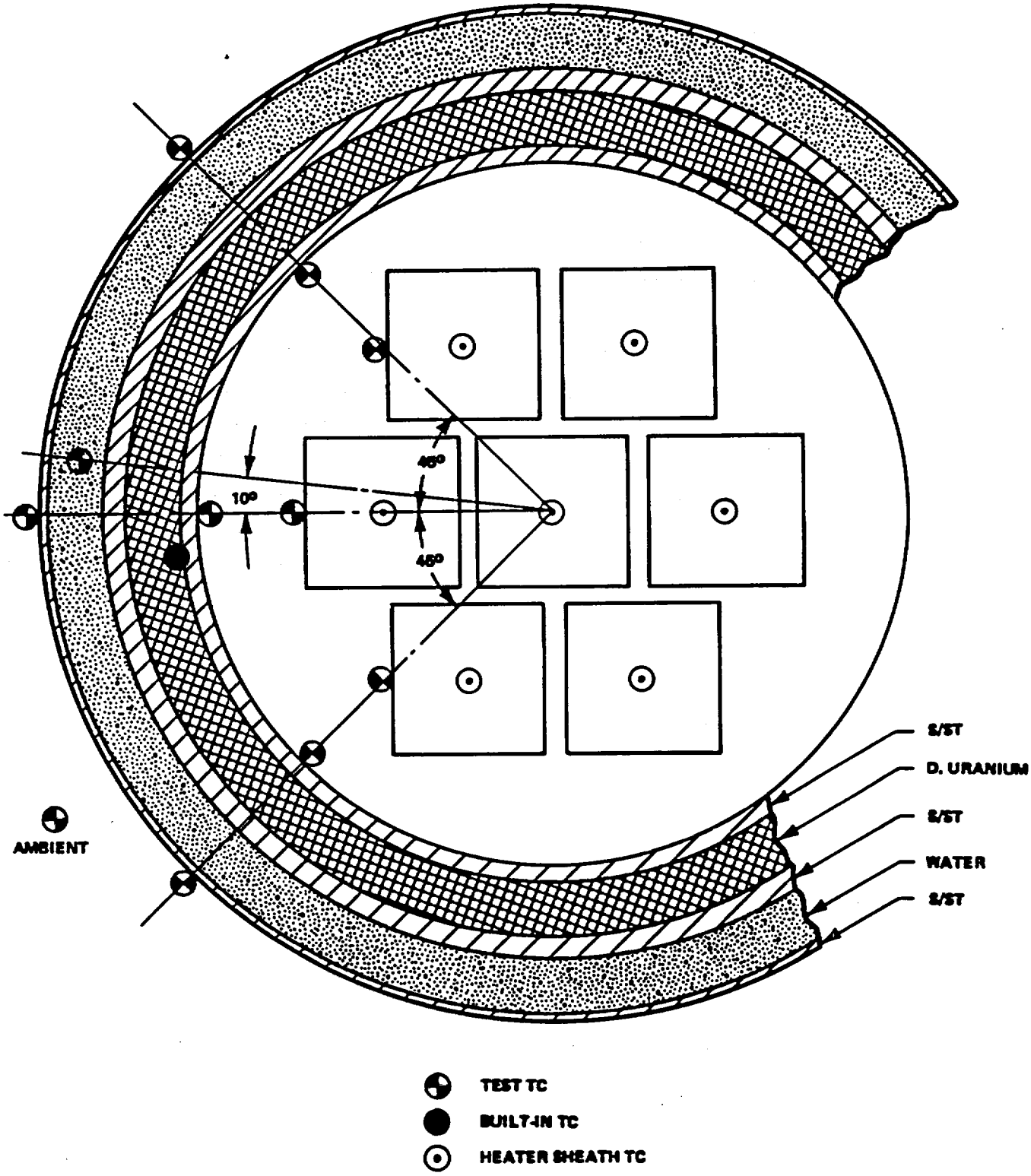

Figure VI-18. Thermocouple Locations

h. One thermocouple at the fuel basket bottom and one thermocouple on the cask surface on the bottom head.

i. One contact pyrometer for surface temperature measurements.

j. An enclosed test area where the effects of ambient temperature variation and air movement can be minimized.

6.7.3 Test Preparation

a. Thermocouples shall be positioned where indicated above.

b. The seven-element basket shall be installed in the cask and the heater units inserted and centered in their appropriate channels. A spacer collar or a modified head will be required for electrical and thermocouple penetrations to the cavity.

c. All components of the electrical and instrumentation system shall be connected and checked for continuity and operability. All thermocouples and instrumentation shall be calibrated.

d. All thermal testing shall be conducted with a General Electric Company appointed representative present. All test procedures shall be in writing and shall be approved by General Electric Company.

6.7.4 Testing

The thermal acceptance criteria applies to the IF 300 cask only under loss-of-mechanical cooling conditions. However for information purposes the thermal testing usually encompasses normal cooling as well as LOMC. Data points are gathered at a number of heat loads in order to fully characterize the thermal capability of the cask. Other thermal-related tests may be conducted.

The collected data forms the basis for establishing the maximum heat load for the cask being tested. It is also used to eatablish base-line temperatures for the periodic evaluation of cask thermal capability.

6.7.5 Thermal Test Report

The following is a summary report of the thermal testing of IF 300 casks serial numbers 301 through 304. This is presented because it establishes the basis for the thermal acceptance criteria.

6.7.5.1 Introduction

To date, General Electric has constructed and tested four model IF-300 Irradiated Fuel Shipping Casks. The thermal demonstration test for the first cask, cask 301, was conducted and a document entitled IF-300 Shipping Cask Demonstration Testing Report* was contained as Appendix B4A-1 to the August 13, 1973 submittal to Docket 70-1220 (now 71-9001). Thermal demonstration tests have also been conducted for casks 302, 303 and 304. Data reduction efforts and results have produced several changes in the test procedure as well as changes in the method of data analysis for these latter three casks and also have prompted a reevaluation and analysis of the cask 301 test data. Therefore, this summary report will not only present the thermal demonstration test summary results for Casks 302, 303 and 304 but will also reevaluate cask 301's performance in light of the additional experience and efforts since submittal of the cask 301 test results in 1973.

6.7.5.2 Test Procedures

Variations between the procedures and methods used for the last three casks and those utilized in the first cask test are identified and explained in the following paragraphs.

*This report is included as an appendix for information purposes. It has been superceded by this summary report.

Cask 301 thermal demonstration tests were conducted in accordance with Stearns-Roger Procedure SR-PP-229, Rev. 3, approved by General Electric, and Subsection 6.7 of the CSAR (NEDO 10034-1). Cask 302 was tested following Stearns-Roger Procedure SR-PP-240, Rev. 1 and Subsection 6.7 of the CSAR. Cask 303 and 304 were tested according to Stearns-Roger Procedure SR-PP-254, Rev. 4, and paragraph 14 of Certificate of Compliance Number 9001. All tests were conducted under both normal cooling and Loss-of-Mechanical Cooling (LOMC) conditions. Two significant differences distinguish these various procedures. For casks 301 and 302, temperature equilibrium data points were obtained at 25%, 50%, 75% and 100% of full power whereas for casks 303 and 304, data points were obtained for 75%, 90%, 95% and 100% of full power. This adjustment provided increased accuracy at the higher power levels. The other significant variation concerns the conditions for determination of thermal equilibrium. Per Certificate of Compliance No. 9001, for test purposes, thermal equilibrium for casks 303 and 304 (and all others) was considered as being achieved when the average cavity water temperature and built-in thermocouple temperature did not rise more than two Farhenheit degrees over a two hour span plus one additional hour for confirmation. For casks 301 and 302, a three Fahrenheit degree per two hour span criterion was used.

6.7.5.3 Test Data Analysis

The Demonstration Testing Report for cask 301 depicted the cask equilibrium temperature distribution (normal and LOMC) based on two ambient air temperatures; first at the actual equilibrium test condition and second at the regulatory 130°F condition. Upon closer examination it was apparent that the thermal response time of the IF-300 inner cavity to a change in ambient temperature is slow (long time constant) due to the mass of the system.

To account for this characteristic, a more realistic estimate of ambient test temperature is an average of ambient temperatures over several hours prior to equilibrium. Fluctuations in ambient

temperatures of 10 to 15 degrees within a short time span which were not indicators of a longer range trend would not likely affect cask temperature distributions.

Similarily it is also difficult to preceive that the cask temperature distribution would be affected by ambient temperatures more than 12 hours past. Thus for casks 302, 303 and 304 as well as for the reevaluation of cask 301, test ambient conditions were calculated as the 12 hour average of measured ambient temperatures prior to equilibrium.

In preparation of the Demonstration Testing Report for cask 301, the cavity bulk water temperature was estimated by averaging the basket thermocouples and the heater thermocouples. However, in later tests, the heater thermocouples tended to record appreciably higher temperatures than the other cavity thermocouples as one might expect. Since incorporation of the heater thermocouples unnecessarily biases the cavity temperatures, cavity bulk water temperatures for casks 302, 303 and 304 tests were estimated by averaging the nine cavity (basket) thermocouples.

It should be noted that in some instances the bulk cavity water temperature and the built-in thermocouple temperature were nearly equal. In light of the position of the various thermocouples, this agreement is understandable if not to be expected. The cavity thermocouples are generally in two groups along the top and bottom of the cask cavity (when in the horizontal position). The built-in thermocouple is between the cavity wall and uranium layer along the side of the cask. Thus while the upper thermocouples read higher than the built-in and the lower thermocouples read lower than the built-in due to the convective cooling mode, the average is often nearly equal to the built-in thermocouple. This confirms the validity of averaging the nine basket thermocouples.

To conform to stipulated regulations, all temperatures for all cask tests were normalized to a common 130°F ambient condition. Normalization from the test ambient temperatures to 130°F was not accomplished by simple addition of the ambient differences to the measured values. Rather some lessor value was used due to the higher heat transfer rate at elevated temperatures. The THTD computer model in the LOMC configuration was run for various power levels and various ambient temperatures. Figure VI-19 is a plot of these runs showing the test-to-130°F ambient correction factor as a function of test ambient temperature for a given power level. The two lines shown are for 75% and 100% power as indicated. Ambient correction factors for 90% and 95% power levels were linearly interpolated from the figure. Subsequent to the cask 301 analysis but in conjunction with the data analysis for casks 302, 303 and 304, a minor error was discovered in the THTD data file which produced the ambient correction factors for the cask 301 report. The correction of this error altered the ambient correction factors slightly. These new factors were utilized for the cask 302, 303 and 304 data analysis as well as for the reevaluation of cask 301.

Subsequent to the cask 301 analysis but in conjunction with the data analysis for casks 302, 303 and 304, a minor error was discovered in the THTD data file which produced the ambient correction factors for the cask 301 report. The correction of this error altered the ambient correction factors slightly. These new factors were utilized for the cask 302, 303 and 304 data analysis as well as for the reevaluation of cask 301.

The immediately preceeding paragraphs identified those differences in test procedure and data analysis which existed between the initial thermal demonstration test of cask 301 and those tests and analyses conducted for casks 302, 303 and 304. The results of the

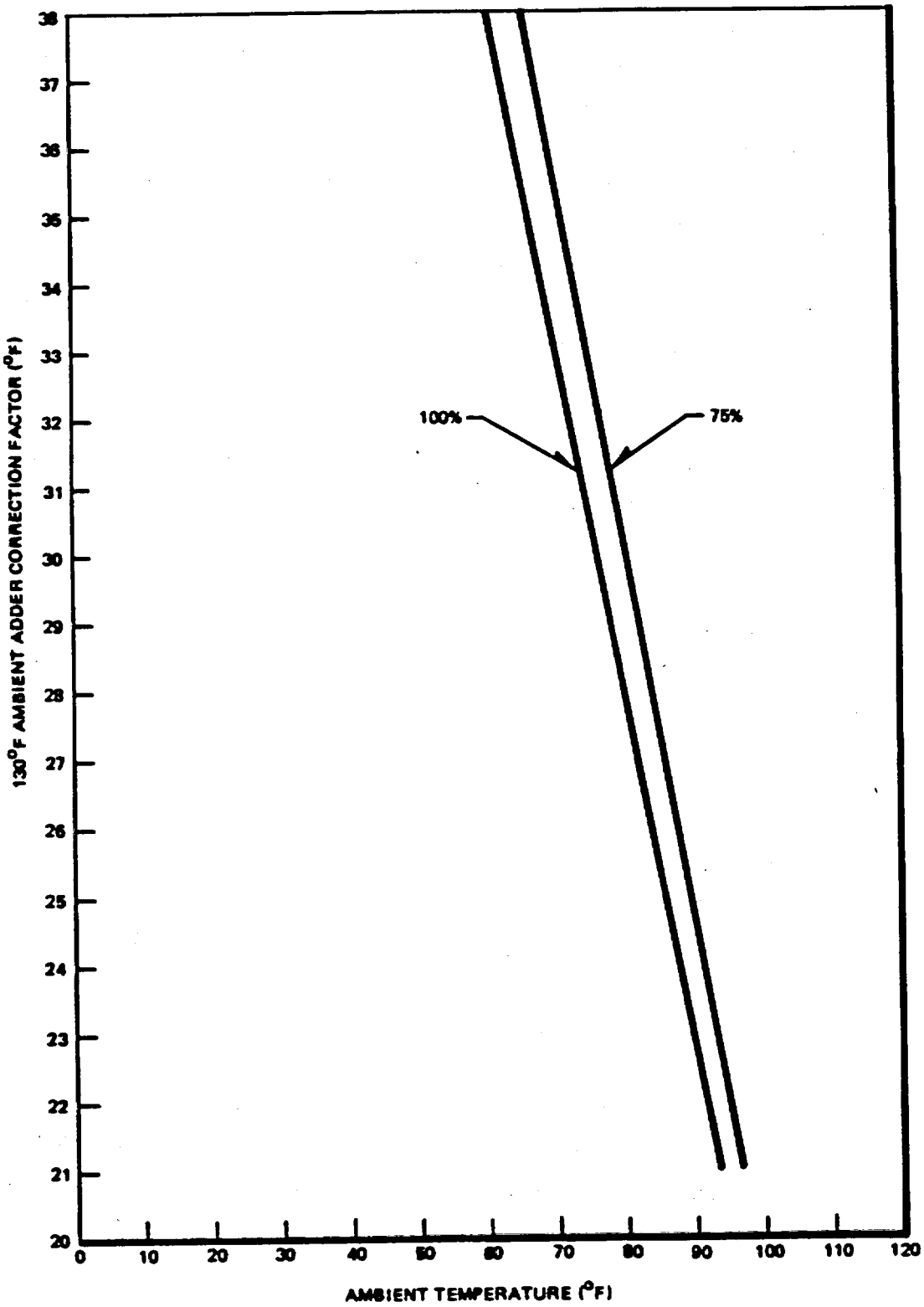

Figure VI-19. Ambient Correction FActors

data reduction for the LOMC tests are summarized in the four tables, Table VI-23 through VI-26. Note that both the revised values for the cask 301 test and the originally reported values are included. Only the LOMC conditions are examined in this report even though normal cooling tests were conducted. The reason for this is that LOMC represents the more critical heat dissipation mode and for the reason is the only thermal condition specified in the testing acceptance criteria. E

Table VI-23 E

CASK 301
LOMC

	Nominal Percent Power							
	25%		50%		75%		100%(1)	
Test Ambient	P(2)	R(3)	P	R	P	R	P	R
Ave. Ambient, °F	83	89	80	75	80	79	79	75
Ave. Cavity Water, °F	177	169	301	302	387	376	421	415
Built-In T.C., °F	164	164	283	283	367	367	400	400
Shield Water, °F	151	151	258	259	328	328	346	346
Bbl. Surface, °F	142	134	242	228	314	294	335	313
Power, KW		19.4		38.2		59.7		77.2
Actual Power, %		25.2		49.8		77.7		100.5
130°F Ambient Adder					29	30.9	24	30.8
Normalized								
Ave. Ambient, °F	130	130	130	130	130	130	130	130
Ave. Cavity Water, °F					412	407	445	446
Built-In T.C., °F					392	398	424	431
Shield Water, °F					353	359	370	377
Bbl. Surface, °F					339	325	359	344

1. Nominal percent power, 100% = 262,000 Btu/hr
2. Previous values per Appendix B4A-1 of August 13, 1973 submittal
3. Revised values per this report

Table VI-24

CASK 302
LOMC

Item	Nominal Percent Power	
Test Ambient	75	100
Ave. Ambient, °F	73	79
Ave. Cavity Water, °F	384	438
Built-In T.C., °F	378	423
Shield Water, °F	335	376
BBL Surface	298	341
Power, KW	57.67	78.38
Actual Power, %	75.1	102.1
130°F Ambient Adder	34.2	28.7
Normalized		
Ave. Ambient, °F	130	130
Ave. Cavity Water, °F	418	467
Built-In T.C., °F	412	452
Shield Water, °F	369	405
BBL Surface, °F	332	370

Table VI-25

CASK 303
LOMC

Item	Nominal Percent Power				
Test Ambient	75	90	90	95	100
Ave. Ambient, °F	78	75	68	75	77
Ave. Cavity Water, °F	382	424	413	426	430
Built-In, TC, °F	384	423	417	427	427
Shield Water, °F	336	368	361	370	370
BBL Surface, °F	301	331	317	328	329
Power, KW	57.4	70.6	67.8	72.6	77.4
Actual Power, %	74.7	91.9	88.3	94.5	100.8
130°F Ambient Adder	31.4	31.8	35.5	30.4	29.7
Normalized					
Ave. Ambient, °F	130	130	130	130	130
Ave. Cavity Water, °F	413	456	449	456	460
Built-In T.C., °F	415	455	453	457	457
Shield Water, °F	397	400	397	400	400
BBL Surface, °F	332	363	352	358	359

Table VI-26

CASK 304
LOMC

E

Item	Nominal Percent Power			
Test Ambient	74	90	95	100
Ave. Ambient, °F	69	64	66	70
Ave. Cavity Water, °F	389	422	424	426
Built-In T.C., °F	389	424	424	427
Shield Water, °F	337	367	368	371
BBL Surface, °F	303	328	330	333
Power, KW	57.7	68.9	72.8	76.6
Actual Power, %	75.1	89.7	94.8	99.7
130°F Ambient Adder	36.4	37.7	36.0	33.4
Normalized				
Ave. Ambient, °F	130	130	130	130
Ave. Cavity Water, °F	425	460	460	459
Built-In T.C., °F	425	462	460	460
Shield Water, °F	373	405	404	404
BBL Surface, °F	339	366	366	366

The bulk cavity water temperatures for each of the four casks normalized to 130°F ambient conditions are plotted in Figure VI-20 as a function of power level. Variations between the casks are less than 5%. Such variations are expected in light of the several sources of random error and deviation which exist in the test setup, i.e., thermocouple error, recorder error, and input power variations. Figure VI-21 does indicate that the LOMC temperature distributions of the IF-300 casks were somewhat higher than originally predicted in the CSAR. A reduction from the 100% design basis heat load (262,000 Btu/hr) was required. E

The original IF-300 Cask Certificate of Compliance placed a limitation of 210,000 Btu/hr on the package heat dissipation rate. The basis for this thermal limitation was the restriction of cavity pressure to <346 psig under LOMC conditions at an ambient temperature of 130°F.

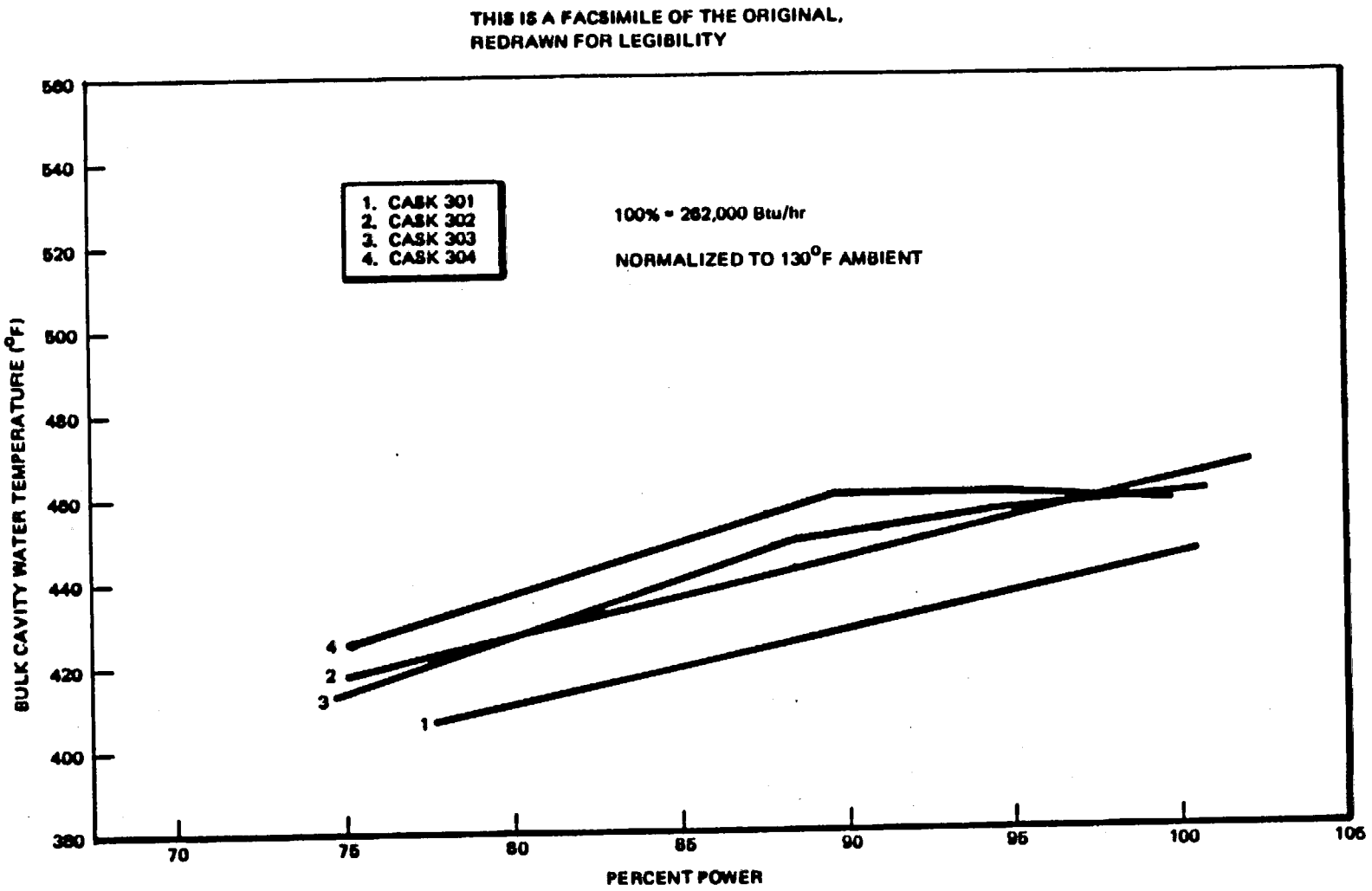

Figure VI-20. Bulk Cavity Water Temperature Comparisons — Loss-of-Mechanical Cooling

The Certificate specified, by reference, a bulk cavity water temperature of no greater than 422°F under the aforementioned LOMC conditions as determined by a thermal demonstration test. This was the cask thermal acceptance criterion.

Based on Figure VI-20, the heat loads shown in Table VI-27 would produce a bulk cavity water temperature of 422°F at an ambient temperature of 130°F. With the exception of cask 301, these heat loads are less than 210,000 Btu/hr, demonstrating that casks 302, 303 and 304 did not meet the original thermal acceptance criterion. E

Table VI-27 E

CASK HEAT LOAD TO

PRODUCE 422°F WATER TEMPERATURE

Cask No.	Heat Load, Btu/hr	% Power
301	221,000	84.5
302	202,000	77.0
303	206,000	78.5
304	194,000	74.0
Certificate #9001 Limit	210,000	80.0

The heat loads shown above in Table VI-27 were considered as wet shipment thermal limits for the respective casks. This became cask nameplate data. E

6.7.5.4 Conclusions

The thermal tests of casks 301-304 showed a maximum variation between casks of 5%, which is quite reasonable considering the number of parameters involved. Some power reduction on casks 302, 303 and 304 was necessary to adhere to the 422°F, 346 psig limitation.

6.7.6 Cask Surface Temperature

At the request of the NRC a cask surface temperature profile measurement was made on unit number 301 under LOMC test conditions.

Temperatures were taken along the neutron shielding barrel length using a contact pyrometer. Readings were taken at three intervals in the approach to steady state at a heat load of 262,000 Btu/hr. The data is shown as Figure VI-21. E

The individual making the measurements stated that contact with the surface was difficult and as a consequence the accuracy of the reading is questionable. Assuming that the difficulty was constant along the length, it is possible to look at the distribution (not the magnitude). The distribution appeared flat over most of the barrel, only falling off at the extreme bottom (and cooler) end. This distribution is quite expected of such a liquid-filled system.

6.7.7 Thermal Test Acceptance Criterion

6.7.7.1 Introduction

IF-300 cask thermal acceptance is based on loss-of-mechanical cooling (LOMC) test temperatures which were normalized to the regulatory conditions of 130°F ambient air. Each cask was tested to determine a heat load value which produced a cavity bulk water temperature of 422°F @ 130°F ambient. The thermal limit for each cask tested was the lesser of the heat load corresponding to a 422°F bulk water temperature or 210,000 Btu/hr. In actual wet shipment use, sufficient expansion volume was established in each cask to assure that the cavity relief pressure of 375 psig was not reached considering the tolerance and accuracy associated with void volume establishment and relief valve set point.

TEMPERATURE ON BARREL – 90° ℄
EVERY THIRD CORRUGATION EXCEPT WELDED SEAM
START WITH FIRST CORRUGATION OF EACH SECTION

(5/29/73) 12:00	(5/29/73) 18:00	(5/29/73) 21:00		
273°F	285°F	292	CORRUGATION NO. 1 (FRONT)	FRONT BARREL SECTION
273	285	300		
275	292	298		
270	295	295		
270	292	300		
270	295	296		
265	290	300	END CORRUGATION	
270	290	300		
270	290	297	CORRUGATION NO. 1 (FRONT)	REAR BARREL SECTION
265	290	300		
270	292	302		
265	282	300		
260	288	300		
260	285	302		
270	290	305	END CORRUGATION	
263	295	305		
255	292	285	CORRUGATION NO. 1 (FRONT)	END BARREL SECTION REAR (VALVE BOX)
230	272	272	CORRUGATION NO. 4	
230	255	270	END CORRUGATION	
		CLOSE TO STEADY STATE		

READINGS TAKEN WITH HAND-HELD PYROMETER

Figure VI-21. Cask Surface Temperature Profile Measurement

E

6.7.7.2 Thermal Acceptance Procedure

The acceptance of a cask from a heat dissipation standpoint was determined as follows:

a. Test the cask at a sufficient number of power settings to allow the determination of the cavity bulk water temperature as a function of heat load.

b. At each power setting allow cask temperatures to reach equilibrium (see e below) and determine the cavity bulk water temperature.

c. Normalize the measured bulk water temperatures to those values which would pertain if the ambient air temperature were 130°F. This is to account for the difference between test and regulatory conditions.

d. The heat load limit for each cask will be that value which would produce a cavity bulk water temperature of 422°F at an ambient air temperature of 130°F based on the test results. Heat load limits in excess of 210,000 Btu/hr shall not be permitted.

e. For test purposes, thermal equilibrium will be considered as being achieved if the average cavity water temperature and built-in thermocouple temperature fail to rise more than two degrees Fahrenheit over a two-hour time span. As confirmation, the test will be conducted for an additional hour using the same criterion. For packages thermally tested prior to September 14, 1973, a three-degree temperature rise in a two-hour time span is acceptable.

f. Following initial heat load determination by the above method, the thermal performance of each cask will be analyzed on an annual basis. Such analyses will be based on cask built-in thermocouple readings and decay heat estimates for each shipment performed in the prior 12 month period. Actual shipment data

will be compared to cask thermal test data, cask thermal computer model output, and previous year's data to assess the unit's thermal characteristics. An annual report will be written by General Electric documenting the analyses. Significant deviations from expected thermal behavior shall result in withdrawal of the affected unit from service until additional investigation and reestablishment of an acceptable heat load or other corrective action is taken.

6.8 SECTION CONCLUSIONS

This section has examined the cask thermal performance under conditions of normal cooling, loss-of-mechanical cooling, 50 percent shield water loss, 30-minute fire, and post-fire equilibrium.

All of these analyses demonstrate that the cask can dissipate the design basis heat load without any adverse affects on the fuel or cask containment functions. The cooling system is shown to be unnecessary for maintenance of acceptable fuel rod temperatures and inner cavity pressures and is thus not a safety item.

Thermal demonstration tests on casks 301 through 304 show that originally there was some variance between calculated and measured temperatures. As a result, a thermal acceptance criteria was established which determined the maximum heat load on a cask-by-cask basis.

The section also discusses the pressure relief and closure components used on the IF-300 and presents data which confirms their acceptability for IF-300 cask usage.

6.9 REFERENCES

6.1 L. B. Shappert, Cask Designers Guide, Oak Ridge National Laboratory (ORNL NSIC-68), February, 1970.

6.2 H. Grober, S. Erk, and U. Grigull: Fundamentals of Heat Transfer, McGraw-Hill, 1961.

6.3 W. M. Kays and A. L. London, Compact Heat Exchangers, National Press, 1955.

6.4 C. S. Williams, Discussion of the Theories of Cavity-Type Sources of Radiant Energy, Journal of the Optical Society of America, Vol. 51, May, 1961.

6.5 W. M. Rohsenow and H. Y. Choi, Heat, Mass, and Momentum Transfer, Prentice-Hall, 1961.

6.6 W. H. McAdams, Heat Transmission, McGraw-Hill, 1954.

6.7 G. M. Dusinberre, Heat-Transfer Calculations by Finite Differences, Int'l. Textbook Co., 1961.

6.8 M. N. Ozisik, Boundary Value Problems of Heat Conduction, Int'l. Textbook Co., 1968.

6.9 R. D. Haberstroh, personal communication.

6.10 J. S. Watson, Heat Transfer from Spent Reactor Fuels During Shipping: A Proposed Method for Predicting Temperature Distribution in Fuel Bundles and Comparison with Experimental Data, ORNL-3439, Oak Ridge National Laboratory.

6.11 F. Kreith, Principles of Heat Transfer, 2nd Ed., Int'l. Textbook Co., 1963.

6.12 Trane Ductulator, Form D100-10-1067, The Trane Company, 1950.

6.13 Trane Air Conditioning Manual, The Trane Company, 1965.

6.14 Thermophysical Properties Research Center, Thermophysical Properties of High Temperature Materials, Vol. 1, Macmillan, 1967.

6.15 H. E. Baybrook, Personal Communication, Allegheny Ludlum Corp., Research Center, Brackenridge, Pa., June, 1969.

6.16 Chromium-Nickel Stainless Steel Data, Section I, Bulletin B, Int'l. Nickel Co., 1963.

6.17 H. C. Hottel and A. F. Sarofim, Radiative Transfer, McGraw-Hill, 1967.

6.18 E. R. G. Eckert and R. M. Drake, Jr., Heat and Mass Transfer, McGraw-Hill, 1959.

6.19 C. A. Meyer, etc., Thermodynamic and Transport Properties of Steam, American Soc. of Mech. Engrs., 1967.

6.20 R. Gordon and J. C. Akfirat, Heat Transfer of Impinging Two-Dimensional Air Jets, Journal of Heat Transfer, February, 1966.

6.21 Chen-Ya Liu, W. K. Mueller, and F. Landis, Natural Convection Heat Transfer in Long Horizontal Cylindrical Annuli.

6.22 A. K. Oppenheim, Radiation Analysis by the Network Method, Transactions of ASME, Vol. 78, pp. 725-735, (1956).

6.23 R. O. Wooton and H. M. Epstein, Heat Transfer From a Parallel Rod Fuel Element in a Shipping Container, Battelle Memorial Institute, 1963.

6.24 J. K. Vennard, Elementary Fluid Mechanics, 4th Edition, John Wiley and Sons, 1962.

6.25 Heat Transfer Data Book, General Electric Company, Corporate Research and Development, Schenectady, N.Y., 1970.

6.26 E. M. Sparrow and R. D. Cess, Radiation Heat Transfer, Wadsworth Publishing Company, Inc. 1966.

6.27 R. L. Cox, Radiative Heat Transfer in Arrays of Parallel Cylinders (ORNL-5239), June 1977.

TABLE OF CONTENTS

VII. CRITICALITY ANALYSIS

		Page
7.1	INTRODUCTION	7-1
7.2	DISCUSSION AND RESULTS	7-1
7.3	CASK FUEL LOADING	7-2
7.4	MODEL SPECIFICATION	7-5
	7.4.1 Description of the Calculational Model	7-5
	7.4.2 Package Regional Densities	7-10
7.5	CRITICALITY CALCULATION	7-14
	7.5.1 Calculational Method	7-14
	7.5.2 Fuel Bundle k_∞ Calculations	7-15
	7.5.3 Cask Calculations	7-16
7.6	CRITICAL BENCHMARK EXPERIMENTS	7-18
	7.6.1 Benchmark Experiments and Applicability	7-18
7.7	REFERENCES	7-21

LIST OF ILLUSTRATIONS

Figure	Title	Page
VII-1	8x8 BWR Water Hole Locations	7-3
VII-2	14x14 PWR Water Hole Locations	7-6
VII-3	15x15 PWR Water Hole Locations	7-7
VII-4	16x16 PWR Water Hole Locations	7-8
VII-5	17x17 PWR Water Hole Locations	7-9
VII-6	BWR Configuration	7-11
VII-7	PWR Configuration	7-12
VII-8	Variation of K_{eff} with Rod Pitch	7-17
VII-9	Variation of K_{eff} with Water Temperature	7-19

N

LIST OF TABLES

Table	Title	Page
VII-1	K-Effective Values	7-2
VII-2	Nominal BWR Dimensions	7-4
VII-3	Nominal PWR Fuel Dimensions	7-5
VII-4	Atom Densities of Cask and Basket Materials	7-10
VII-5	Atom Densities of Fuels	7-13
VII-6	Infinite Array Calculations	7-15
VII-7	Cask k_{eff} Values ($\pm 1\sigma$)	7-16
VII-8	Summary of Critical Experiments	7-20

VII. CRITICALITY ANALYSIS

7.1 INTRODUCTION

The IF-300 shipping cask has been designed to transport irradiated reactor fuel bundles from both pressurized water reactors (PWR) and boiling water reactors (BWR). The IF-300 cask utilizes interchangeable inserts or baskets in the cask cavity for fuel bundle support. There are three types of fuel baskets for 7 PWR, 18 BWR, and 17 BWR channelled fuel assemblies. The purpose of this chapter is to identify, describe, discuss and analyze the principle criticality engineering-physics design of the packaging, components and systems important to safety and necessary to comply with the performance requirements of 10 CFR Part 71 for the 7-cell PWR and 18-cell BWR baskets licensed prior to 1991. The 17-cell BWR channelled fuel basket design is addressed in Volume 3, Appendix A.

7.2 DISCUSSION AND RESULTS

Criticality control for the PWR and BWR fuel licensed prior to 1991 in the IF-300 cask is achieved through the use of boron carbide (B_4C) filled stainless steel tubes permanently affixed to the fuel baskets as opposed to borated stainless steel poison plates used in the 17-cell BWR channelled fuel basket. The IF-300 cask is shown in quarter symmetry in Figures VII-1 and VII-2, showing the PWR and BWR geometries licensed prior to 1991 and B_4C tube locations. These absorber rods are manufactured by the General Electric Company following the same standards, where applicable, used for BWR control blade absorber tubes. Quality control checks include B_4C density determinations, helium leak checking and material certifications on both tubing and end plugs.

The criticality analysis calculations were performed with the MERIT computer program, a Monte Carlo program which solves the neutron transport equation as an eigenvalue or a fixed source problem and includes the effects of neutron shielding. This program is especially written for the analysis of fuel lattices in thermal nuclear reactors. MERIT has the capability to perform calculations in up to three dimensions and with neutron energies between 0 and 10 MeV. MERIT uses cross sections processed from the ENDF/B-IV library tapes. The qualifications of MERIT is addressed in Section 7.5.

The IF-300 cask was shown to be critically safe for the transport of both PWR and BWR fuels supplied to domestically designed reactors. Both abnormal and accident conditions were considered. Detailed results of the analysis are contained in Section 7.4 and fuel descriptions are contained in Section 7.2. In summary, the maximum cask k-effective values for PWR and BWR fuels are in Table VII-1.

These values calculated for one sigma include MERIT calculation uncertainty and bias.

Table VII-1
K-EFFECTIVE VALUES

	PWR	BWR
k_{eff} (4.0% enrichment)	0.955 ± 0.004	0.880 ± 0.005

7.3 CASK FUEL LOADING

Prior to 1991, the IF-300 cask was designed to carry either 18 BWR fuel bundles or 7 PWR fuel bundles. As described in Volume 3, Appendix A, it was licensed to also carry 17 BWR channelled fuel bundles in 1991. This section addresses the former types of fuel.

BWR fuel bundles are primarily manufactured by General Electric and are square arrays of Zircaloy tubes containing the UO_2 fuel pellets. These arrays are either the earlier Group I 7 x 7 design or the current Group II 8 x 8 design which are held in position by a tie plate at the upper end and a nozzle at the lower end. Longitudinal spacing and support is provided by a series of spacer assemblies along the length of the fuel rods. The design basis BWR bundle in this analysis has the dimensions shown in Table VII-2.

The BWR design does not contain control rods within the bundles, but some BWR bundle designs may contain non-fueled rods, (water-holes) in one or two rod locations as shown in Figure VII-1.

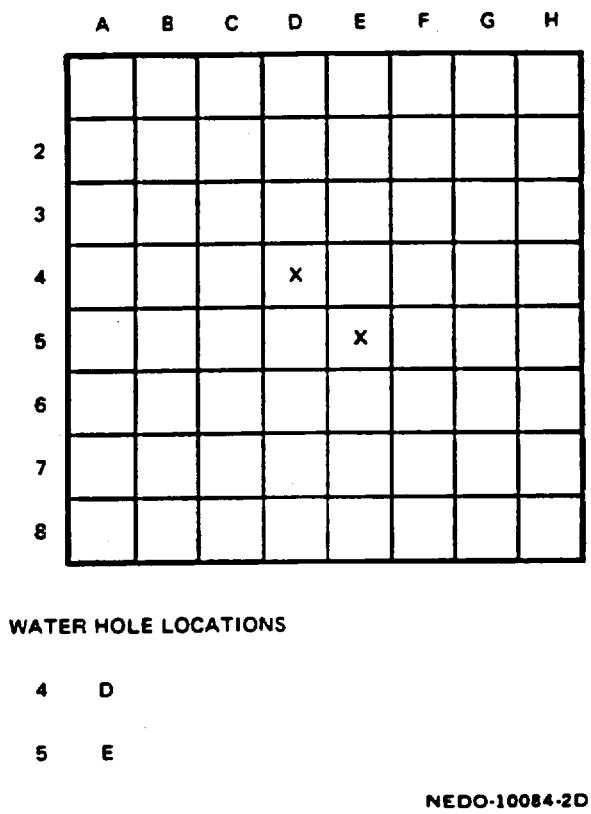

Figure VII-1. 8x8 BWR Water Hole Locations

Table VII-2

NOMINAL BWR DIMENSIONS

	Group I 7x7, in.	Group II 8x8, in.
Pellet Diameter	0.478	0.416
Rod Outside Diameter	0.463	0.493
Clad Thickness	0.037	0.034
Rod Pitch	0.738	0.640

Pressurized water reactors are manufactured by three companies domestically: Westinghouse(W), Combustion Engineering (CE), and Babcock and Wilcox(BW). There are some differences between fuel bundle designs for various PWR vendors, but all fuel fabricators use a square array of tubes containing UO_2 pellets. Current product line fuel uses Zircaloy as the cladding material. Some earlier PWR's used stainless steel cladding. Earlier PWR fuel Group I designs utilizes 14x14 and 15x15 rod arrays.

Current generation PWR fuels Group II designs are either 17 x 17 or 16 x 16 rod arrays. For all PWR fuel types, the rods are held in a lattice geometry by top and bottom flow nozzles. Spacer assemblies along the length of the bundles maintain rod spacing and provide support.

PWR bundles utilize control rod systems within the fuel bundles. Depending on bundle type, some fuel rods may be replaced by thimble tubes which act as guides for control rods or burnable poison rods. These various rod assemblies are generally not shipped with the spent fuel bundles, thus leaving the thimbles filled with the cask coolant (water-holes) as shown in Figures VII-2 through VII-5.

In addition, most bundles are shipped without the central instrumentation tube. The design basis PWR bundles in this analysis have the dimensions given in Table VII-3.

7.4 MODEL SPECIFICATION

7.4.1 Description of the Calculational Model

The IF-300 cask was explicitly modeled in two-dimension geometry and 1/4 symmetry using MERIT. Only slight differences exist between the calculational model and the actual hardware and are as follows:

1. The model assumes that basket channels have circulation openings along their full length whereas the actual openings are segmented. The model uses less stainless steel between the bundles which is conservative in this case.

2. The corrugated barrel and neutron shield water are ignored. The four inch thick uranium metal gamma shield acts as a reflector, effectively isolating the cask cavity neutronically from fissile material in other casks.

3. The basket's stainless steel structural rings are conservatively ignored.

Table VII-3

NOMINAL PWR FUEL DIMENSIONS

	Group I Fuels			Group II Fuels		
	W(15x15)	BW(15x15)	CE(14x14)	W(17x17)	BW(17x17)	CE(16x16)
Pellet dia.	0.368	0.377	0.383	0.3225	0.324	0.325
Rod O.D.	0.422	0.430	0.440	0.374	0.379	0.382
Clad Thickness	0.0243	0.0265	0.026	0.0225	0.0235	0.025
Rod Pitch	0.563	0.568	0.580	0.496	0.502	0.5063

	A	B	C	D	E	F	G	H	I	J	K	L	M	N
1														
2														
3						X			X					
4				X							X			
5														
6			X			X			X			X		
7														
8														
9			X			X			X			X		
10														
11				X							X			
12						X			X					
13														
14														

WATER HOLE LOCATIONS

3	F, I
4	D, K
6	C, F, I, L
9	C, F, I, L
11	D, K
12	F, I

NEDO-10084-2D

Figure VII-2. 14x14 PWR Water Hole Locations

	A	B	C	D	E	F	G	H	I	J	K	L	M	N	O
1															
2															
3						X				X					
4				X								X			
5															
6			X			X				X			X		
7															
8								X							
9															
10			X			X				X			X		
11															
12				X								X			
13						X				X					
14															
15															

WATER HOLE LOCATIONS

3	F, J
4	D, L
6	C, F, J, M
8	H
10	C, F, J, M
12	D, L
13	F, J

NEDO-10084-2D

Figure VII-3. 15x15 PWR Water Hole Locations

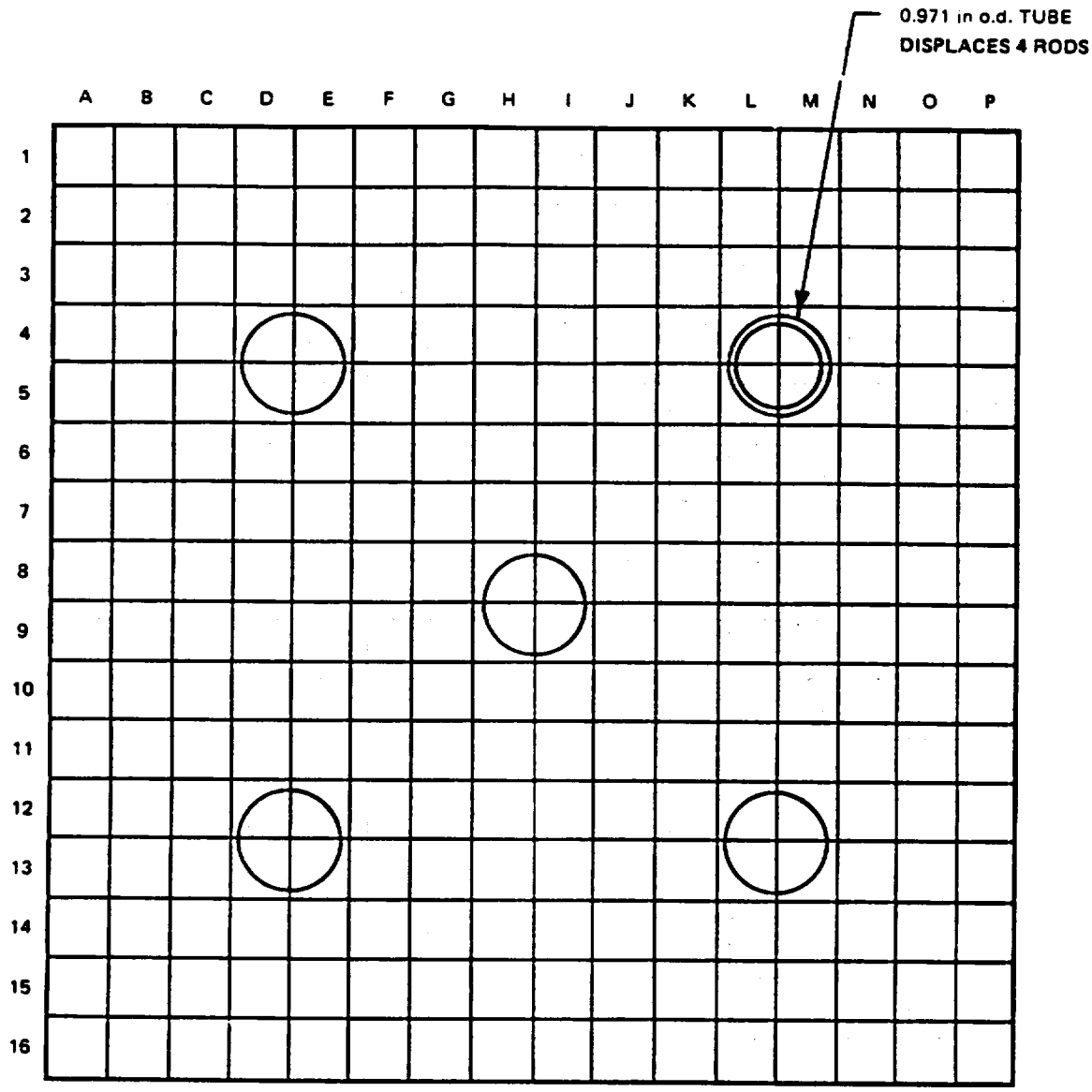

WATER HOLE LOCATIONS

4	D, E, L, M
5	D, E, L, M
8	H, I
9	H, I
12	D, E, L, M
13	D, E, L, M

NEDO-10084-2D

Figure VII-4. 16x16 PWR Water Hole Locations

	A	B	C	D	E	F	G	H	I	J	K	L	M	N	O	P	Q
1																	
2																	
3						X			X			X					
4				X										X			
5																	
6			X			X			X			X			X		
7																	
8																	
9			X			X			X			X			X		
10																	
11																	
12			X			X			X			X			X		
13																	
14				X										X			
15						X			X			X					
16																	
17																	

WATER ROD HOLES

3	F, I, L
4	D, N
6	C, F, I, L, O
9	C, F, I, L, O
12	C, F, I, L, O
14	D, N
15	F, I, L

NEDO-10084-2D

Figure VII-5. 17x17 PWR Water Hole Locations

7.4.2 Package Regional Densities

The material densities, areas (2 dimension model) and atom densities for constituent nuclides of all materials other than fuel which are used in the calculational models are shown in Table VII-4. The material identification numbers are as shown on Figures VII-6 and VII-7.

Table VII-4

ATOM-DENSITIES OF CASK AND BASKET MATERIALS

I.D.	Zone	Material	Density g/cc	Area* cm^2	Atom Density Atoms/bn-cm
1	Outer shell	SST	7.93	381.63	
		Fe			0.633056E-01
					0.165391E-01
					0.651010E-02
2	Shield	Uranium	18.82	869.98	
		U-235			0.106128E-03
		U-238			0.475275E-01
3	Inner shell	SST	7.93	102.33	(same as 1)
4	Water (20°C)	Water	0.99832	**	
		H-1			0.667625E-01
		O-16			0.333048E-01
5	Channel	SST	7.93	4.65	(same as 1)
6	Poison Rods	B_4C	1.76	28.95	
		B-10			0.151997E-01
		C-12			0.189785E-01
7	Connecting Rod	SST	7.93	3.98	(same as 1)

*1/4 Symmetry
**Water area = 3135.35 cm^2 - (all other components, including fuel)

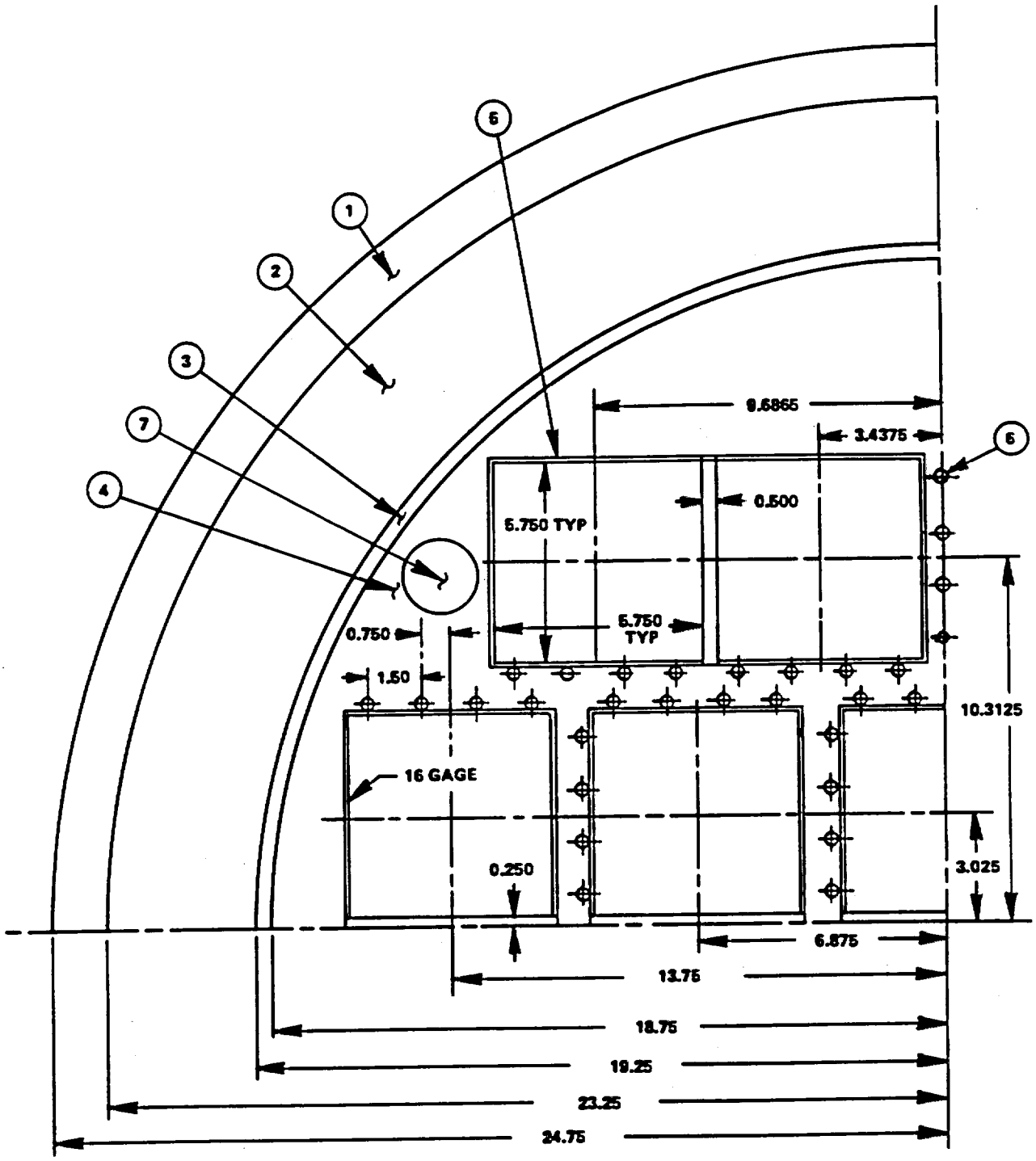

NOTE: 16 GAGE SHEET = 0.0598 inch THICK

Figure VII-6. BWR - Configuration

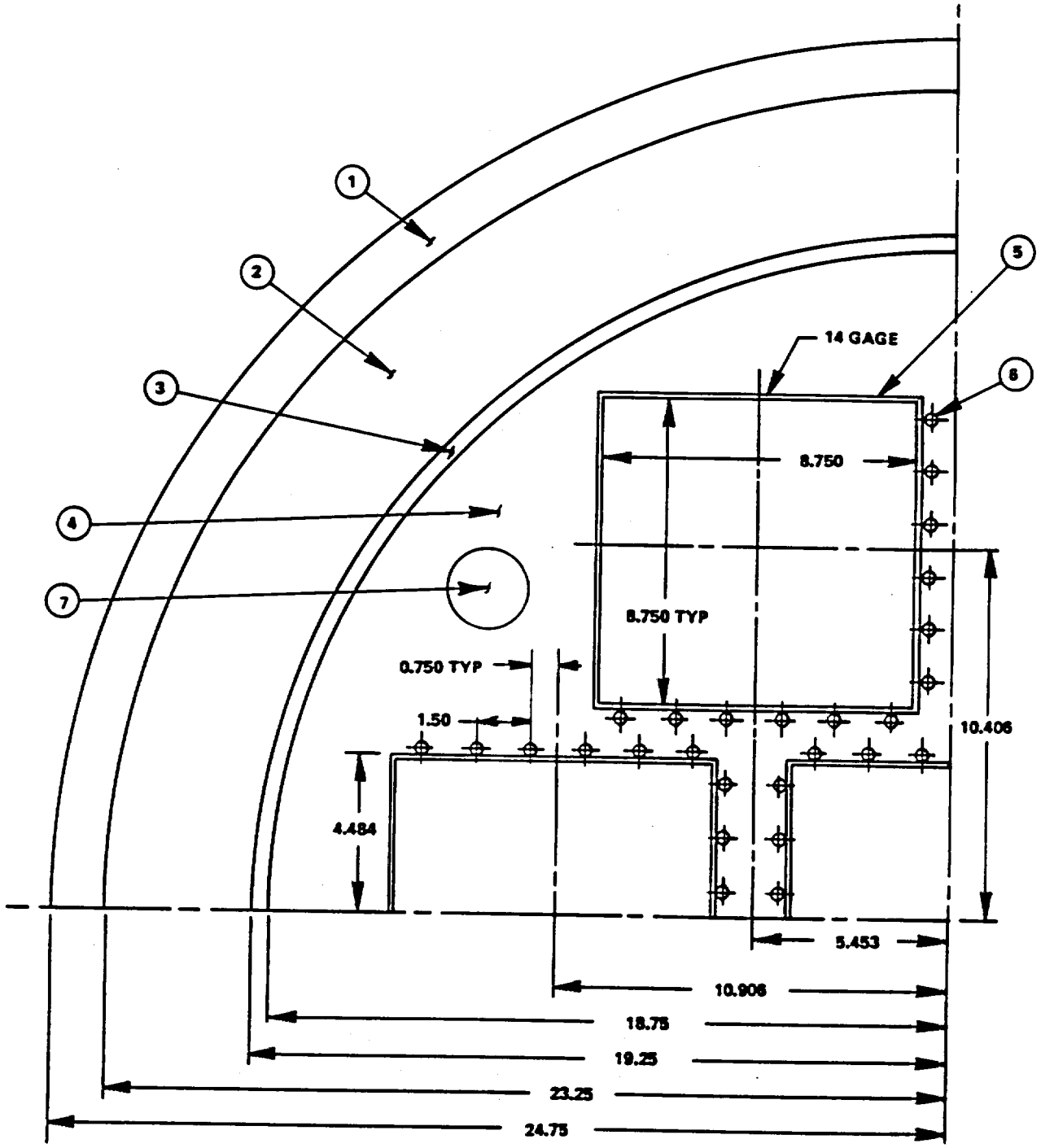

NOTE: 14 GAGE SHEET = 0.0747 inch THICK

Figure VII-7. PWR - Configuration

Table VII-5 provides the material densities, areas and isotopic atom densities for the various fuel types. Both BWR and PWR fuel bundles were assumed to be enriched uniformally to 4.0%. No credit was taken for burnup depletion of fissile isotopes, the presence of burnable poisons, or fission product poisoning.

Table VII-5

ATOM DENSITIES OF FUELS

Fuel Type	Isotope	Density g/cc	Area cm^2/bundle	Atom Density Atoms/bn-cm
7x7				
clad		6.55	15.06	
	Zr-90			0.43333E-01
fuel		9.9488	62.07	
	U-235			0.898795E-03
	U-238			0.212986E-01
	O-16			0.442865E-01
8x8				
clad		6.55	20.24	
	Zr-90			0.4333330E-01
fuel		9.9757	58.57	
	U-235			0.901208E-03
	U-238			0.213558E-01
	O-16			0.444054E-01
14x14				
clad		6.55	35.24	
	Zr-90			0.43333E-01
fuel		10.05	127.16	
	U-235			0.908173E-03
	U-238			0.215208E-01
	O-16			0.447485-01
15x15				
clad		6.55	40.73	
	Zr-90			0.433330E-01
Fuel		10.25	146.95	
	U-235			0.926320E-03
	U-238			0.219514E-01
	O-16			0.456437E-01

Table VII-5

ATOM DENSITIES OF FUELS (Continued)

Fuel Type	Isotope	Density g/cc	Area cm^2/bundle	Atom Density Atoms/bn-cm
16x16				
clad		6.55	42.69	
	Zr-90			0.433330E-01
fuel		9.98	131.78	
	U-235			0.901573E-03
	U-238			0.213644E-01
	O-16			0.444233E-01
17x17 W				
clad		6.55	42.32	
	Zr-90			0.433330E-01
fuel		10.00	144.77	
	U-235			0.903840E-03
	U-238			0.214182E-01
	O-16			0.445351E-01
17x17 B&W				
clad		6.55	44.71	
	Zr-90			0.433330E-01
fuel		9.81	147.45	
	U-235			0.886429E-03
	U-238			0.210056E-01
	O-16			0.436772E-01

7.5 CRITICALITY CALCULATION

This section describes the calculational method used to determine the effective multiplication factor of the IF-300 cask loaded with each of the fuel bundle types described in Sections 7.2 and 7.3.2.

7.5.1 Calculational Method

The IF-300 cask criticality analysis was performed in three parts. Part 1 determined the most reactive (k-infinite or k_∞) BWR and PWR bundle types. Part 2 analyzed the cask containing the most reactive BWR and PWR bundle types at 20°C and determined the k-effective (k_{eff})

values. Part 3 determined the effect of temperature and rod spacing variations on cask k-effective.

MERIT was used for all calculations, both the infinite fuel bundle arrays to determine the most reactive configurations and the cask calculations. Results of the fuel k_∞ calculations appear in Section 7.5.2 and results of the cask calculations appear in Section 7.5.3.

7.5.2 Fuel Bundle k_∞ Calculations

Infinite array calculations were performed for each of the types of PWR and BWR fuels in order to select the bundles of maximum reactivity to use in the cask calculations.

It was not expected that the k_∞ values would show significant differences between older and newer generations of fuel bundle design. The results shown in Table VII-6 confirm this.

Table VII-6
INFINITE ARRAY CALCULATIONS

Fuel Type	K_∞ @ 20°C, 4% Enr
Group I early design	
7x7 GE	1.385
14x14 CE	1.450
15x15 BW	1.457
Group II current design	
8x8 GE	1.388
16x16 CE	1.440
17x17 BW	1.457
17x17 W	1.456

From the above results the 8x8 BWR and the B&W 17x17 PWR fuels were selected as representative fuel bundle types with which to perform cask k-effective calculations.

The effects of the regulatory accident (10 CFR 71 Appendix B) on the cask reactivity were also considered. The cask is designed such that the only accident effect, as far as criticality is concerned, is the loss of the neutron shield water and possible loss of the cavity coolant water. The basic calculations were performed without the neutron shield. Therefore, the effect of the loss of it is included in the analysis. The temperature effects on k_{eff} demonstrated that the complete loss of water is the extreme case of reduced density, causing a reduction in cask k_{eff}.

Another possible effect of the regulatory accident on a loaded cask might be a change in the fuel rod pitches due to fuel spacer deformation. Although permanent fuel bundle deformation is not expected, the effect of pitch variation on cask k_{eff} was considered. Figure VII-8 shows that the designed nominal pitch is at or near the maximum k_{eff} pitch.

7.5.3 Cask Calculations

BWR and PWR configurations in the IF-300 cask were evaluated using representative fuels selected as a result of the infinite array calculations. The basic calculations were performed at 20°C. Also, an infinite array of casks was also considered. The infinite array calculation was conservative* as summarized in Table VII-7.

Table VII-7

CASK k_{eff} VALUES

Fuel Configuration	Single Cask @20°C	Infinite Array of Casks @20°C
BWR (4.0%, water holes)	0.874	--
BWR (4.0%, no water holes)	0.871	0.885
PWR (4.0%, water holes)	0.949	0.962
PWR (4.0%, no water holes)	0.933	--

*Performed by assuming that all leakage neutrons were reflected back into the system. This substantially overpredicts k_∞ in that no actual array density could approach this theoretical limit. Even so, the small increase in k_∞ with respect to k_{eff} indicates that the fuel in a single cask is essentially isolated from the surrounding environment and is not sensitive to the presence of other packages.

7.7 REFERENCES

1. Cross Section Working Group Benchmark Specifications, ENDF-202 November 1974.

2. M. N. Baldwin, et al., Physics Verification Program - Part III, Babcock & Wilcox (BAW-3647-6), January 1970.

3. G. T. Fairburn, et al., Pu Lattice Experiments in Uniform Test Lattice of UO_2-1.5% PuO_2 Fuel, Babcock & Wilcox (BAW-1357), August 1970.

4. S. R. Bierman, E. D. Clayton, B. M. Durst, "Critical Separation Between Subcritical Clusters of 2.35 Wt. % U_{235} Enriched UO_2 Rods in Water with Fixed Neutron Poisons" (PNL-2438).

5. S. R. Bierman, B. M. Durst, E. D. Clayton, "Critical Separation Between Subcritical Clusters of 4.29 Wt. % U_{235} Enriched UO_2 Rods in Water with Fixed Neutron Poisons" (NUREG/CR-0073).

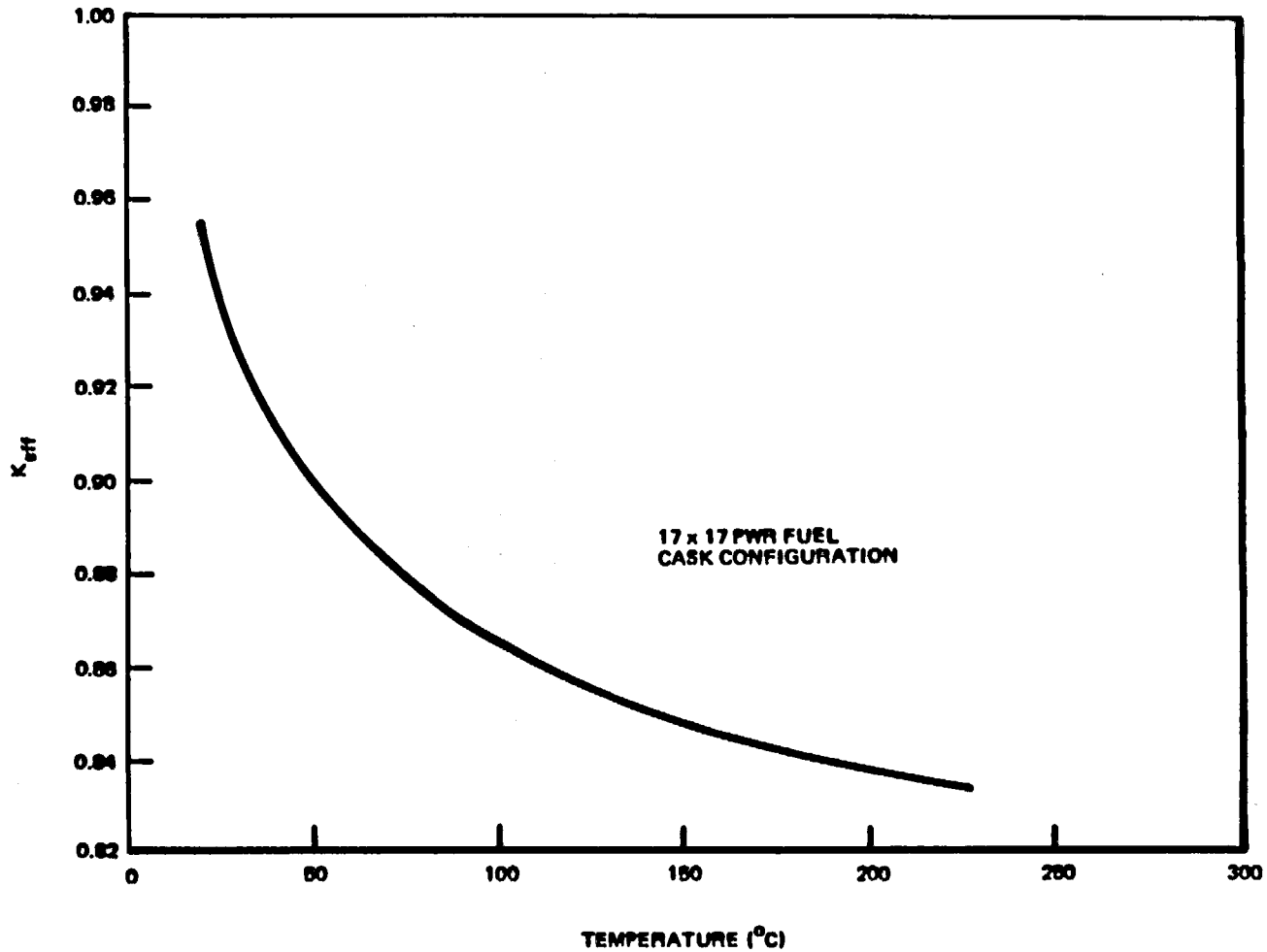

Figure VII-9. Variation of K_{eff} with Water Temperature

Table VII-8

SUMMARY OF CRITICAL EXPERIMENTS

Experiment	MERIT	Reference
(1) ORNL-1	0.9911 ± 0.0028	1
(2) ORNL-2	0.9933 ± 0.0046	1
(3) TRX-1	0.9998 ± 0.0013	1
(4) TRX-2	0.9924 ± 0.0010	1
(5) PNL-1	1.0194 ± 0.0055	1
(6) PNL-2	1.0143 ± 0.0060	1
(7) B&W UO_2	0.9950 ± 0.0021	2
(8) B&W P_uO_2	0.9960 ± 0.0018	3
(9) NRC Criticals		
PNL-2438-020	0.9918 ± 0.0022	4
PNL-2438-033	0.9928 ± 0.0021	4
CR-0073-012	0.9952 ± 0.0028	5

Based on these MERIT qualification programs, a bias of 0.006 ± 0.003 (1σ) Δk has been established with respect to the uranium critical experiments cited in Table VII-8. Therefore, MERIT tends to underpredict K_{eff} by approximately 0.6 percent Δk.

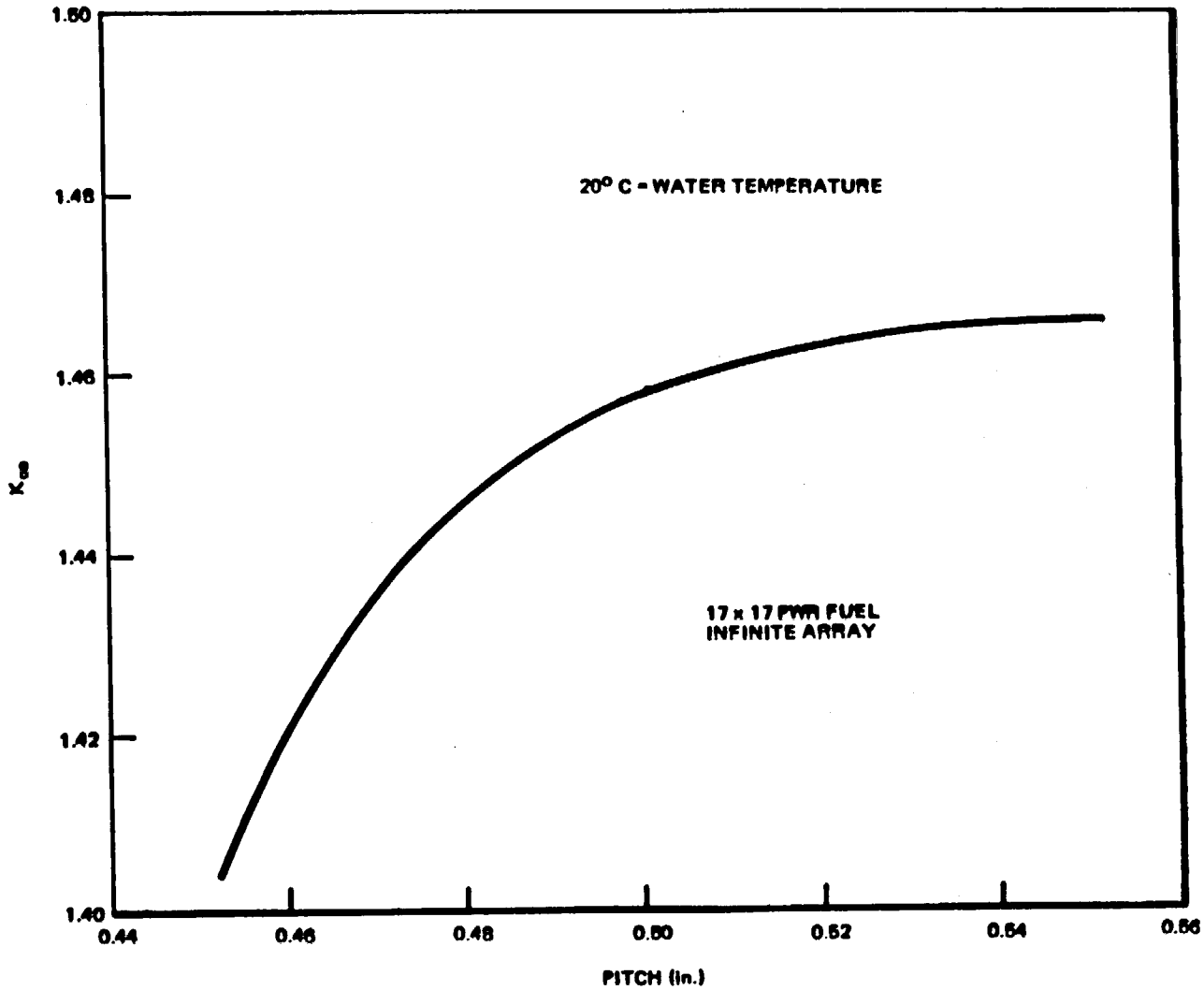

Figure VII-8. Variation of K_{eff} with Rod Pitch

The effects of changes in internal water density as a function of temperature were analyzed. As Figure VII-9 shows, the cask exhibits a negative reactivity temperature coefficient, that is, cask k_{eff} decreases with increasing temperature.

7.6 CRITICAL BENCHMARK EXPERIMENTS

In this section, MERIT calculations of critical experiments are discussed. MERIT has been thoroughly verified for programming, sample procedures, particle tracking, random number generation, fission source distribution, statistical evaluation, resonance cross section evaluation, edits and other functions of the program.

7.6.1 Benchmark Experiments and Applicability

The qualification of the MERIT program rests upon extensive qualification studies demonstrating the overall performance of MERIT and the ENDF/V-IV cross section data. Critical experiments include:

1. CSEWG thermal reactor benchmark problems:

   TRX-1, TRX-2, ORNL-1, ORNL-2, PNL-1, PNL-2

2. Babcock & Wilcox Small Lattice Facility

3. USNRC sponsored critical experiments for fuel racks and shipping containers.

The results of these experiments are summarized in Table VII-8.

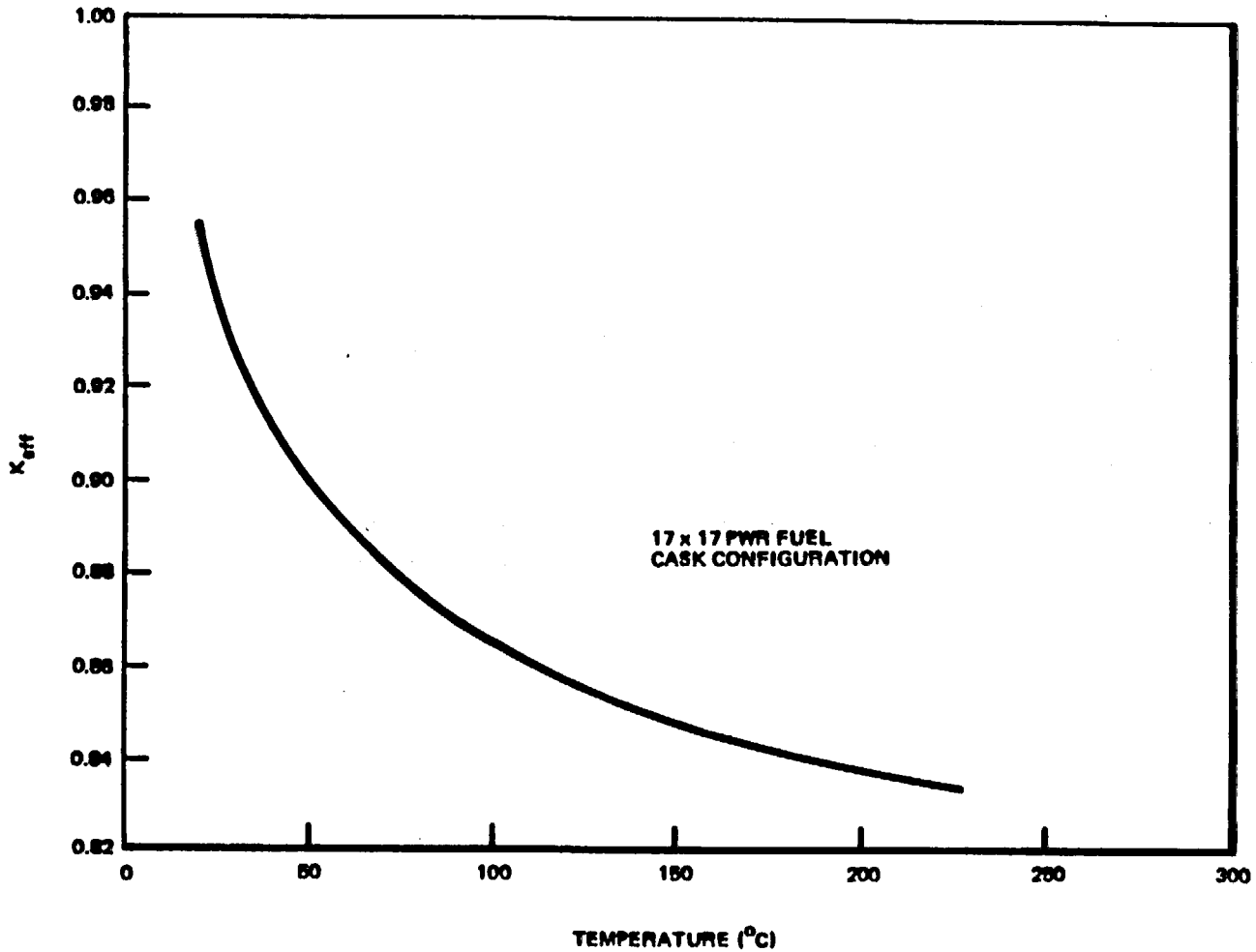

Figure VII-9. Variation of K_{eff} with Water Temperature

Table VII-8

SUMMARY OF CRITICAL EXPERIMENTS

Experiment	MERIT	Reference
(1) ORNL-1	0.9911 ± 0.0028	1
(2) ORNL-2	0.9933 ± 0.0046	1
(3) TRX-1	0.9998 ± 0.0013	1
(4) TRX-2	0.9924 ± 0.0010	1
(5) PNL-1	1.0194 ± 0.0055	1
(6) PNL-2	1.0143 ± 0.0060	1
(7) B&W UO_2	0.9950 ± 0.0021	2
(8) B&W P_uO_2	0.9960 ± 0.0018	3
(9) NRC Criticals		
PNL-2438-020	0.9918 ± 0.0022	4
PNL-2438-033	0.9928 ± 0.0021	4
CR-0073-012	0.9952 ± 0.0028	5

Based on these MERIT qualification programs, a bias of 0.006 ± 0.003 (1σ) Δk has been established with respect to the uranium critical experiments cited in Table VII-8. Therefore, MERIT tends to underpredict K_{eff} by approximately 0.6 percent Δk.

7.7 REFERENCES

1. Cross Section Working Group Benchmark Specifications, ENDF-202 November 1974.

2. M. N. Baldwin, et al., Physics Verification Program - Part III, Babcock & Wilcox (BAW-3647-6), January 1970.

3. G. T. Fairburn, et al., Pu Lattice Experiments in Uniform Test Lattice of UO_2-1.5% PuO_2 Fuel, Babcock & Wilcox (BAW-1357), August 1970.

4. S. R. Bierman, E. D. Clayton, B. M. Durst, "Critical Separation Between Subcritical Clusters of 2.35 Wt. % U_{235} Enriched UO_2 Rods in Water with Fixed Neutron Poisons" (PNL-2438).

5. S. R. Bierman, B. M. Durst, E. D. Clayton, "Critical Separation Between Subcritical Clusters of 4.29 Wt. % U_{235} Enriched UO_2 Rods in Water with Fixed Neutron Poisons" (NUREG/CR-0073).

TABLE OF CONTENTS

VIII. SHIELDING

		Page
8.1	FUEL BASES AND SOURCE TERMS	8-1
8.1.1	8.1.1 Gamma Radiation	8-1
	8.1.2 Fast Neutron Radiation	8-1
8.2	SHIELDING METHODOLOGY	8-6
	8.2.1 Gamma Shielding	8-6
	8.2.2 Neutron Shielding	8-10
	8.2.3 Combined Dose Rate	8-18
	8.2.4 Calculational Results	8-19
8.3	INTERNAL SHIELDING	8-20
8.4	AIR-FILLED CAVITY	8-20
8.5	DOSE-RATE ACCEPTANCE CRITERIA	8-20

LIST OF ILLUSTRATIONS

Figure	Title	Page
VIII-1	Nuclear Reaction Sequence in UO_2 Fuel	8-4
VIII-2	Total Spontaneous Fission and (α, η) Neutron Emission Rate vs. Fuel Burn-Up. 120 Days Cooling	8-5
VIII-3	Geometry of the Shielding Calculational Model Containing Seven PWR Fuel Bundle	8-8
VIII-4	One-Dimensional Calculational Shielding Model with 4.5-Inch Thickness of Water on the Outer Surface of the Proposed IF 300 Shipping Cask	8-9
VIII-5	Uranium Shielding Experiment at ORNL	8-13
VIII-6	Measurement and Calculation for ORNL SNAP Reactor with No Shielding Present	8-15
VIII-7	Measurements and Calculations for ORNL SNAP Reactor Shielded with 4-1/2 Inches of Depleted Uranium	8-16

LIST OF TABLES

Table	Title	Page
VIII-1	Irradiated Fuel Parameters	8-2
VIII-2	Energy Groups	8-2
VIII-3	Gamma Dose Rates by Group	8-7
VIII-4	Material Thicknesses for Side, Flange and Axial Calculations	8-18
VIII-5	Gamma and Neutron Shielding Results	8-19

E

VIII. SHIELDING

8.1 FUEL BASES AND SOURCE TERMS

Section III describes the BWR and PWR design basis fuels and Section IV indicates the maximum number of each type which the IF-300 cask will hold as licensed prior to 1991. Volume 3, Appendices A and B describe BWR and PWR fuels licensed since 1991. Considering 18 BWR bundles or 7 PWR bundles, the latter represents the more severe shielding problem because of its higher specific operating power and higher exposure potential due to greater enrichment. For this reason, the IF-300 cask shielding analysis is based on consideration of 7 PWR design basis bundles. Volume 3, Appendix A describes the shielding analysis for the IF-300 cask with 17 channelled BWR fuel assemblies. Table VIII-1 gives the parameters of both reference fuel loadings for comparison. The source term has two components, gamma and fast neutron.

8.1.1 Gamma Radiation

The gamma source comes from the decay of radioisotopes produced in the fuel during reactor operation. The gamma source strength is a function of fuel operating specific power, irradiation time and cooling time. Table VIII-2 shows a seven group distribution for fuels licensed prior to 1991 (see Volume 3, Appendices A and B for fuels licensed since 1991). The seven group distribution is based on 875 operating days at a specific power of 40 kW/kgU, followed by 120 days of cooling. This forms the shielding computer solution input.

8.1.2 Fast Neutron Radiation

Recent work indicates that light water reactor fuel with a burnup of greater than 20,000 MWd/T will contain sufficient concentrations of transplutonium isotopes to make neutron shielding in a shipping cask a necessity.

The isotopes that form the primary neutron source in high exposure fuel are Curium 242 and Curium 244. In a U-235 fueled reactor, the formation of one atom of CM-242 requires four neutron capture events, while Cm-244 requires six neutron captures. Thus the concentration of these isotopes will depend, roughly on the fuel exposure to the fourth and to the sixth power until the concentrations approach their

TABLE VIII-1

IRRADIATED FUEL PARAMETERS

PWR Parameters:

Specific Power	=	40 kWth/kgU
U/Assembly	=	465 kg
Average Power/Assembly	=	18.28 MWth
Peaking Factor	=	1.2
Peak Power/Assembly	=	21.94 MWth
Power/Basket*	=	153.6 MWth
Vol of 7 bundles	=	1.178×10^6 cm^3

BWR Parameters:

Specific Power	=	30 kWth/kgU
kgU/Assembly	=	198 kgU
Average Power/Assembly	=	5.85 MWth
Peaking Factor	=	1.2
Peak Power/Assembly	=	7.02 MWth
Power/Basket*	=	126.36 MWth
Vol of 18 bundles	=	1.616×10^6 cm^3

*Denotes power of fuel while in reactor

TABLE VIII-2

ENERGY GROUPS

Group	Energy Range	Effective Energy	MEV/Fission
I	>2.6 MeV	2.8 MeV	- NEG -
II	2.2 - 2.6	2.38	1.54×10^{-5}
III	1.8 - 2.2	1.97	4.22×10^{-4}
IV	1.35 - 1.80	1.54	2.42×10^{-4}
V	0.9 - 1.35	1.30	1.08×10^{-4}
VI	0.4 - 0.9	0.80	4.16×10^{-2}
VII	0.1 - 0.4	0.40	6.02×10^{-4}

The seven-group distribution is taken from data published by K. Shure in WAPD-BT-24.

equilibrium values. Because of this, the neutron dose will be small with exposures less than 20,000 MWd/T. Figure VIII-1 show the curium production reaction chain.

The Cm-242 and Cm-244 produce neutrons by two types of mechanisms: spontaneous fission and (α, n) reactions with the oxygen in the fuel. ORNL-4357, "Curium Data Sheets," gives the $^{242}CmO_2$ neutron emission rates as 2.34 x 107 n/sec-gm from (α, n) and 2.02 x 10^7 from spontaneous fission. The (α, n) and spontaneous fission yields of $^{244}CmO_2$ are 5.05 x 10^5 and 5.05 x 10^7 respectively. The document also indicates that the (α, n) and spontaneous fission neutron spectra are quite similar to the energy spectrum of neutrons from thermal fission of U-235.

The concentration of Cm-242 and Cm-244 in spent BWR and PWR fuels of exposures up to ~44,000 MWd/T has been measured and reported in WCAP-6085, BNWL-45 and GEAP-5746. In addition, calculations of the curium concentrations have been made using effective cross sections based on the measured data. These calculations are reported in GEAP-5355, BNWL-1010, and by E.D. Arnold of Oak Ridge National Laboratory. As expected, the Cm-242 and Cm-244 concentrations depend on the spectrum and total fluence seen by the fuel. Thus, for a specified exposure, the magnitude of the curium concentrations for various fuel types will cover a range which is determined by the enrichments and spectra considered. These various measurements and calculations have been combined to yield a band of probable values for neutron emission rate. Figure VIII-2 is a graph of neutron emission rate from Cm-242 and Cm-244 vs. fuel exposure. The upper limit of the band represents low enrichment fuels, the lower limit is for high enrichment fuels.

The design basis neutron source strength for the IF-300 cask is 3 x 10^9 neutrons per second for fuels licensed prior to 1991. Calculations show that the exposure which will yield this source is 35,000 MWd/T for a capacity loading of either BWR or PWR fuel. See Volume 3, Appendices A and B for fuels licensed since 1991.

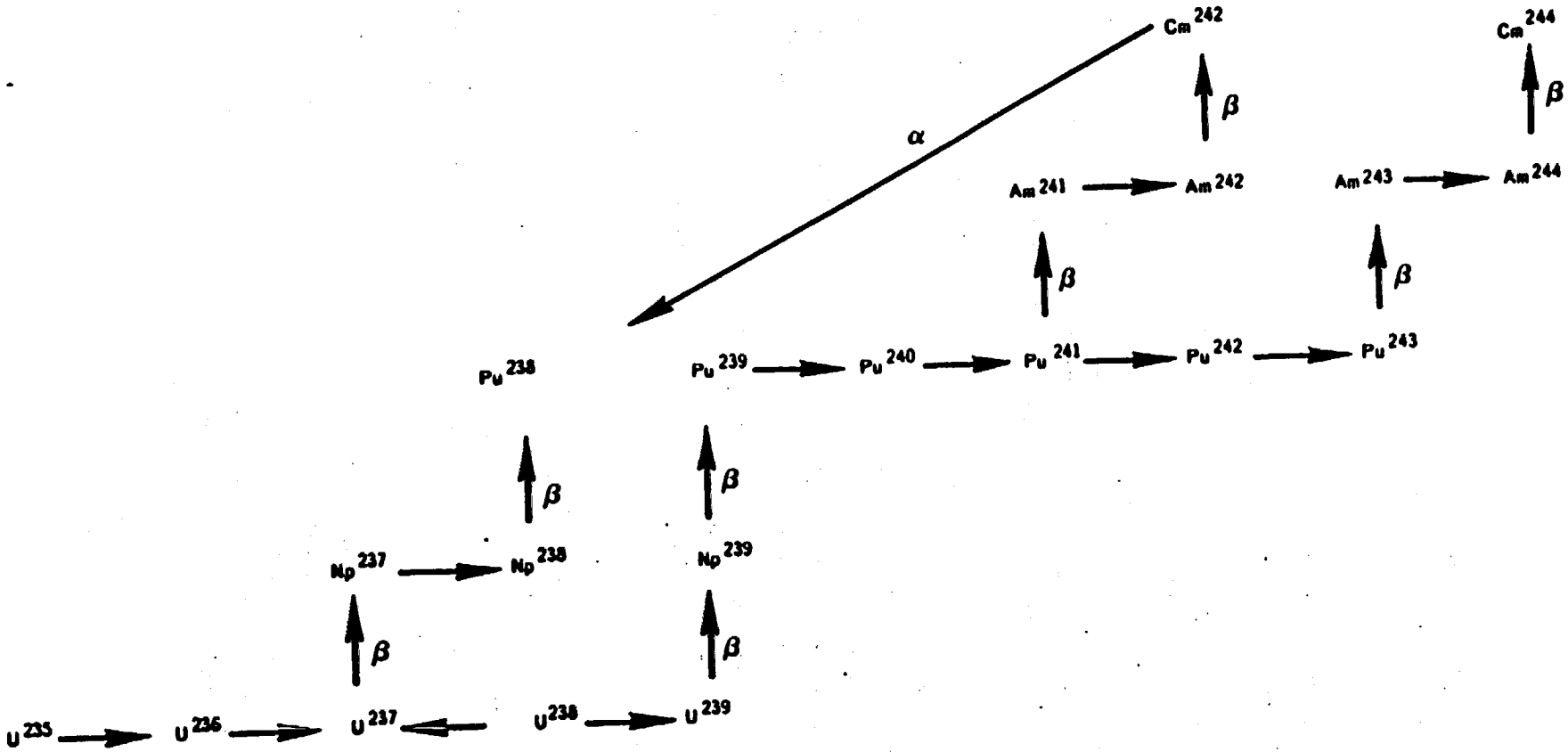

Figure VIII-1 Nuclear Reaction Sequence in UO_2 Fuel

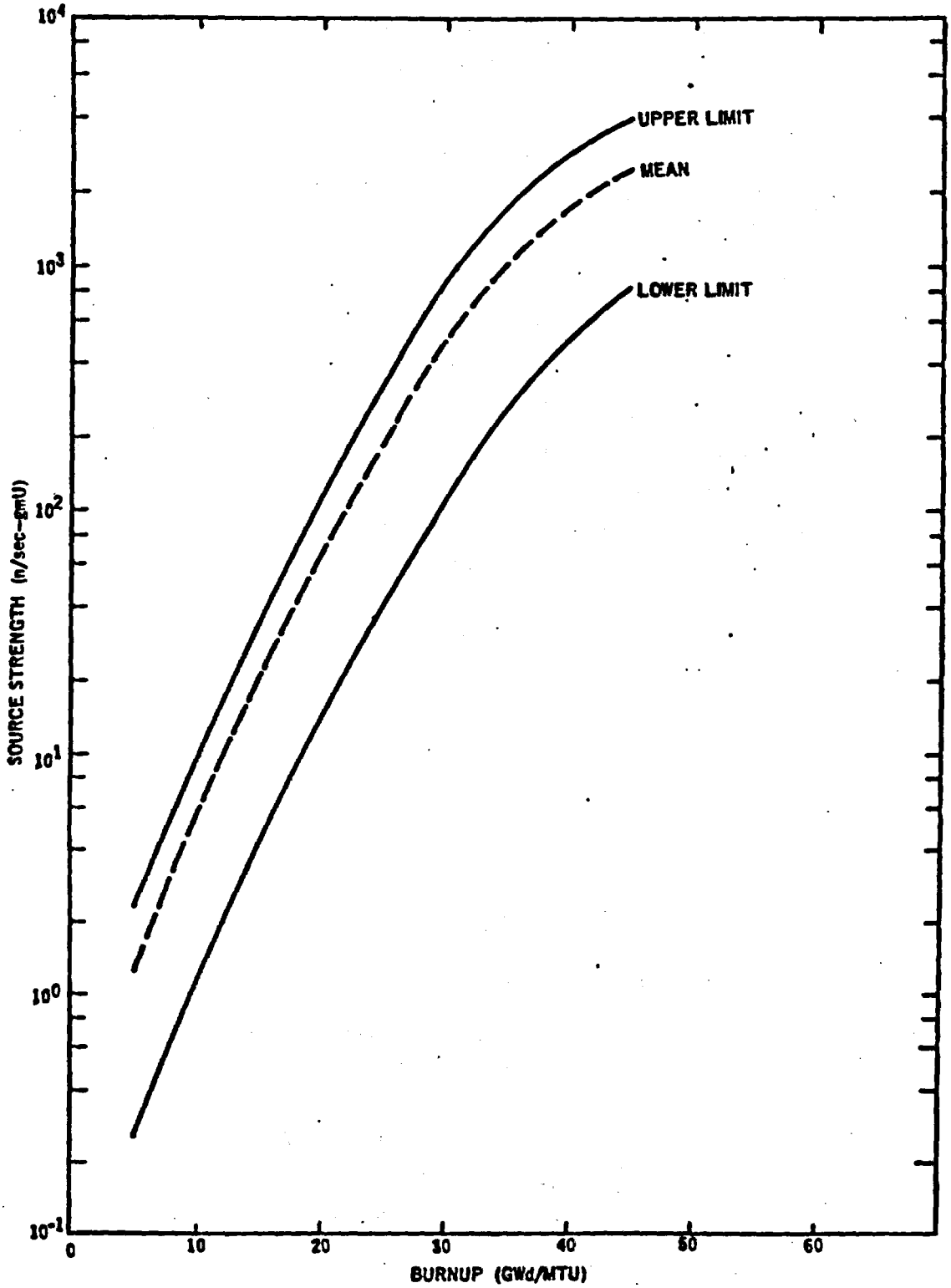

Figure VIII-2 Total Spontaneous Fission and (α, η) Neutron Emission Rate vs. Fuel Burn-Up. 120 Days Cooling.

8.2 SHIELDING METHODOLOGY

Dose rates for normal operation are computed at 10 feet from the cask centerline. This location is also 6 feet from the nearest accessible surface as specified in the regulations. For these computations normal operations means a water-filled cavity. Subsection 8.4 discusses the air-filled cavity case.

8.2.1 Gamma Shielding:

8.2.1.1 The necessary gamma shielding was determined by computer calculations using the QAD* point kernel code system. As seen in Table VIII-2, seven major energy groups were taken into consideration. However, it was found that groups 2, 3, and 4 contribute practically all of the dose. Table VIII-3 shows the dose rate distribution. The effective energies of each group were determined by finding the average energies, E_i, of the respective groups using the expression:

$$E_i = \frac{\int_{G_i} E_i \frac{\mu}{\rho} (E)\, S_\Gamma (E)\, dE}{\int_{G_i} \frac{\mu}{\rho} (D)\, S_\Gamma (E)\, dE} \qquad (1)$$

where:

E_i = average energies in group G_i.

$\frac{\mu}{\rho}$ = Mass attenuation for uranium

S_Γ = Gamma source in photons/fission-sec-watt @ 1000 sec cooling time

Equation (1) will give the average energy per group for a 1000 sec cooling time. However, for a 120 day, 1.04×10^7 sec, cooling time -- which is what the calculation is based upon -- the average energy for each group should be less than that shown in Table VIII-3. Since a 120 day cooling time would represent a softer spectrum, there is some measure of conservatism.

*Richard E. Malenfant, "QAD: A Series of General Purposes Shielding Programs," LA-3573 (April 1967)

TABLE VIII-3

GAMMA DOSE RATES BY GROUP

Group	Effective Energy (MeV)	Dose Rate (mR/hr) 4 inches of Uranium
1	2.8	0.0
2	2.38	0.27
3	1.97	3.80
4	1.54	0.48
5	1.30	0.0
6	0.80	0.0
7	0.40	0.0
	Total Gamma D/R	4.55

The source term was represented as an annular ring of six PWR bundles surrounding one cylindricized PWR bundle (see Figures VIII-3 and VIII-4). For the radial (side) calculations, the assumption was made that the power generated by each bundle is 1.2 times the average. Figure III-3, illustrating power distribution, indicates this is a reasonable assumption since the distribution of fission product gamma sources 120 days after shutdown will be influenced principally by the power distribution during the 120 days of irradiation prior to shutdown.

The QAD-P5A version of the QAD point kernel code system was used to evaluate the IF 300 gamma shielding design. The QAD system is programmed to calculate both fast neutron and gamma-ray penetration of various shield configurations. QAD was not used in this case to compute fast neutron penetration since the results are considered to be less accurate than an ANISN-type calculation.

The QAD system permits source, shield, and detector point geometries to be described in three dimensions. This system provides an estimate of uncollided gamma-ray flux, dose rate and energy deposition at specified detector points.

FIGURE WITHHELD UNDER 10 CFR 2.390

Figure VIII-3 Geometry of the Shielding Calculational Model Containing Seven PWR Fuel Bundles

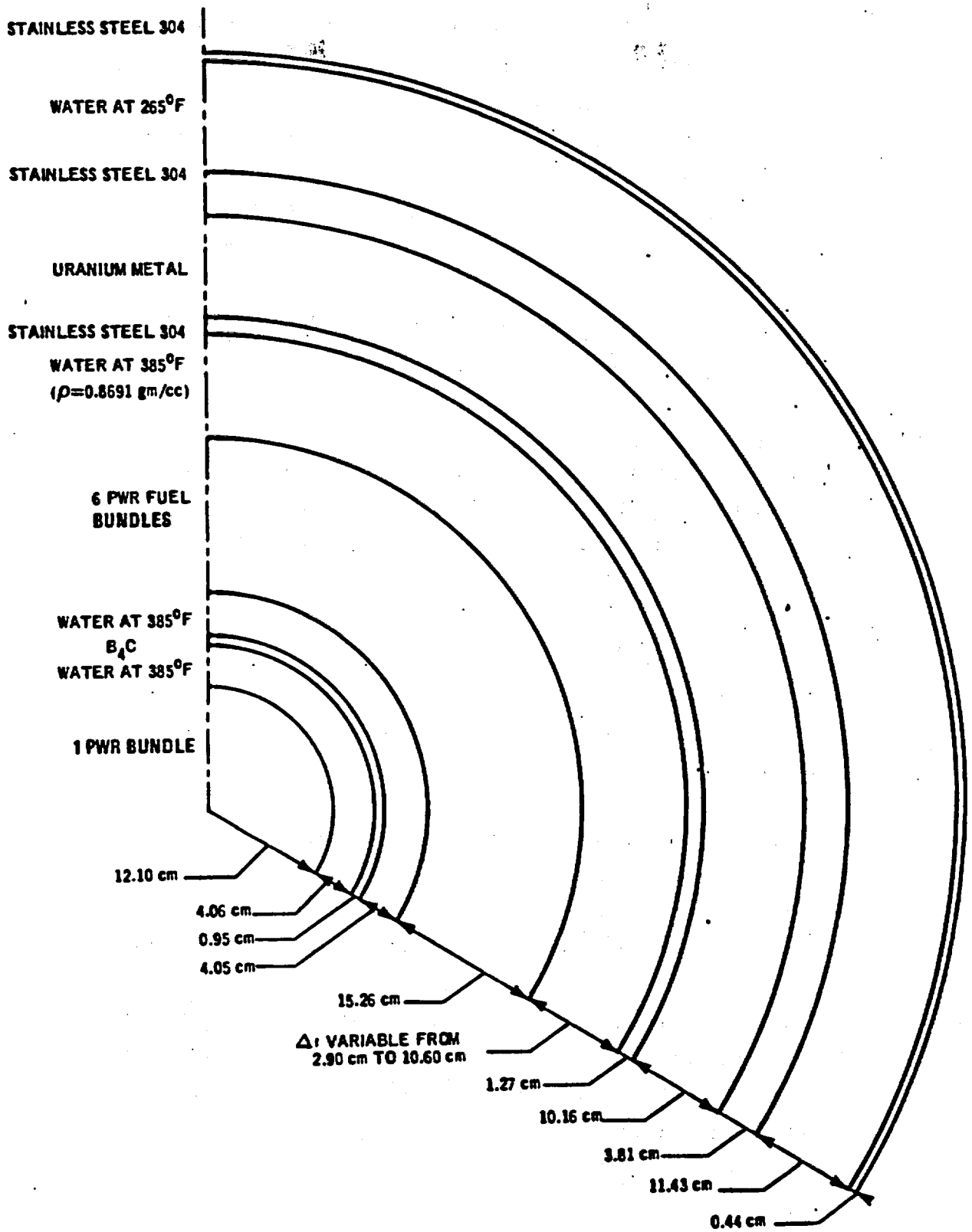

Figure VIII-4 One-Dimensional Calculational Shielding Model with 4.5-Inch Thickness of Water on the Outer Surface of the Proposed IF 300 Shipping Cask

Input data consist of a description of the source distribution and intensity by a number of point isotropic sources and a mathematical representation of the physical geometry with quadratic surfaces. The QAD-P5A version includes a built-in library of gamma-ray attenuation coefficients and buildup factor coefficients. However, since buildup factors for uranium are not included, a correction was applied to the uncollided gamma-ray flux computations.

The gamma shielding results for the IF 300 geometry (Figure VIII-3) are shown in Table II-7.

8.2.2 Neutron Shielding

The If 300 cask geometry (Figures VIII-3 and 4) was analyzed for neutrons shielding considering two basic cases:

- Water within the cask cavity and shielding jacket. (normal case)
- Loss of internal and external shielding water. (accident case).

The neutron source used was 3×10^9 n/sec as described in subsection 8.1.

Due to the complexity of this type of calculation, a computer solution was employed and a benchmark problem was run to confirm the results. The computer code used is designated SN1D. The code uses 27 energy groups ranging from thermal to 16.5 MeV.

8.2.2.1 SN1D is a one-dimensional, discrete ordinates, S_n transport code with general anisotropic scattering. It is a modified version of ANISN, [1] is written in FORTRAN-IV, and is operational on the GE-635 computer.

The major features of the code are:

1. Data is input in a free-style format; this revision to ANISN reduces the number of input errors. Cross sections and sources may be input from tape.

[1] W.W. Engle, Jr., K-1693 (March 30, 1967)

2. Dynamic storage is used for almost all data; SN1D will attempt to find the optimum configuration of fast core memory and peripheral storage for each problem. Peripheral storage of cross sections, fixed sources, fluxes and currents is made only when dictated by the size of the problem.
3. SN1D will solve a wide variety of transport problems. Various boundary conditions are allowed in slab, cylinder and sphere problems. In addition to fixed source and multiplication constant calculations, a number of search options whereby one can vary dimensions, concentrations or cross sections in order to arrive at a predetermined eigenvalue are available. Distributed or shell sources may be specified at any positions within the configuration. In addition, the adjoint calculation can be made.
4. Output includes the eigenvalue, scalar and angular fluxes, sources, any material activities desired (both by interval and zone), neutron balance data, few group condensation and cell homogenization.

The major differences between SN1D, and its predecessor, ANISN, are as follows:

1. As noted above, data is now input in a free-style format.
2. The cross section table format has been revised. Problems having no upscatter are not significantly affected, but storage requirements for upscatter problems are significantly reduced.
3. A provision for entering group and zone dependent bucklings has been added.
4. A provision for temperature correcting the thermal group cross sections has been added.
5. A provision for entering a distributed source from peripheral storage has been added.
6. A provision for peripheral storage, in a distributed source format, of specified activities by interval has been added.

7. A provision for entering the appropriate transverse dimension, effecting only the normalization, has been added.
8. An outer iteration acceleration routine, applied to the fission source, has been added.
9. A Chebyshev acceleration routine, applied to the inner iterations, has been added.
10. Source normalization has been replaced by power normalization.

8.2.2.2 To verify the code and the cross section libraries it was determined that a benchmark problem should be performed. Considerable work has been done with water shields, so the primary objective was to test the uranium cross sections and determine how the code would handle a shield which itself generated a neutron source.

An experiment using uranium shielding was obtained through C.E. Clifford, Oak Ridge National Laboratory. This experiment, illustrated in Figure VIII-5 consist of: (1) a SNAP reactor; (2) a uranium slab; and (3) a detector. The neutron spectrum from the SNAP reactor is very similar to the spectrum resulting from spontaneous fission in Cm-244; and the depleted uranium slab has the same U-235 content as that specified for the cask.

The SN1D calculation was set up the following way:

Referring to Figure VIII-5, an assumed point source, $S_o(1)$, at item 1, is the measured flux, $\phi(3)$, at item 3 multiplied by $4\pi R^2$, where $R^2 = 28$ feet.

$$S_o(1) = 4\pi R^2 \phi(3)$$

If v is the volume of the SNAP reactor, the volume source is,

$$S_v(1) = \frac{S_o(1)}{v \text{ cm}} \phi(3)$$

$S_v(1)$ is the source input for SN1D.

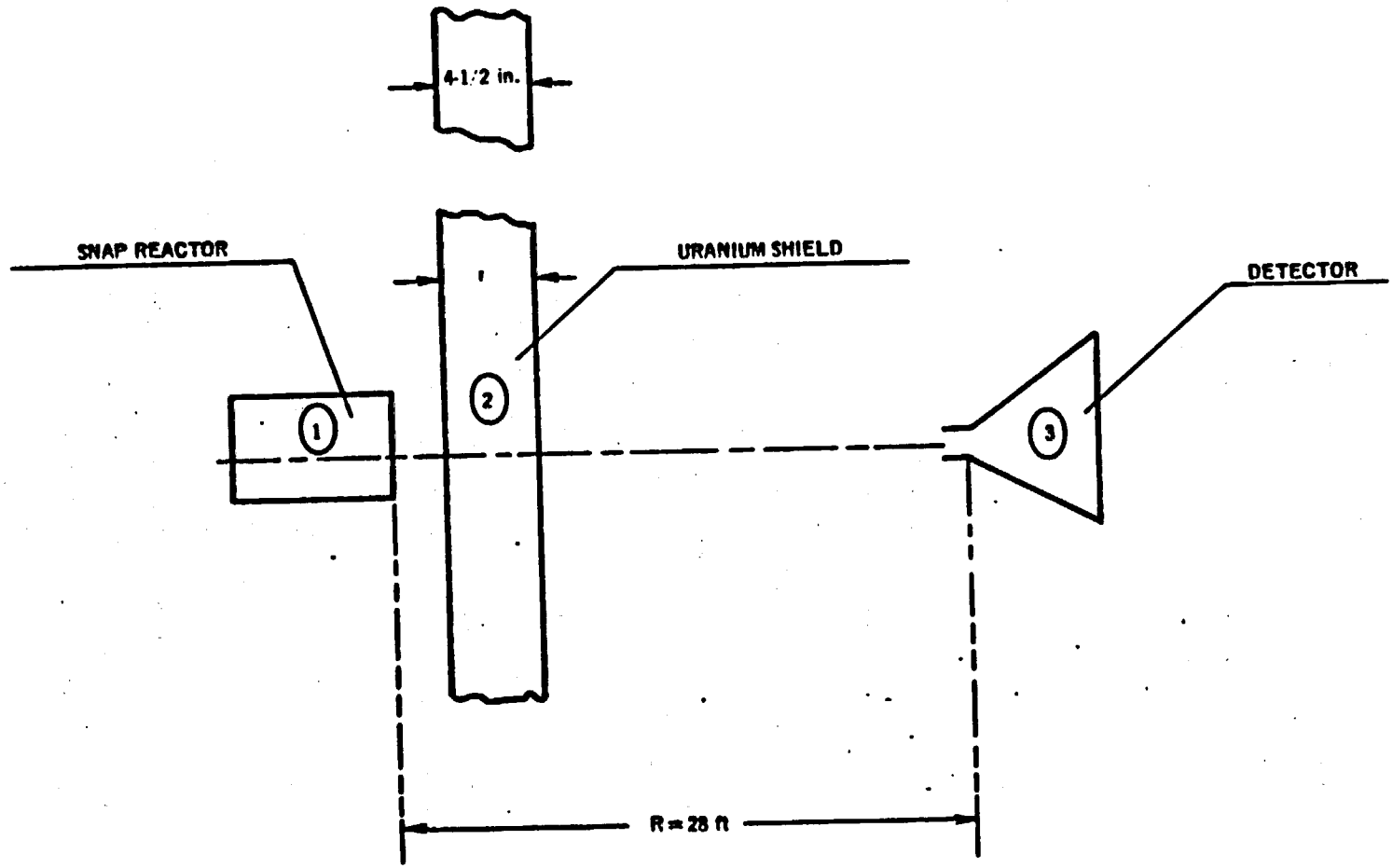

Figure VIII-5 Uranium Shielding Experiment at ORNL

The resulting neutron flux was then calculated at item 3, with and without the uranium shield in place. Calculations were performed both in (P_3, S_6) transport theory and diffusion theory. These are shown in Figures VIII-6 and VIII-7.

The agreement shown between the calculated model and the experiment is strong support for using SN1D and the indicated cross sections to calculate the shield for the IF 300 cask.

The neutron dose rate calculated for the cask primarily results from neutrons with energies greater than 0.2 MeV. Experimental measurements were taken between 0.8 and 15.0 MeV. The results in the test region -- computed versus measured -- imply a calculated accuracy down to at least 0.1 MeV.

8.2.2.3 Figure VIII-3 shows the three areas of concern for shielding purposes. As in the gamma case, the source term was homogenized. Results from the SN1D calculations for the "water" and "no water" cases are shown in Table II-4.

The adequacy of approximating the seven PWR fuel assemblies in the one-dimensional geometry of Figure VIII-4 was verified by running a two-dimensional version of the base radial case. The SN2D results agreed with the one-dimensional approximation to an accuracy of four percent.

The basic concept of this neutron shield involves both the water and the uranium. The hydrogen in the water has a large neutron scattering cross section per unit mass. Because the neutron and proton have about the same mass, the neutron on the average loses about half of its energy at each collision with hydrogen. Hydrogen also has a large capture cross section for thermal and epithermal neutrons. The uranium down scatters neutrons through inelastic collisions. In the thermal and epithermal energy range, uranium has a moderate

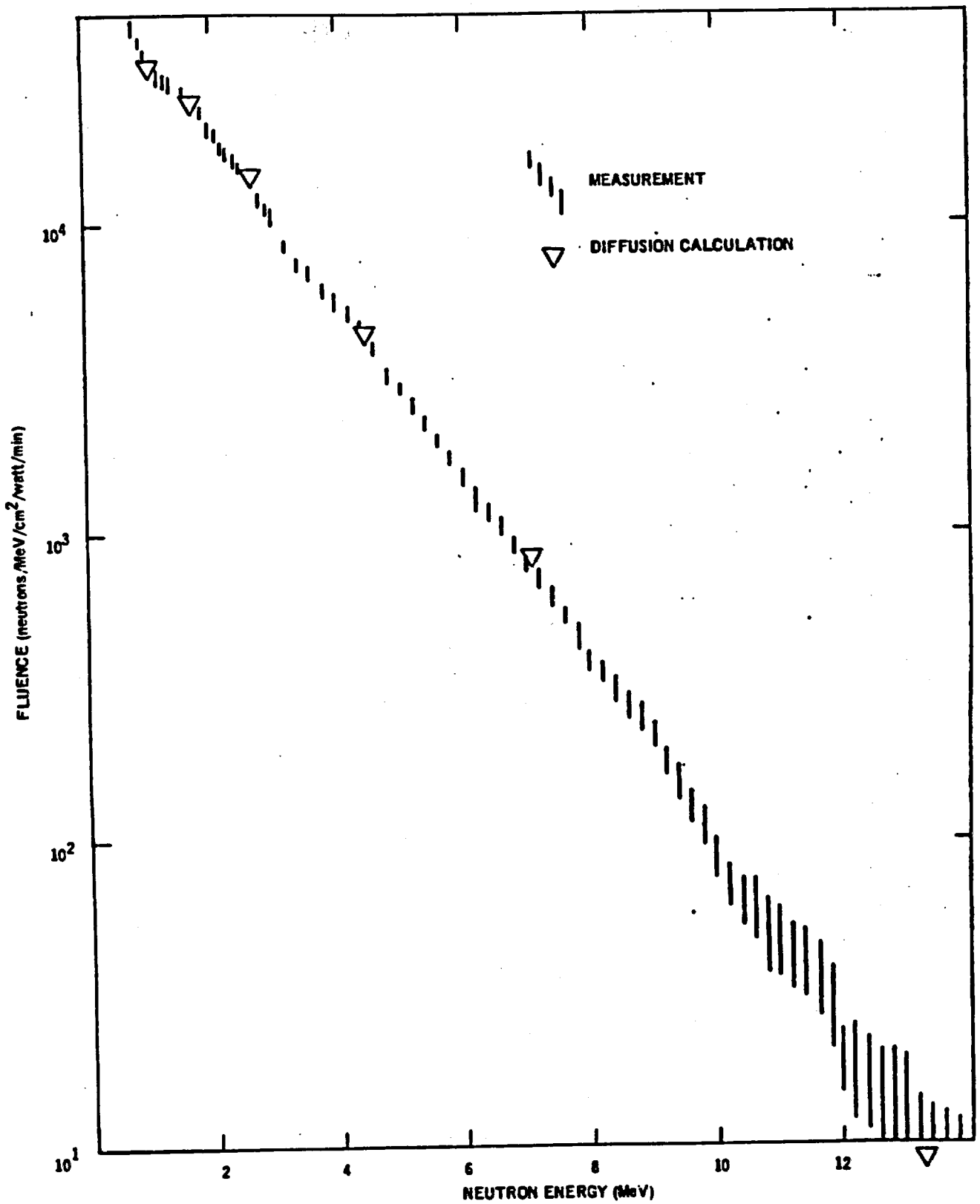

Figure VIII-6 Measurement and Calculation for ORNL SNAP Reactor with No Shielding Present

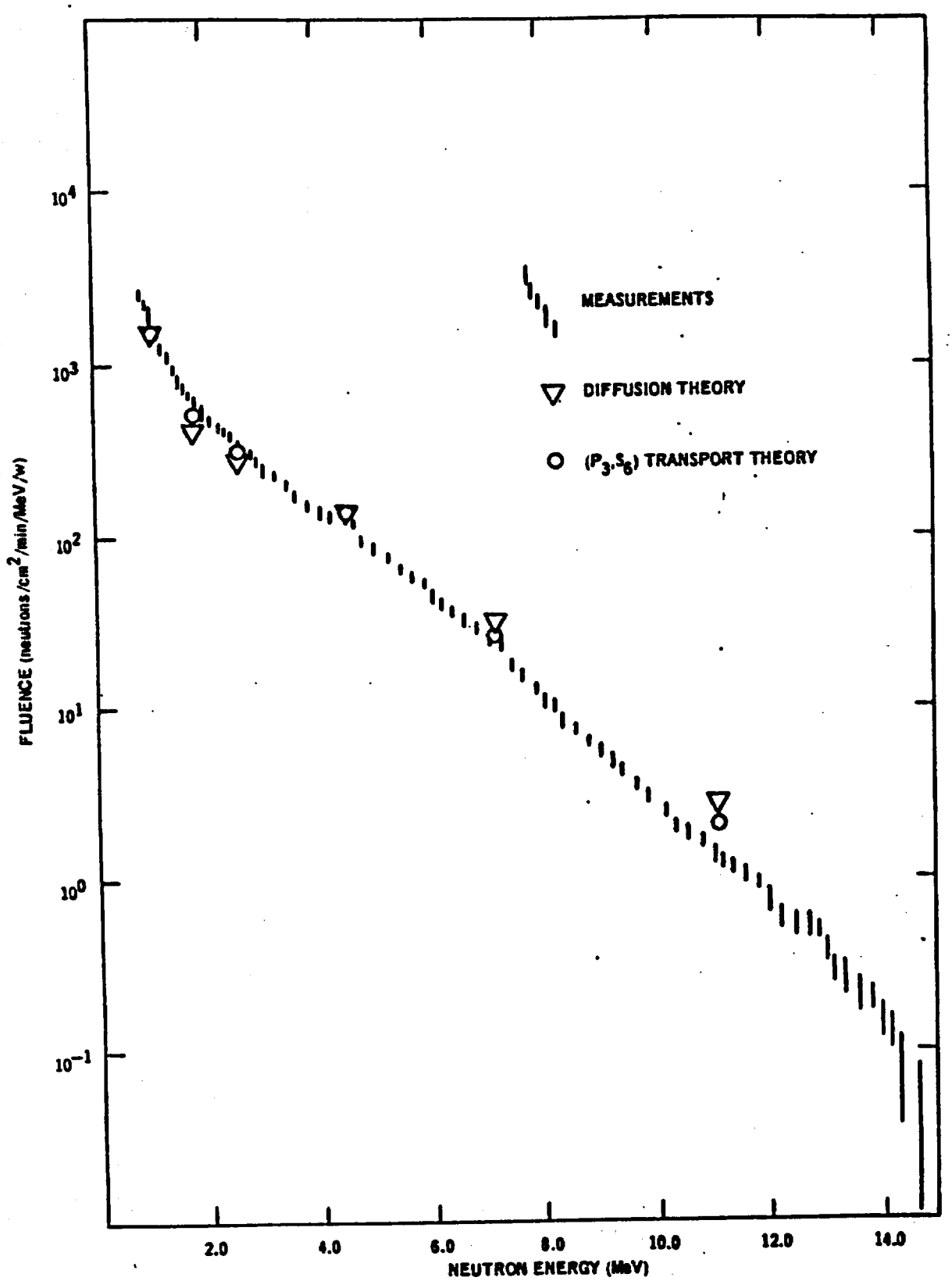

Figure VIII-7. Measurements and calculations for ORNL SNAP Reactor Shielded with 4-1/2 Inches of Depleted Uranium

capture cross section. Thus the combined water/uranium shield reduces the neutron dose rate by (1) decreasing the neutron population by capture, and (2) down scattering the neutrons to a lower energy level resulting in a lower RBE factor. Thus, the uranium acts as both the gamma shield and significant percentage of the neutron shield.

In the accident case where the water is assumed lost, the inelastic scattering in the uranium is still efficient enough to keep the neutron dose rate well below the prescribed limit.

SN1D has been programmed to consider the thermal fissioning of any U-235 in the shield and the source volume as well as the fast fissioning of U-238. Neither of these reactions contribute significantly to the exterior neutron dose rate. The buildup of Pu-239 in the shield is also negligible.

8.2.2.4 The neutron dose rate at the cask flange (P_4) and both ends (P_2 and P_3) was also computed using the SN1D computer program. Slab geometry was assumed for all of these calculations, including the flange. A correction in the neutron source at the ends of the active fuel regions was made based on the end-of-life power distribution as illustrated in Figure III-1.

For comparison, material thicknesses for the side, flange and axial calculations are shown in Table VIII-4.

8.2.2.5 External secondary gamma radiation resulting from neutron captures in the water jacket makes a small but measurable contribution to the gamma dose rate 10 feet from the cask axial centerline.

The assumption was made that all neutrons absorbed in the water region resulted in the emission of a 2.23 MeV gamma photon. Assuming no self-attenuation by the water, the capture gamma dose rate at ten feet from the cask axial centerline was computed to be 0.4 mR/hr.

TABLE VIII-4

MATERIAL THICKNESSES FOR SIDE, FLANGE AND AXIAL CALCULATIONS

			Axial	
Material	Side (in.)	Flange (in.)	Top-End (in.)	Bottom-End (in.)
Water	2.2-4.2	18.00	18.00	6.00
Stainless Steel	0.50	6.50	1.00	1.00
Uranium	4.00	-	3.00	3.75
Stainless Steel	1.50	-	1.50	1.50
Water	5.0-7.0	-	-	-
Stainless Steel	0.125	-	-	-

8.2.2.6 Table VIII-4 shows that for the side shielding case, the interior water thickness varies from 2.2 to 4.2 inches and the exterior water thickness varies from 5.0 to 7.0 inches. The variation in these dimensions is a result of irregular geometry in the former case and the corrugated exterior in the latter.

Considering the average thicknesses of both components, the resulting neutron dose rate was calculated to be 3.3 mRem/hr. Local variations at the cask surface due to interior geometry become undetectable at the distance of 6 feet from the accessible surface. These local variations are never more than a factor of two higher than the surface average. The peak dose-rate on the nearest accessible surface is substantially less than the 200 mR/hr limit.

8.2.3 Combined Dose Rate

Table VIII-5 tabulates the combined dose rates for the side, flange and ends of the IF300 shipping cask.

The gamma and neutron dose rates were first computed for the cask geometry as shown in Figures VIII-3 and VIII-4, and then corrected for the variable geometry and the secondary gamma radiation. Both components have been multiplied by an axial peaking factor of 1.2 (see Figure III-1). The resulting combined dose rate at ten feet from

the cask axial centerline (six feet from the nearest accessible surface) is the side of the screened and locked enclosure. This enclosure extends to the edge of the eight-foot wide equipment skid. Since the cask centerline is on the skid centerline, a point six feet from the skid edge is also ten feet from the cask centerline (see Section IV - Equipment Description).

TABLE VIII-5

GAMMA AND NEUTRON SHIELDING RESULTS*

	R_{10} 10 ft from Cask Centerline	R_3 Accident 3 ft from Cask Surface	F_9 9 ft from Flange	T_9 9 ft from Top Head	B_9 9 ft from Bottom End
Gamma (mr/hr)	5.46	17.6	< 0.2	3.0	2.8
Neutron (mRem/hr)**	3.96	440.0	< 0.02	≤ 0.6	0.4
Total (mRem/hr)	9.42	457.6	< 0.22	≤ 3.6	3.2
Regulatory Limit (mRem/hr)***	10	1000	10	10	10

* Locations of R_{10}, R_3, F_9, T_9, and B_9 illustrated in Figure VIII-3 for fuels licensed prior to 1991. See Volume 3, Appendices A and B for fuels licensed since 1991.

** Includes fission in uranium shield.

*** 10CFR71 and 49CFR173.

8.2.4 Calculational Results:

49CFR173 prescribes the allowable dose rates as 10 mr/hr total radiation at a point 6 feet from the nearest accessible surface of the package equidistant from the ends; or 200 mr/hr at the cask surface, whichever is greater. The former pertains to the IF-300 cask. Furthermore, 10CFR71 specifies a limit of 1 R/hr three feet from the cask surface following the accident conditions. Table VIII-5 indicates that the IF-300 cask shielding meets both normal and accident shielding requirements.

8.3 INTERNAL SHIELDING

Supplementary shielding has been added to the upper end of the BWR fuel basket. The computer analysis of these stainless steel-clad uranium metal components and their supporting structures is contained as an appendix to the structures analysis Section V of this SAR.

8.4 AIR-FILLED CAVITY SHIELDING

The IF-300 cask cavity may be air-filled rather than water-filled provided the heat load is less than 40,000 Btu/hr. This low decay heat rate can be produced by various combinations of fuel exposure and cooling time (i.e. high exposure - long cooled, low exposure - short cooled, etc.)

For dry shipments the reduced allowable heat load reduces the gamma and neutron source strengths. The expected dose rates under both accident and normal conditions are less than dose rates calculated for wet shipments.

8.5 DOSE-RATE ACCEPTANCE CRITERIA

10CFR, § 71.51(a)(2) limits the post-accident dose rate to 1,000 millirems per hour at 3 feet from the external surface of the package. The IF-300 cask contents must be so limited as to meet § 71.51(a)(2). This limitation is implemented by applying multipliers to the normal condition dose rate measurements which are taken prior to shipment. If the sum of the adjusted measurements exceeds an established value the shipment cannot be made.

8.5.1 The measurements, adjustments and limits are applied as follows:

$$(\text{Gamma D/R})(11.3) + (\text{Neutron D/R})(111.0) \leq 1{,}000 \text{ mr/hr}$$

The gamma and neutron dose rate measurements are to be taken at a distance of 6 feet from the side of the cask skid (10 feet from the cask centerline). These measurements have been normalized to normal conditions as calculated in Section 8.5.2.

8.5.2 Basis for Multipliers

Table VIII-5 gives the calculated dose rates for both normal and accident conditions. The ratio of R_3 to R_{10} represents the increase in dose rate from normal conditions at 10 feet from the cask centerline to accident conditions at three feet from the cask surface (R_3/R_{10}). The 3 foot accident limit is 1000 millirem per hour.

8.5.2.1 Gamma Multiplier

From Table VIII-5, the gamma R_3/R_{10} ratio is:

$$(R_3/R_{10}) = \frac{17.6}{5.46} = 3.22$$

Calculations indicate that as a result of the cask side drop there could be a 1/8 inch wide separation of the interface between two stepped uranium shielding pieces. This gap increases the gamma dose rate by a factor of 3.5. Thus the gamma multiplier is:

$$\text{Gamma multiplier} = 3.22 \times 3.5$$
$$= 11.3$$

8.5.2.2 Neutron Multiplier

From Table VIII-5 the neutron R_3/R_{10} ratio is

$$(R_3/R_{10}) = \frac{440.0}{3.96} = 111.0$$

The 1/8 inch shielding separation discussed in 8.5.2.1 does not effect the neutron dose rate thus the neutron multiplier is the R_3/R_{10} ratio.

$$\text{Neutron multiplier} = 111.0$$

TABLE OF CONTENTS

IX. SAFETY COMPLIANCE

			Page
9.1	INTRODUCTION		9-1
9.2	10CFR71		9-1
	9.2.1	General Standards for All Packaging (71.31)	9-1
	9.2.1.1	No Internal Reactions	9-1
	9.2.1.2	Positive Closure	9-1
	9.2.1.3	Lifting Devices	9-1
	9.2.1.4	Tie Down Devices	9-2
	9.2.2	Structural Standards for Large Quantity Shipping (71.32)	9-2
	9.2.2.1	Load Resistance	9-2
	9.2.2.2	External Pressure	9-2
	9.2.3	Criticality Standards for Fissile Material Packages (71.33)	9-2
	9.2.3.1	Maximum Credible Configuration	9-2
	9.2.3.2	Optimal Moderation	9-3
	9.2.3.3	Fully Reflected	9-3
	9.2.3.4	Results	9-3
	9.2.4	Evaluation of a Single Package (71.34)	9-3
	9.2.5	Standards for Normal Conditions of Transport for a Single Package (71.35)	9-3
	9.2.6	Standards for Hypothetical Accident Conditions for a Single Package (71.36)	9-4
9.3	49CFR173		9-4
	9.3.1	General Packaging Requirements (173.393)	9-4
9.4	SECTION GUIDE		9-5
9.5	BASIC COMPONENTS		9-6

LIST OF TABLES

Table	Title	Page
IX-1	IF-300 Basic Components	9-7

IX. SAFETY COMPLIANCE

9.1 INTRODUCTION

This section is designed to recap and summate this report in light of the requirements of 10CFR71 - Subpart C, and 49CFR173.

9.2 10CFR71

9.2.1 General Standards for All Packaging

9.2.1.1 No Internal Reactions

The cask surfaces and the fuel baskets are stainless steel. This material does not react with steam or water either chemically or galvanically. The fuel is designed to be nonreactive in waterfilled systems. The uranium shield is totally clad in stainless steel. A copper diffusion barrier separates the stainless steel from the uranium to prevent the formation of an alloy under high temperature conditions. The entire shipping package is chemically and galvanically inert.

9.2.1.2 Positive Closure

The IF-300 cask head is held in place by 32 bolted studs. The mating flanges are designed to accept a Grayloc metallic gasket with a minimum design pressure of 600 psi. Shear steps are provided in the flange to prevent damage to the gasket under impact. Two tapered guide pins ensure proper head alignment during installation.

9.2.1.3 Lifting Devices

The analysis of Section V indicates that the lifting structures of both the cask and the lid are capable of supporting three times their respective weights without generating stresses in excess of their yield strengths (FS > 1.0).

The cask design is such that there are no possible lifting points other than those intended. In addition, the failure of any of the intended lifting structures will not result in a redistribution of shielding or a loss of cask integrity.

9.2.1.4 Tie Down Devices

Section V shows that both the front and rear cask supports are capable of sustaining the combined 10 g longitudinal, 5 g transverse and 2 g vertical forces without generating stresses in excess of their yield strengths (FS > 1.0).

The cask is designed to have only one tiedown method. The failure of either, or both, supports will not impair the ability of the package to meet other requirements. There will be no shielding redistribution or loss of cask integrity.

9.2.2 Structural Standards for Large Quantity Shipping

9.2.2.1 Load Resistance

With the package considered as a simple beam loaded with five times its own weight, the cask body outer shell safety factors in shear and bending are 20.4 and 8.6 respectively, based on allowable stresses.

9.2.2.2 External Pressure

When subjected to an external pressure of 25 psig, the package outer shell safety factors in elastic stability and axial failure exceed unity, based on allowable stresses.

9.2.3 Criticality Standards for Fissile Material Packages

This section addresses the 7-cell PWR and 18-cell BWR fuel baskets licensed prior to 1991. Volume 3, Appendices A and B address fuels and baskets licensed since 1991.

9.2.3.1 Maximum Credible Configuration

Fuel element spacing is provided by the stainless steel basket. The stress analysis of Section V shows that during accident conditions there is no redistribution of fuel. The normal transport arrangement is the maximum credible configuration.

9.2.3.2 Optimal Moderation

The criticality analysis of Section VII shows that the water filled cask is the most reactive configuration. There is a significant reduction in K_{eff} as the water density is reduced.

9.2.3.3 Fully Reflected

The criticality analysis used full reflection as part of calculation. The presence of depleted uranium as a shield makes the cask highly reflective by design.

9.2.3.4 Results

Calculations show that both of the reference design fuel loadings have a K_{eff} significantly less than 0.95 under the above conditions. Both the BWR and PWR baskets require criticality control. This is accomplished using boron carbide-filled rods, fixed to the basket structure.

9.2.4 Evaluation of a Single Package

The IF 300 spend fuel shipping cask was designed for both the normal transport and hypothetical accident conditions of 10CFR71. The effects of these conditions were evaluated using standard computational techniques. It was considered unnecessary to perform model testing. The completed cask will have undergone a series of thermal demonstration tests prior to acceptance (see Section VI).

The cask tiedowns have been sized only for the normal transportation conditions. Only the cask is considered under the accident criteria.

9.2.5 Standards for Normal Conditions of Transport for a Single Package

The thermal analysis of Section VI considers the cases of 130°F still air and -40°F still air. The stress analysis and material description of Section V discusses the 0.5 times atmospheric pressure and the water spray criteria. The penetration test and the free drop fall within the accident analysis of Section V.

The IF 300 cask is so designed that there will be no release of radioactive material or coolant. The contained coolant activity will remain below the limits prescribed in 10CFR 71. And, there is neither a loss of package effectiveness nor a gas or vapor mixture which, upon ignition, could lead to a loss of effectiveness.

The analysis of Section VII indicates that even in the most reactive condition, the cask contents remain substantially subcritical. The package and contents geometries remain unchanged under all normal conditions of transport.

9.2.6 Standards for Hypothetical Accident Conditions for a Single Package

Section V analyzes the effects of the 30-foot free drop and the 40-inch puncture tests on the IF 300 cask. Section VI examines the 30-minute fire criteria.

Under the hypothetical accident conditions, the external radiation (gamma and neutron) is less than 1 R/hr at 3 feet from the cask. Under the assumed loss of shielding water condition and following the 30 minute fire, no radioactive releases are made from the cask.

There is no redistribution of fissile material to a more reactive condition following the hypothetical accident. The Section VII analysis indicates that the normal shipping configuration is the most reactive array. The basic package geometry remains unchanged under the hypothetical accident conditions.

9.3 49CFR173

9.3.1 General Packaging Requirements

The IF 300 cask in meeting the requirements of 10CFR71 also complies with the criteria under 49CFR173. The only non-current requirement is normal shipping dose rate. Article 173.393 limits the cask dose rate at six feet from the nearest accessible surface to 10 mr/hr. Section VIII shows that this criteria is adequately met.

All cask closure nuts will be safety wired prior to shipment. In addition, enclosure access doors and panels are locked during transit.

Under the normal shipping conditions, the nearest accessible surface temperature remains below the 180°F limit.

9.4 BASIC COMPONENTS (Safety Related) E

Certain components and structures of the IF-300 casks are safety related and as such are identified as Basic Components. Basic Components of the IF-300 are listed in Table IX-1 according to their nuclear functions which are a) containment of radioactive material within 10CFR71 limits, b) nuclear shielding, and c) criticality control. IF-300 Basic Components are designed, fabricated, assembled, tested, used and maintained under an NRC approved quality assurance program that satisfies the requirements in 10CFR71 Subpart H, "Quality Assurance". E

Table IX-1
IF-300 BASIC COMPONENTS
(Safety Related)

I. CONTAINMENT

- Cavity End Plate
- Inner Shell
- Vent Pipe Assembly
- Locating Key
- Body Flange
- PWR Head Forging
- PWR Head Subassembly
- BWR Head Forging
- BWR Head Liner
- Trunnion Assembly
- Valve Boxes
- BWR Head End Plate
- BWR Head Liner Ring
- BWR Sleeve Nuts
- PWR Sleeve Nuts
- Studs
- Cavity Globe Valves
- Valve Pipe Cap or Plugs
- Valve Hardware
- Grayloc Seal Ring
- Fins
- Cavity Drain Line Assembly
- Rupture Disk Device

II. NUCLEAR SHIELDING

Uranium shield (cask barrel, closure head, bottom; basket shield), Neutron shield (corrugated barrel, valve boxes, expansion tank, piping, valves, blind flanges, liquid.)

III. CRITICALITY CONTROL

BWR Baskets
PWR Basket

nutech
INTERNATIONAL

TABLE OF CONTENTS

X. OPERATION, MAINTENANCE AND TESTING

			Page
10.1	OPERATING PROCEDURES		10-1
	10.1.1	Procedures for Cask Loading	10-1
	10.1.2	Procedures for Unloading the Package	10-2
	10.1.3	Transport of an Empty Cask with Type B Contents	10-6
	10.1.4	Transport of an Empty Cask with Less Than Type B Contents	10-6
10.2	MAINTENANCE PROCEDURES		10-7
	10.2.1	Annual Inspections	10-7
	10.2.2	Annual Component Replacement	10-8
	10.2.3	Annual Leakage Testing	10-8
10.3	TESTING		10-8
	10.3.1	Tests at Fabrication	10-8
	10.3.2	Leakage Testing	10-9
10.4	REFERENCES		10-15

N

LIST OF TABLES

Table	Title	Page
X-1	Crud and Fission Gas Release Fractions	10-11
X-2	Inputs to Leakage Path Diameter Calculations	10-13

N

X. OPERATION, MAINTENANCE, AND TESTING

10.1 OPERATING PROCEDURES

Instructions for use of the IF-300 Transportation System are published in the General Electric document "Operating Instructions, IF-300 Irradiated Fuel Transportation System", GEI-92817. This manual describes the complete handling sequence for preparation, loading, transport, and unloading. The manual is used for operator training as well as on-the-job direction. During actual operation of the cask the manual may be supplemented with a General Electric technical advisor, training classes, and site specific procedures, as applicable.

The operating procedures are summarized below:

10.1.1 Procedures for Cask Loading

Operations at the loading facility include the span of activities from receiving and inspecting the cask to preparing the loaded cask for shipment. Each loading facility must provide fully trained personnel and detailed operating procedures to cover all of the activities. N

10.1.1.1 Cask Receiving and Inspection

a. The IF-300 railroad car is oriented, chocked, and braked.
b. A visual inspection for damage and leakage is made and a radiological survey of the cask is initiated in accordance with the requirements of 10CFR20.

10.1.1.2 Preparing for Cask Removal from the Rail Car

a. The cask enclosures are opened.
b. The valve box covers are removed.
c. Cask tie-down pins are removed and the lifting trunnions are installed.
d. The cask lifting yoke is picked up and engaged with the cask trunnions.
e. Proper engagement of the yoke hooks and trunnions is verified.

10.1.1.3 Moving the Cask to the Preparation Area

a. The cask is rotated to the vertical position, lifted free of the tilting cradle, moved to the preparation area, and set down.

10.1.1.4 Preparing to Load the Cask

a. The cask lifting yoke is removed from the cask and set aside.
b. The cask exterior is cleaned and the inner cavity filled with water.
c. The cask head sleeve nuts are loosened and removed.
d. The yoke is repositioned on the cask and the head removal cables are inspected, attached and adjusted.
e. The cask is lifted and lowered into the loading basin.
f. The cask is lowered to the basin floor and the yoke is disengaged.
g. The cask closure head is removed.
h. The head is raised out of the basin, rinsed, inspected, and stored.
i. The cask cavity is inspected to verify, for irradiated fuel shipments, that the proper fuel baskets are in place or, for irradiated hardware shipments, that the inner cavity is empty.

10.1.1.5 Loading Irradiated Fuel into the Cask

a. The list of irradiated fuel bundles, transfer procedure, and cask loading diagram are obtained.
b. Fuel bundles are grappled one at a time and moved to the appropriate cell in the basket. Fuel assembly seating is verified.
c. The identification marking is verified for each fuel bundle moved and the records are correspondingly marked.

N

10.1.1.6 Loading Irradiated Hardware

a. A cask liner for the hardware to be transported is placed in the loading basin.
b. The hardware is loaded into the liner using appropriate component spacers to limit the movement of the hardware.
c. The liner cover is installed and the liner lifted and placed in the IF-300 cask.

10.1.1.7 Installing the Cask Closure Head

a. The cask closure head is lifted and the gasket and gasket retaining clips are inspected for damage or looseness.
b. The head is slowly lowered onto the cask over the guide pins. This operation is closely watched to assure that the head is properly aligned.

10.1.1.8 Returning the Cask to the Preparation Area

a. The yoke is re-engaged with the cask trunnions.
b. The connection is visually inspected to verify proper engagement.

c. The cask is slowly raised (while monitoring radiation levels) until the top of the cask reaches the level of the fuel pool curb.
d. Four cask closure head sleeve nuts are installed, hand tight.
e. The cask is removed from the pool (while again monitoring radiation levels), washed, and placed in the preparation area.
f. The yoke is removed and set aside.

10.1.1.9 Securing the Cask Closure Head

a. Parallelism of the head and cask flanges is tested and the head sleeve nuts are torqued to 370 ft-lbs minimum.
b. After metal-to-metal contact (.007 inch gap or less) is achieved between the head and cask flanges, the head sleeve nuts are lockwired for security.

10.1.1.10 Flushing of the Cask Inner Cavity

a. When desired, the cask inner cavity may be flushed with demineralized water until sample analysis conforms with pre-determined limits. This step is not mandatory.

10.1.1.11 Draining of the Cask Inner Cavity N

a. A pressure regulated helium supply is connected to the cask cavity vent valve.
b. A drain hose is connected to the cask cavity fill/drain valve and directed into a radwaste drain or back into the pool.
c. After opening the cask cavity vent and fill/drain valves, helium is introduced through the vent valve at 15 psig.
d. When helium is observed to flow out of the cask cavity drain hose, the fill/drain valve is closed and the cask cavity pressurized to 15 psig.
e. The drain hose is removed.
f. The cask cavity vent valve is closed and the helium supply removed.

10.1.1.12 Assembly Verification Leakage Testing

a. Leakage testing of the cask closure seal, vent valve, fill/drain valve, and rupture disk device is performed with a thermal conductivity sensing instrument. This type of instrument is sensitive to any gas stream having a thermal conductivity different from the ambient air in which the instrument is being used.
b. The test instrument is set up and used according to written procedures and the manufacturer's instructions.
c. With the instrument calibrated to a sensitivity of at least 2×10^{-1} cm^3/sec (helium), the vent valve, fill/drain valve, and rupture disk device are checked for indications of leakage.

d. With the instrument calibrated to a sensitivity of at least 2 x 10^{-2} cm^3/sec (helium), the closure seal is checked for indications of leakage. (The sensitivity of this test is increased to account for the dilution which would occur between a potential point of closure seal leakage and the nearest point of measurement.)

e. If leakage is detected during either of the above checks, the offending components are repaired or replaced and then re-tested for leakage.

f. Valve must be checked to be open if pipe cap or plugs are used.

10.1.1.13 Preparing the cask for Transport of Irradiated Fuel

a. Steps 10.1.1.11a thru c are repeated. Nitrogen may be used to supply the third cask volume of inert gas.

b. The supply of helium (nitrogen) is discontinued when at least one additional cask volume has been supplied to the inner cavity. (One cask volume equals 83 cubic feet when shipping irradiated fuel.)

c. the excess helium (nitrogen) within the inner cavity is bled off thru the fill/drain valve until the cavity pressure has decayed to 0 psig. This completes the process of inerting the cask cavity.

d. The vent and fill/drain valve is closed and the connecting hoses and gages are removed.

e. The cask, skid, and rail car are decontaminated in accordance with regulatory requirements.

f. The cask is lifted with the yoke, positioned on the tilting cradle, and lowered to its horizontal position.

g. The yoke is removed.

h. The trunnions are removed and the cask tiedown pins installed.

i. The valve box covers are replaced.

j. The radiological survey of the cask and rail car is completed.

10.1.1.14 Preparing the Cask for Transport of Irradiated Hardware

a. A drain hose is connected to the cask cavity fill/drain valve and directed into a radwaste drain or back into the pool.

b. Steps 10.1.1.13c thru j are repeated.

10.1.1.15 Closing the Equipment Skid

a. The cask enclosures are closed, locked, and sealed.

10.1.2 Procedures for Unloading the Package

Operations at the unloading facility are largely the same as loading operations with the major exception being the increased radiological awareness required for receiving a loaded cask. Each unloading facility must provide fully trained personnel and detailed operating procedures to cover all activities.

10.1.2.1 Cask Receiving and Inspection

a. Steps 10.1.1.1a and b are repeated.

10.1.2.2 Preparing for Cask Removal from the Rail Car

a. Steps 10.1.1.2a thru e are repeated.
b. The cask inner cavity temperature may be recorded prior to disconnecting the thermocouple.

10.1.2.3 Moving the Cask to the Preparation Area

a. Step 10.1.1.3a is repeated.
b. If the cask inner cavity temperature was not recorded in step 10.1.2.2b, it is now recorded.

10.1.2.4 Preparing to Unload Irradiated Fuel

a. Steps 10.1.1.4a and b are repeated.
b. A pressure gage is installed on the vent line.
c. The cask cavity is flushed and sampled, giving due consideration to the cask internal temperature and pressure. N
d. The cask head sleeve nuts are loosened and all but four are removed.
e. The yoke is repositioned on the cask and the head removal cables are inspected, attached, and adjusted.
f. the cask is lifted from the preparation area and lowered into the loading basin. The last four sleeve nuts are removed while the cask is suspended over the basin with the top of the cask one foot above the water.
g. Steps 10.1.1.4f thru h are repeated.

10.1.2.5 Preparing to Unload Irradiated Hardware

a. If the cask is to be unloaded underwater, steps 10.1.2.4a thru d are followed.
b. If the cask is to be unloaded in air at a waste disposal site, the cask is cleaned and prepared for unloading following a procedure developed by the burial site, reviewed by General Electric, and tested in a dry run at the burial site using unirradiated hardware.
c. The disposal site procedure will specify when and where the cask head sleeve nuts will be loosened and removed.

10.1.2.6 Unloading Irradiated Fuel from the Cask

a. The list identifying fuel bundles to be unloaded is obtained.
b. The fuel bundle identification and location in the cask is verified.
c. The fuel bundles are unloaded one at a time in accordance with the fuel transfer procedure.

10.1.2.7 Unloading Irradiated Hardware from the Cask

a. Unloading of irradiated hardware in air at a disposal site will follow a disposal site procedure.
b. If the irradiated hardware is unloaded underwater, the liner is lifted from the cask and positioned in the water basin as specified by procedure.

10.1.2.8 Installing the Cask Closure Head

a. Steps 10.1.1.7a and b are repeated.

10.1.2.9 Returning the Cask to the Preparation Area

a. If the cask has been unloaded underwater, steps 10.1.1.8a thru f are repeated (without radiation monitoring). Step 10.1.1.8d is optional.
b. If the cask has been unloaded dry, disposal site procedures will be followed.

10.1.2.10 Securing the Cask Closure Head

a. Steps 10.1.1.9a and b are repeated.

10.1.3 Transport of an Empty Cask with Type B Contents

The following operations are typically performed subsequent to transport of irradiated fuel:

10.1.3.1 Draining of the Cask Inner Cavity

a. Steps 10.1.1.11a thru d are repeated.

10.1.3.2 Assembly Verification Leakage Testing

a. Steps 10.1.1.12a thru e are repeated.

10.1.3.3 Preparing the Empty Cask for Transport

a. A drain hose is connected to the cask cavity fill/drain valve and directed into a radwaste drain or back into the pool.
b. Steps 10.1.1.13c thru j are repeated.

10.1.3.4 Closing the Equipment Skid

a. The cask enclosures are closed, locked, and sealed.

10.1.4 Transport of an Empty Cask with Less Than Type B Contents

The following operations are typically performed after transport of irradiated hardware:

10.1.4.1 Draining of the Cask Inner Cavity

If the cask has been unloaded underwater:

a. Steps 10.1.1.11a thru c are repeated with the exception that the use of air may be substituted for the use of helium.
b. When the applied cover gas is observed to flow out of the cask cavity drain hose, the vent valve is closed and the excess pressure within the cavity is allowed to decay to 0 psig.
c. The fill/drain valve is closed and the connecting hoses and gages are removed.

10.1.4.2 Assembly Verification Leakage Testing

a. Leakage testing is not performed on IF-300 casks when transporting less than Type B quantities of radioactive materials.

10.1.4.3 Preparing the Empty Cask for Transport

a. Steps 10.1.1.13e thru j are repeated.

10.1.4.4 Closing the Equipment Skid

a. The cask enclosures are closed, locked, and sealed. N

10.2 MAINTENANCE PROCEDURES

The General Electric document "Maintenance Instructions, IF-300 Irradiated Fuel Shipping Cask", GEI-92821, provides maintenance procedures for all functional components of the IF-300 Transportation System.

Maintenance procedures affecting the cask and cask components are summarized below:

10.2.1 Annual Inspections

10.2.1.1 Cask Cavity, Exterior, Head, Etc.

a. The cask cavity, cask exterior, closure head, and related components are inspected annually for signs of damage or degradation.

10.2.1.2 Neutron Shielding

a. The neutron shielding liquid is inspected annually for purity, presence of foreign matter or radioactivity, and if applicable, ethylene glycol percentage.
b. The neutron shielding relief valves are inspected annually for functionality and verification of set pressure.

10.2.2 Annual Component Replacement

10.2.2.1 Rupture Disk

a. The rupture disk is replaced on an annual basis, just prior to annual leakage testing. The rupture disk is inspected for corrosion or other defects during the disk replacement process.

10.2.3 Annual Leakage Testing

10.2.3.1 Cask Cavity

a. Leakage testing of the cask closure seal, vent valve, fill/drain valve, and rupture disk device is performed annually with a thermal conductivity sensing instrument or a helium mass spectrometer leak detector.
b. The test instrument is set up and used according to written procedures and the manufacturer's instructions.
c. With the instrument calibrated to a sensitivity of at least 3.5 x 10^{-4} cm^3/sec (helium), the vent valve, fill/drain valve, and rupture disk device are checked for indications of leakage.
d. With the instrument calibrated to a sensitivity of at least 3.5 x 10^{-5} cm^3/sec (helium), the closure seal is checked for indications of leakage. (The increased sensitivity of this test accounts for the dilution which would occur between a potential point of closure seal leakage and the nearest point of measurement) N
e. If leakage is detected during either of the above checks, the offending components are repaired or replaced and then re-tested for leakage.

10.2.3.2 Neutron Shielding

a. The neutron shielding containment with vent/fill valves attached is hydrostatically tested annually at a pressure of 80-100 psig.

10.3 TESTING

This subsection discusses or references the tests which are or have been applied to the cask or to selected cask components. These tests may be initial determinations or they may be periodic.

10.3.1 Tests at Fabrication

10.3.1.1 Cask Inner Cavity

a. The cask inner cavity, closure, closure seal, piping and valves were hydrostatically tested at 600 psig at room temperature.

10.3.1.2 Neutron Shielding Cavity

a. The neutron shielding cavity, piping, vent/fill valves, and closures have been hydrostatically tested at 200 psig at room temperature. Both neutron shielding cavity sections were tested simultaneously.

10.3.1.3 Rupture Disk Device

a. See Section 6.6

10.3.1.4 Neutron Shielding Containment Relief Valve

a. See Section 6.6 (200 Psig Pressure Relief Valve)

10.3.1.5 Inner Cavity/Neutron Shielding Cavity Fill, Drain, and Vent Valves

a. See Section 6.6 (1-Inch Globe Valve)

10.3.1.6 Thermal Testing

a. See Section 6.7

10.3.1.7 Gamma Shielding

a. During fabrication, the uranium castings were radiographed and then checked, after stacking, by gamma scan techniques to assure that there are no radiation leaks and the uranium material is sufficiently sound such that the requirements in Section 8.5 can be satisfied. N

10.3.1.8 Functional Testing

a. Prior to delivery for use, the IF-300 casks were given a complete functional test. This test involved the removal and replacement of the two irradiated fuel baskets, the two heads, rotation and removal of the cask from the equipment skid, operation of the cooling systems, operation of the enclosures, and remote engagement and disengagement of the lifting systems.

10.3.2 Leakage Testing

Leakage testing on the IF-300 cask is done in accordance with the requirements of 10CFR71, Regulatory Guide 7.4, and ANSI Std. N14.5.

10.3.2.1 Package Containment Requirements

a. For normal conditions of transport, the containment criteria is "... no loss or dispersal of radioactive contents, as demonstrated to a sensitivity of 10^{-6} A_2 per hour,..." (Ref. 10.1)

b. For hypothetical accident conditions, the containment criteria is "... no escape of Kr^{85} exceeding 10,000 curies in one week, no escape of other radioactive materials exceeding a total amount A_2 in one week..." (Ref. 10.1)

10.3.2.2 Release Rate Limits

a. Using the assumptions and methods listed below, an A_{2e} (A_2 equivalent) of 162 curies is calculated for the contents of the IF-300 cask (excluding the Kr^{85} in fuel rod plenums):

- Data from PWR fuel assemblies (Ref.10.2) is used to identify the radionuclides in the crud on LWR fuel assemblies, and estimate the activity associated with each radionuclide at fuel assembly discharge. (Use of PWR crud data is conservative.)

- A decay period of two years from fuel assembly discharge is assumed in calculating A_{2e}. Two years corresponds approximately to the minimum cooling time needed for a fuel assembly with normal burn-up to comply with the heat load requirements of the IF-300 cask.
- The following formula (Ref. 10.3) is used to calculate the value of A_{2e}:

$$A_{2e} = 1 \;/\; \Sigma \frac{f'}{A_{2e}} \qquad \text{Eq'n 10-1}$$

where: A_{2e} = Equivalent A_2 of the mixture of radionuclides
f' = Activity fraction (at two years) of the individual radionuclides in the mixture.
A_2 = Tabulated A_2 values for the individual radionuclides in the mixture.

b. Therefore, the release rate limits for the conditions of interest are:

$R_N = A_2 \times 10^{-6}$ Ci/Hr
$= \underline{4.51 \times 10^{-8} \text{ Ci/Sec}}$ (Normal Conditions of Transport)

$R_{A1} = A_2$ Ci/Wk
$= \underline{2.68 \times 10^{-4} \text{ Ci/Sec}}$ (Hypothetical Accident Conditions) (Excluding Kr^{85})

$R_{A2} = 10{,}000$ Ci/Wk
$= \underline{1.65 \times 10^{-2} \text{ Ci/Sec}}$ (Hypothetical Accident Conditions) (Kr^{85} Only)

10.3.2.3 Radionuclide Concentrations

a. Based on the data of Reference 10.2, the activity due to the crud of one 2 year cooled PWR fuel assembly is 1074 Ci. (Use of PWR crud data is conservative.)

b. Based on data from NEDO-10084-2, the activity due to the fission gas inventory (Kr^{85}) of one 2 year cooled BWR fuel assembly is 727 Ci. (Use of BWR fission gas data is conservative).

c. The minimum cavity free volume for the IF-300 cask is 82.2 ft^3 (PWR configuration, Section 6.5).

d. The release fractions of Table X-1 are used in calculating radionuclide concentrations.

For normal conditions, a.) the release fraction for crud is based on an upper bound estimate of the percentage of crud that could remain airborne (i.e. available for release) during transport, and b.) the release fraction for fission gas is based on the thermal calculations of Section 6 and General Electric's extensive experience in shipping irradiated fuel assemblies.

For hypothetical accident conditions, a.) the release fraction for crud is based on the values reported in SAND80-2124 (Ref.10.4), and b.) the release fraction for fission gas is based on the very conservative assumption that all of the fuel assemblies fail as a result of hypothetical accident conditions. N

TABLE X-1

CRUD AND FISSION GAS RELEASE FRACTIONS

	Normal Conditions	Accident Conditions
Crud, %	1	25
Fission Gas, %	0	100

e. Radionuclide concentrations are calculated with the following equation:

$$C_x = Act_x / V \qquad \text{Eq'n 10-2}$$

where: C_x = Radionuclide concentration for condition "x"

Act_x = Activity available for leakage for condition "x", including the effect of release fraction

V = Cavity free volume

f. Therefore, the radionuclide concentrations for the conditions of interest are:

$C_N = \underline{3.23 \times 10^{-5}\ Ci/cm^3}$ (Normal Conditions of Transport)

$C_{A1} = \underline{8.08 \times 10^{-4}\ Ci/cm^3}$ (Hypothetical Accident Conditions) (Excluding Kr^{85})

$C_{A2} = \underline{5.61 \times 10^{-3}\ Ci/cm^3}$ (Hypothetical Accident Conditions) (Kr^{85} Only

10.3.2.4 Leakage Rate Limits

a. Leakage rate limits are calculated with the following equation:

$$L_x = R_x / C_x \qquad \text{Eq'n 10-3}$$

where: L_x = Leakage rate limit at condition "x"
R_x = Release rate limit at condition "x"
C_x = Radionuclide concentration at condition "x"

b. Therefore, leakage rate limits for the conditions of interest are:

$L_N = \underline{1.40 \times 10^{-3}\ cm^3/sec}$ (Normal Conditions of Transport)

$L_{A1} = \underline{3.32 \times 10^{-1}\ cm^3/sec}$ (Hypothetical Accident Conditions) (Excluding Kr^{85})

$L_{A2} = \underline{2.94\ cm^3/sec}$ (Hypothetical Accident Conditions) (Kr^{85} Only)

10.3.2.5 Limiting Leakage Path Diameter

a. Gas leakage for laminar, transitional, or molecular flow modes can be estimated with the following equation (Ref. 10.5):

$$L = 3810 \frac{D^3}{a} \left(323 \frac{D}{\eta} (P_u^{\ 2} - P_d^{\ 2}) + \sqrt{\frac{T}{M}} (P_u - P_d) \right) \qquad \text{Eq'n 10-4}$$

where: L = leakage rate, cm^3/sec
D = leak path diameter, cm
a = leak path length, cm
P_u = upstream pressure, atm-abs
P_d = downstream pressure, atm-abs
η = gas viscosity, cp
T = gas temperature, °K
M = gas molecular wt., amu

b. Upstream pressures and gas temperatures are obtained from the thermal analyses of Section 6.3. LOMC data is used for normal conditions of transport and PFE data is used for hypothetical accident conditions.

c. By assuming a leak path length of 1 cm, leak path diameters associated with the leakage rates of interest (L_N, L_{A1}, L_{A2}) can be calculated. Table X-2 documents the inputs used in calculating the following leak path diameters:

D_N = $\underline{13.5 \times 10^{-4}\ cm}$ (Normal Conditions of Transport)

D_{A1} = $\underline{21.5 \times 10^{-4}\ cm}$ (Hypothetical Accident Conditions) (Excluding Kr^{85})

D_{A2} = $\underline{37 \times 10^{-4}\ cm}$ (Hypothetical Accident Conditions) (Kr^{85} Only)

Comparing the above leak path diameters, it is concluded that normal conditions of transport (i.e. LOMC) are the most limiting leakage conditions.

N

TABLE X-2

INPUTS TO LEAKAGE PATH DIAMETER CALCULATIONS

Inputs	Normal Conditions of Transport	Hypothetical Accident Conditions (Excluding Kr^{85})	Hypothetical Accident Conditions (Kr^{85} Only)
L, cm^3/sec	1.4×10^{-3}	3.32×10^{-1}	2.94
a, cm	1.0	1.0	1.0
P_u, atm-abs	2.99	19.1	19.1
P_d, atm-abs	1.0	1.0	1.0
η, cp	0.025	0.029	0.029
T, °K	469	548	548
M, amu	28.71 (air)	28.71 (air)	28.71 (air)

10.3.2.6 Reference Air Leakage Rate

a. Using equation 10-4, a leak path length and diameter of 1 cm and 13.5 microns, respectively, and standard air conditions (25°C and 1 atm-abs), the reference air leakage rate is:

L_{Ref} = $\underline{2.45 \times 10^{-4}\ atm\text{-}cm^3/sec}$

This leakage rate is equivalent to L_N.

10.3.2.7 Annual Leakage Test Requirements

a. Type B packages must be leakage tested within the preceding 12-month period. The test procedure sensitivity for this "annual" test must be less than or equal to one-half the reference air leakage rate, L_{Ref}, or its equivalent. (Ref. 10.5)

b. For the IF-300 cask, helium at room temperature and 1 atm-gage is used for the annual leakage test. Using equation 10-4 and a leak path length and diameter of 1 cm and 13.5 microns, respectively, a helium leakage rate of 7.1×10^{-4} cm^3/sec is calculated.

This leakage rate is equivalent to L_N and L_{Ref}.

c. Since the leakage test procedure sensitivity must be less than or equal to one-half the calculated leakage rate, the required test procedure sensitivity for the annual leakage test is 3.5×10^{-4} cm^3/sec (helium) or less.

10.3.2.8 Assembly Verification Leakage Testing

a. Type B packages must also be leakage tested prior to each shipment. The required test procedure sensitivity in this instance, however, is less stringent than that of the annual leakage test. Per Reference 10.6, leakage testing prior to each shipment...

> "should be sensitive enough to preclude the release of an A_2 quantity in 10 days, but need not be more sensitive than 10^{-3} atm-cm^3/sec and can be no less sensitive than 10^{-1} atm-cm^3/sec."

b. By using the methods presented in 10.3.2.2 thru 10.3.2.4 above, the following parameters are calculated for a release rate of A_2 Ci in 10 days:

$$R_A = \underline{1.88 \times 10^{-4} \text{ Ci/sec}}$$

$$C_A = C_N = \underline{3.23 \times 10^{-5} \text{ Ci/cm}^3}$$

$$L_A = \underline{5.80 \text{ cm}^3\text{/sec}}$$

Substituting L_A, a leak path length of 1 cm, and LOMC conditions into equation 10-4, the resulting leak path diameter is 110 microns. Standardized to air at 25°C and 1 atm-abs, this leak path diameter would result in a leakage rate of 9.65×10^{-1} atm-cm^3/sec (air).

c. For a minimum leakage test procedure sensitivity of 10^{-1} atm-cm^3/sec (at standard air conditions), the use of equation 10-4 results in a leak path diameter of 62 microns when a leak path length of 1 cm is assumed.

d. Helium at 1 atm-gage is used for assembly verification testing. For a leak path length and diameter of 1 cm and 62 microns, respectively, the use of equation 10-4 and test conditions results in a leakage rate of 2.88×10^{-1} cm^3/sec (helium).

Thus, for the IF-300 cask, the assembly verification test procedure must have a sensitivity of 2.88×10^{-1} (helium) to be equivalent to a sensitivity of 1×10^{-1} atm-cm^3/sec at standard air conditions.

10.4 REFERENCES

1. 10CFR71.51 N

2. EPRI NP-2735, Expected Performance of Spent LWR Fuel Under Dry Storage Conditions, Battelle, Colombus Laboratories, Dec. 1982.

3. R. H. Jones, R.T. Reese, A Method for Determination of A_2 for a Mixture of Radionuclides, presented at PATRAM '83, New Orleans, LA, May 15-20, 1983.

4. E.L. Wilmot, Transportation Accident Scenarios for Commercial Spent Fuel, SAND80-2124, Sandia National Laboratories, February 1981.

5. ANSI Std. N14.5-1977, American National Standard for Leakage Tests on Packages for Shipment of Radioactive Materials.

6. Letter, dated Nov. 14, 1984, C.E. MacDonald to J.E. VanHoomissen, regarding GE's application for renewal of C of C 9001.